STRENGTHENING OF REINFORCED CONCRETE FRAMES BY CUSTOM SHAPED HIGH STRENGTH CONCRETE MASONRY BLOCKS

A THESIS SUBMITTED TO
THE GRADUATE SCHOOL OF NATURAL AND APPLIED SCIENCES
OF
MIDDLE EAST TECHNICAL UNIVERSITY

BY

GÜRAY ARSLAN

IN PARTIAL FULFILLMENT OF THE REQUIREMENTS
FOR
THE DEGREE OF MASTER OF SCIENCE
IN
CIVIL ENGINEERING

JANUARY 2009

Approval of the thesis:

STRENGTHENING OF REINFORCED CONCRETE FRAMES BY CUSTOM SHAPED HIGH STRENGTH CONCRETE MASONRY BLOCKS

submitted by **GÜRAY ARSLAN** in partial fulfillment of the requirements for the degree of **Master of Science in Civil Engineering Department, Middle East Technical University** by,

Prof. Dr. Canan Özgen _____
Dean, Graduate School of **Natural and Applied Sciences**

Prof. Dr. Güney Özcebe _____
Head of Department, **Civil Engineering**

Assoc. Prof. Dr. M. Uğur Polat _____
Supervisor, **Civil Engineering Dept., METU**

Examining Committee Members:

Prof. Dr. Mehmet Utku _____
Civil Engineering Dept., METU

Assoc. Prof. Dr. M. Uğur Polat _____
Civil Engineering Dept., METU

Prof. Dr. Turgut Tokdemir _____
Engineering Science Dept., METU

Assoc. Prof. Dr. Uğurhan Akyüz _____
Civil Engineering Dept., METU

Assist. Prof. Dr. Özgür Kurç _____
Civil Engineering Dept., METU

Date: 26.01.2009

I hereby declare that all information in this document has been obtained and presented in accordance with academic rules and ethical conduct. I also declare that, as required by these rules and conduct, I have fully cited and referenced all materials and results that are not original to this work.

Name, Last name: Güray ARSLAN

Signature:

ABSTRACT

STRENGTHENING OF REINFORCED CONCRETE FRAMES BY CUSTOM SHAPED HIGH STRENGTH CONCRETE MASONRY BLOCKS

ARSLAN, Güray
M.Sc., Department of Civil Engineering
Supervisor: Assoc. Prof. Dr. Uğur POLAT

January 2009, 124 pages

Located on one of the highly active seismic fault systems in the world, the building stock in Turkey is mainly composed of reinforced concrete frames with 4-5 stories. Due to design and construction deficiencies resulting from the use of unqualified personnel and insufficient supervision, many of these buildings lack lateral stiffness, ductility and strength. For many structures, there is a need to alleviate these deficiencies by means of some rehabilitation techniques prior to earthquakes. One approach also used very widely in Turkey is to fill some of the frame bays by cast-in-place R/C panels. The procedure appears to be very practical at first glance. It also appears to be very economical as far as the production of the panels is concerned. However, the production phase is slow, dirty, destructive and disruptive to occupants. Moreover, it requires relatively skilled personnel and special equipment. Therefore, the real life experience shows that the actual cost in practice is much higher when all other hidden costs are taken into account.

The aim of this experimental study is to explore the potential of using infill walls made of custom shaped and high strength concrete blocks as a simpler and more practical alternative to cast-in-place R/C panels to increase the lateral load bearing capacity of frame structures. The effectiveness of FRCM (Fiber Reinforced Cementitous Matrix) system on damaged structures is also investigated in this study.

Keywords: R/C Frame, Strengthening, Custom Shaped Concrete Block, High Strength Concrete Block, FRCM

ÖZ

BETONARME ÇERÇEVE YAPISAL SİSTEMLERİN ÖZEL GEOMETRİLİ VE YÜKSEK DAYANIMLI BETON BLOKLAR İLE GÜÇLENDİRİLMESİ

ARSLAN, Güray
Yüksek Lisans, İnşaat Mühendisliği Bölümü
Tez Yöneticisi: Doç. Dr. Uğur POLAT

Ocak 2009, 124 sayfa

Dünyanın en aktif deprem kuşaklarından birisi üzerinde yer alan ülkemizin mevcut yapı stoku büyük ölçüde 4-5 katlı betonarme çerçeve yapısal sisteme sahip binalardan oluşmaktadır. İnşaat aşamasındaki yetersiz denetim ve kalifiye olmayan işçilik nedeni ile oluşan tasarım ve yapım kusurları yüzünden bu binaların çoğu yatay rijitlik, süneklik ve dayanım yönünden yetersiz kalmaktadır. Sonuç olarak bu kusurları giderip gerekli deprem güvenliğini sağlamak üzere böyle yapıların uygun bir yaklaşım ile güçlendirilmesi gereği ortaya çıkmaktadır. Bu amaçla ülkemizde de yaygın olarak kullanılan bir yaklaşım çerçeve sistemdeki bazı açıklıkların yerinde döküm betonarme paneller ile doldurulmasıdır. Ancak ilk bakışta çok pratik ve panellerin üretimi düşünüldüğü zaman ekonomik gibi görünen bu yöntem, imalat aşamasında oldukça tahripkar, kirli ve yavaş olup özel işçilik ve ekipman gerektirmektedir Bu nedenle ekonomik gibi görünen bu yöntemin tüm giderler düşünüldüğünde son maliyet olarak çok da ekonomik olmadığı gerçek uygulamalarda açıkça görülmektedir.

Bu çalışma ile betonarme çerçeve sistemlerde yerinde döküm betonarme paneller yerine daha basit ve pratik bir yaklaşım olarak özel geometrili ve yüksek dayanımlı beton bloklarla oluşturulan dolgu duvarların kullanılması potansiyelinin deneysel ve analitik olarak araştırılması amaçlanmaktadır. Bu çalışmada FRCM sistemlerin hasarlı yapılar üzerindeki etkisi de ayrıca incelenmiştir.

Anahtar kelimeler: Betonarme Çerçeve, Güçlendirme, Özel Geometrili Beton Blok, Yüksek Dayanımlı Beton Blok, FRCM

To mankind

ACKNOWLEDGMENTS

This study was carried out under the supervision of Assoc. Prof. Dr. M. Uğur POLAT. I would like to express great appreciation to him for his support, advice and patience during this study.

I want to thank to Assoc. Prof. Dr. İsmail Özgür YAMAN for his suggestions and comments for the preparation of mix design of concrete blocks.

Also, I would like to thank ŞahİsmailTEKİN for his helps during the experiments.

I gratefully acknowledge the financial support given by the Scientific and Technical Research Council of Turkey (TUBITAK).

Finally, I would like to thank my family for their invaluable support during this long period.

TABLE OF CONTENTS

LIST OF TABLES

LIST OF FIGURES

CHAPTER 1

INTRODUCTION

1.1 General

Most of the residential buildings in Turkey are reinforced concrete structures. The buildings showing nonductile behaviour are seismically deficient. Such nonductile behaviour of these reinforced concrete frames is due to inadequate flexural and shear capacity and lack of confinement in beams, columns and beam-column joints; and strong beam-weak column. Since these kinds of frames lack sufficient lateral stiffness, ductility and strength, the buildings experience large lateral displacements under the earthquake loads. Therefore, great many of the reinforced concrete structures suffered severe damage in recent earthquakes. To improve the seismic behaviour of these structures, the retrofitting of them is required for life safety.

Many seismic retrofitting techniques have been developed to improve the seismic performance of existing undamaged buildings prior to being subjected to earthquakes. Generally, there are two main approaches to increase the seismic capacity of existing structures. The first approach is a member-level rehabilitation which involves increasing the ductility capacity of members. In this approach, the seismic performance of individual deficient members such as beams, columns, beam-column joints and walls are improved by using concrete, steel or fiber reinforced polymer (FRP) jacketing. The second approach is structural system-level rehabilitation. This approach involves global modifications to the structural system. Addition of structural walls, steel braces, base isolators and damping devices has a very effective impact on the structural response to seismic loads [1].

Strengthening of individual deficient structural members is feasible if the number of these members is limited and if the overall drift requirements of the structural system are satisfied [2]. If these requirements are not satisfied properly, structural system-level rehabilitation becomes a convenient and economical solution to reduce the risk of damage.

The basic policy of seismic strengthening for existing buildings is the same as a policy of new building design [3]. According to the strengthening policy, the technique to improve the seismic performance of existing buildings is determined.

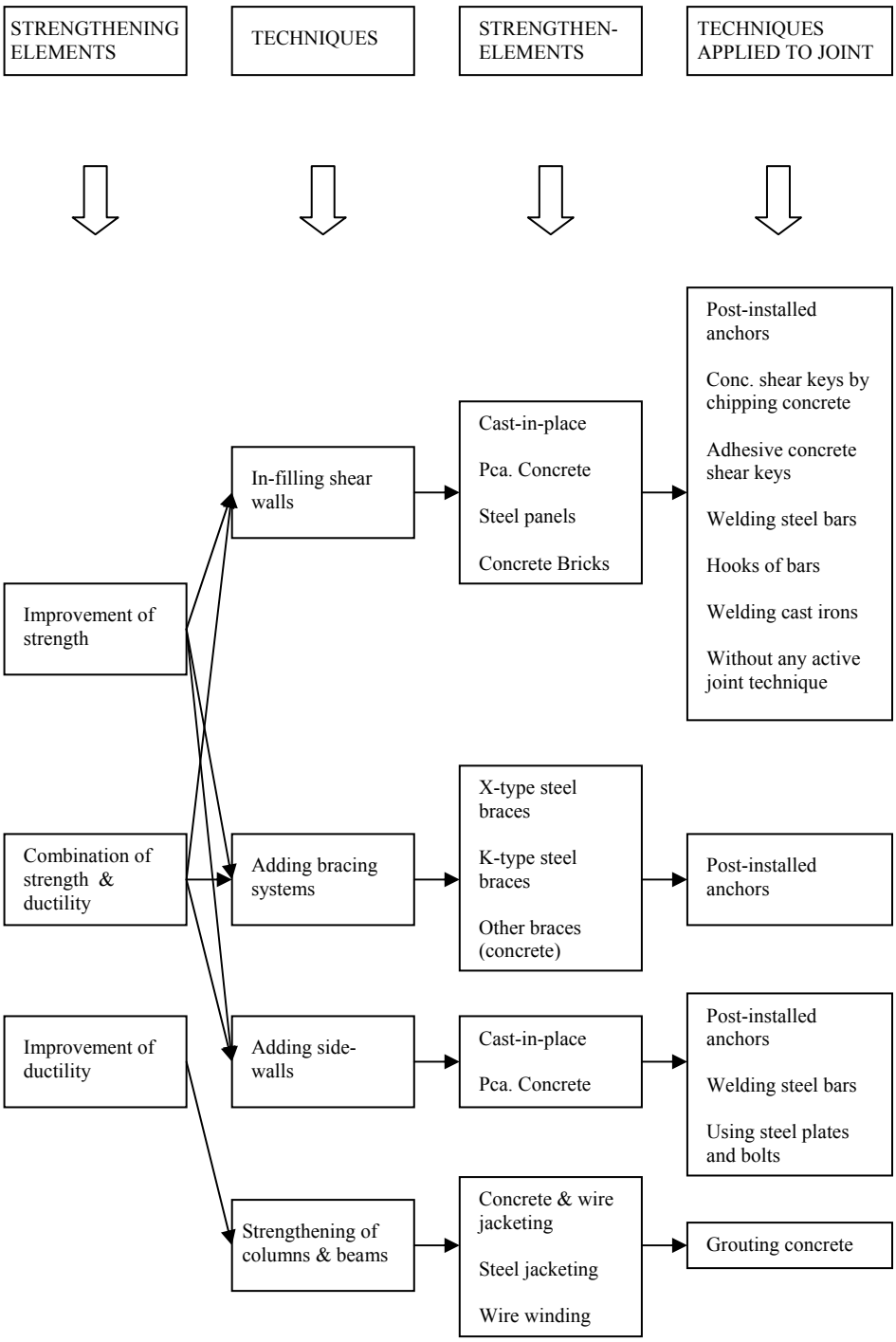

Figure 1.1 - Relationship Between Strengthening Policy and Strengthening Techniques [3]

One of the most common strengthening techniques applied to existing buildings in Turkey is adding new reinforced concrete shear walls to reinforced concrete frames. However, there are some disadvantages to this approach. The cost, time constraints, the need for large formwork during construction, problems associated with casting large quantities of concrete in an existing building, and limiting or usually preventing the use of the building in the course of the construction operations are some of them. Therefore, some new alternative techniques are necessary to overcome these problems.

1.2 Object and Scope of this Study

The aim of this study is to investigate the potential of using infill walls made of custom shaped and high strength concrete blocks as a simpler and more practical alternative to cast-in-place reinforced concrete panels to increase the lateral load bearing capacity of frame structures. This method of seismic strengthening is expected to be a much more practical and feasible technique, and not disturbing to the occupants. Also, this technique does not require skilled personnel, extensive formwork and special equipment.

One of the specimens of the testing program was retrofitted with FRCM (Fiber Reinforced Cementitous Matrix) system in its damaged state. Thus, the effectiveness of FRCM system on the damaged reinforced concrete structural elements was also investigated in this research.

A total of six twin frames are planned and tested in this study. The basic test frame is composed of two one-bay, two-story reinforced concrete frames attached back to back by a strong foundation beam. The aim of forming this kind of a frame is to test two frames in a single run by benefiting from the advantage of symmetry. The test program is as follows:

1. Bare frame: unstrengthened frame used as a reference (lower limit),
2. Frame with cast-in-place R/C infill wall: used as a reference (upper limit),
3. Frame with infill wall made of 30 MPa concrete blocks with wavy edges,
4. Frame with infill wall made of 30 MPa rectangular concrete blocks
5. Frame with infill wall made of 70 MPa concrete blocks with wavy edges,
6. Frame with infill wall made of 70 MPa rectangular concrete blocks

In an effort to see the increase in ductility of the concrete block masonry walls provided by external reinforcement the test frame with infill wall made of 30 MPa rectangular concrete blocks was also tested after retrofitting it in its damaged state by FRCM composite mesh.

There are mainly three parameters which are expected to influence the effectiveness and the capacity of the infill walls made of high strength concrete blocks. These are the compressive strength of concrete blocks, the concrete block geometry, and the adhesive strength of the mortar forming the joints between the concrete blocks. A preliminary experimental study was conducted for the selection of the appropriate mortar. In these experiments three concrete blocks were joined by an epoxy based two-component mortar brand named Concresive 1406 and produced by BASF-YKS and tested as shown in Figure 1.2. It was seen that its adhesion to the concrete blocks was extremely good and its shear strength was sufficient to force the shear failure into the concrete blocks as shown in Figure 1.3 for even the highest compressive strength concrete blocks to be used in this study.

Therefore, two parameters remain to be investigated in this study for the strengthening of reinforced concrete frames by using infill walls made of high strength concrete blocks.

- Concrete block strength
- Concrete block geometry

Figure 1.2 - Experimental Setup for the Shear Strength of Concrete Blocks Joined by Concresive 1406 Mortar

Figure 1.3 - Failure of Concrete Blocks Joined by Concresive 1406 Mortar

CHAPTER 2

LITERATURE SURVEY

2.1 General

Rehabilitation of reinforced concrete frame structures to increase their seismic capacities has always been an attractive subject and investigated by various researchers in the literature. Some of the significant previous studies on the subject are summarized below.

2.2 Previous Studies

Ersoy and Uzsoy [4] tested one story, one-bay reinforced concrete frames under monotonic loading to investigate the effects of strengthening with cast-in-place reinforced concrete infills.

In this study the researchers have investigated the following main parameters:

- Aspect ratio
- Infill thickness
- Effect of vertical loads
- Connection between frame and panel
- The ratio of beam stiffness to column stiffness

The results of the study can be listed as:

- Lateral load carrying capacity increased by approximately 700% and the lateral deflection at failure reduced by 65%.
- The bond between the panel and the frame did not affect the lateral load capacity and rigidity of strengthened frames significantly.
- The elastic lateral rigidity of the frame increased by 500%.

Govindan, Lakshmipathy and Santhakumar [5] investigated experimental comparison of the behavior of a seven-story brick masonry infilled reinforced concrete frame with that of a reinforced concrete frame without infill subject to lateral loads, and assessed the failure mode of the brick-infilled frame.

Based on the test results, the following conclusions were drawn:

- The load carrying capacity of infilled frames was twice that of reinforced concrete frame without infill.
- The initial stiffness of infilled frame was 5.0 times that of comparable reinforced concrete frame.
- Reinforced concrete frame showed 3.29 times better cumulative ductility.
- The total energy dissipation capacity of the infilled frame was 1.5 times that of the reinforced concrete frame without infill.
- The damage to the infill during the final stages of loading was considerable and there was a danger of brick-work crushing and spilling, resulting in debris which could endanger occupants.

Phan, Cheok and Todd [6] analyzed existing experimental results from 54 tests of lightly reinforced concrete frames to develop guidelines for seismic strengthening of LRC frame buildings.

The main variables in this study were:

- Infill wall type (cast-in-place, CIP and precast)
- Wall thickness
- The amount of anchor area
- Anchor type

According to this study the following suggestions were reported as design guidelines for strengthening with infill walls:

- Infill wall thickness, of both CIP and precast infill walls, should be not less than 2/5 the thickness of the bounding column or the top beam of the frame, whichever is smaller, and should not be greater than the thickness of the top beam.

- Based on experimental observation, the ratio of the total cross sectional area of the connecting anchors to the area of the infill walls at the wall/frame interface (Ac/Aw) should not be less than 0.8% for successful connection between the wall and the existing frame.
- Even though the flexural reinforcement ratio was not a variable in this study, successful infill wall performance was observed in experiments where the reinforcement ratio, in both the vertical and horizontal directions, was greater than or equal to 0.75%.

Frosch [7] made tests on fourteen two-story nonductile frames to develop minimum design and detailing requirements for the precast infill wall system. The main variables in the experimental investigation were:

- Shear key configuration
- Shear key size
- Panel spacing
- Vertical steel
- Grout strength
- Panel thickness

The following conclusions were obtained from the experimental research:

- Joint failures occurred at the top of the horizontal grout interface due to lack of adhesion between the panel and the grout caused by air entrapment during grouting of the joint.
- The shear key configuration (alignment and spacing) had no significant effect on the peak strength and no effect on the residual capacity.
- The shear key size had no significant effect on the peak capacity and no effect on the residual.
- The relative strength between the grout and panel concrete influenced the joint behavior. The lower strength material controlled the peak capacity and failure surface location. The residual capacity, however, was not affected.

- The peak and residual capacity of the walls increased directly with the wall thickness.
- Increasing the vertical reinforcement increased both the peak and residual capacities of the specimen.

Erdem et. al. [8] tested two 1/3 scale, two-story, three-bay undamaged frames to compare two types of strengthening techniques experimentally. Both undamaged frames were designed such that they had the common deficiencies of existing buildings in Turkey. One of the frames was strengthened with RC infill while the other frame was strengthened with CFRP strengthened hollow clay blocks. The test specimens were subjected to reversed cyclic quasi-static loading.

The following conclusions were drawn in the light of the 1/3-scale tests:

- Both strengthening techniques increased the stiffness and strength of frames significantly. The lateral strength increased by approximately 500%. The stiffness of the strengthened frames was about ten times that of the bare frame.
- The initial stiffness of the frame which was strengthened with RC infill was higher compared to the frame strengthened with CFRP applied hollow clay block infill wall.
- The capacity of the frame where the hollow clay block infills have been strengthened using CFRP strips depends on the amount and effectiveness of CFRP anchor dowels.
- Although the strengths of both specimens were almost the same, the strength degradation of Specimen S2 (strengthened with CFRP applied hollow clay block infill wall) beyond the peak was more pronounced.

Süsoy [9] made an experimental research to investigate the behaviour of the seismic strengthening method by bonding precast concrete panels on hollow brick masonry infill walls of existing reinforced concrete frames in order to convert the infill into a load carrying system. The test frames were one story-one bay reinforced concrete frames of one-third scale.

The main parameters studied for this study were:

- Panel geometry
- Panel to panel connections
- Panel to frame connections
- Effect of lap-splice and axial load

The following conclusions were obtained from this study:

- The experiments showed that strengthening with precast concrete panels was found to be a very effective and convenient method for strengthening seismically vulnerable reinforced concrete structures.
- Average strength increase was 2.5 times with respect to the reference specimen after strengthening with precast panels. Initial lateral stiffness increased about 3.3 times.
- Test results show that welded connections and shear keys were found to be unnecessary, only epoxy was shown to be satisfactory for all panel connections.
- Strengthened infill failed by excessive diagonal cracking on the panels, and the frame failed by crushing or failure at the column bases or at the beam-column joints. After the failure of the infill, the behavior of the system became similar to a frame behavior. Stronger infills provided higher lateral load capacity, but hampered frame action, thus, limiting the ductility.
- The method proved to be effective also for specimens with lap-spliced reinforcement, although bar slip problems were observed.
- Utilization of one-story, one-bay reinforced concrete test frames were proved to be successful and almost equivalent to two-story, one-bay test frames, as they have provided similar results.

Baran [10] tested total fourteen one-bay two story frames, two being unstrengthened reference frames to investigate the effect of high strength precast concrete panels bonding on hollow brick masonry infill walls. To reflect the common deficiencies observed at the site, some weaknesses such as inadequate confinement at the end zones of the columns, low quality concrete, lapped-splices with inadequate splice

length at floor levels and inadequate transverse reinforcement in the joints were introduced in the test frames.

Main parameters studied experimentally were:

- Precast concrete panel geometry
- Panel to panel connections; shear keys, welding, epoxy alone etc.
- Panel to frame connections
- Internal or external panel applications
- Number and spacing of anchorage bolts in the case of external panels

The following conclusions obtained from fourteen tests conducted:

- The increase in lateral load carrying capacity of the strengthened frames varied between 2.24 times and 2.77 times with respect to the reference frame.
- The increase in the initial stiffness of the strengthened frames varied between 1.72 times and 3.07 times with respect to the reference frame.
- The increase in the energy dissipation capacities of the strengthened frames varied between 1.44 times and 3.86 times.
- According to the test results, the magnitude of the story drift index was significantly reduced as a result of the strengthening of the frames.
- Frames strengthened by panels connected only by the use of epoxy mortar proved to be so successful that both shear keys and welded connections came to be redundant.
- In most of the tests, it was observed that the frames dissipated energy when damage occurred in the panels together with the frame itself.
- Bond problems due to lapped-splices on the longitudinal reinforcements would not be critical in the cases when the axial load level on the columns are not very low.
- According to the analytical studies, equivalent strut method estimated the initial stiffness of the strengthened specimens more reasonably than the equivalent column whereas the lateral load carrying capacities of the specimens was well predicted by equivalent column method.

Kesner and Billington [11] made an experimental research. In this research, an infill wall system was developed for use in steel framed structures using precast panels made of engineered cementitious composite materials (ECC). The infill panels were constructed using the ECC material reinforced similar to traditional precast concrete panels.

Main parameters studied in this experiment were:

- Panel geometry
- Reinforcement type
- Material type

The following conclusions were obtained from this study:

- The ECC panels exhibited greater strength compared to the concrete panel. The increased strength of the ECC panels was attributed to the tensile carrying capacity of ECC and the improved bond characteristics between ECC and reinforcing steel.
- In the panel testing, two different types of reinforcing were used in the panels. The use of the 9.5 mm perimeter bar in addition to the welded wire fabric (WWF) reinforcement was found to significantly increase the stiffness, strength (peak and residual) and energy dissipation in the panels.
- Two different panel shapes were examined in the program, a rectangular panel and a tapered panel. The tapered panel was developed to represent a more optimal panel shape.

Kara [12] tested nine one-bay two story frames to investigate the strengthening of non-ductile concrete frames by introducing partial infills into existing frames.

Parameters of this study were:

- The infill length to height ratio
- The arrangements of infills into frame openings
- The existence of edge member at the free and of infill.

Test results showed that:

- Partial infills significantly improved the lateral load carrying capacity stiffness and energy dissipation capacity of the bare frame.
- The more infill length to height ratio of partial infill was utilized, the more lateral load capacity, stiffness was observed.
- The most successful results were obtained when the partial infill wall was connected to both columns and beams of the frame.
- The existence of edge members, also affected the specimen's lateral load carrying capacity, stiffness and energy dissipation capacity.

Yüksel, Ilki, Erol, Demir and Karadoğan [13] tested six two story-one bay reinforced concrete frames, two bare, two infilled and two with CFRP retrofitted infill walls under constant vertical load and reversed cyclic lateral loads. Test data were evaluated in terms of strength, stiffness and failure mechanisms.
Based on this study, the following conclusions were drawn:

- The lateral strength and stiffness of the infilled specimens are significantly higher than bare frame specimens.
- Although one or two diagonal cracks were formed on the infill walls, crucial damage of the infills, prior to retrofitting of the specimens, was corner crushing. The contribution of infill walls to the lateral load capacity of specimen seemed to end after corner crushing.
- Retrofitting the specimens by CFRP prevented corner crushing and diagonal cracks spreaded over the whole infill. Although the infill walls were severely damaged at the end of the tests, total collapse of infill walls was not observed.
- Retrofitting infilled frame specimens by CFRP increased lateral load capacities and lateral stiffness. The sudden load drops, observed at base shear versus top displacement curves due to diagonal CFRP rupture, showed that the contribution of diagonal CFRP on overall behavior is substantial.
- Energy dissipation capacity of the system was increased by the means of CFRP application.

Garevski, Hristovski and Stojmanovska [14] designed and tested three 1/3 scale models (2 story R/C frame specimens) of a 4 story R/C frame building prototype on the shaking-table at the IZIIS Laboratory, Skopje, Macedonia. The first test specimen was a 3D RC frame structure with infill walls. The second specimen had additional CFRP strips applied on both faces of the infill walls using epoxy. The third specimen was retrofitted with pre-cast concrete panels epoxy glued to the wall and frame members. The main goal was to verify the validity and applicability of different seismic retrofitting techniques

From the performed experimental investigations the following conclusions were obtained:

- The experiments have shown that using the proposed techniques for retrofit of these kinds of structural systems, the overall behavior under seismic excitation can significantly be improved. The maximum displacements dropped from 16.8 cm for the non-retrofitted specimen to 8.7 cm and 2.26 cm for the retrofitted specimens for the strongest applied earthquake record.
- Specimen 3 strengthened with epoxy glued pre-cast panels exhibited significant increase in the load carrying capacity and stiffness as well as considerable ductility improvement and increased energy dissipation.
- As compared to other retrofit and strengthening methods, both of the strengthening techniques CFRP and pre-cast concrete panels have proved to be applicable more easily and more rapidly and also do not require evacuation of the occupants.

CHAPTER 3

TEST SPECIMENS

3.1 General

The test specimens used in this experimental study are one-bay, two-story reinforced concrete frames. The main test frame is composed of two frames connected back to back by a strong foundation beam. The aim of forming this kind of a frame is to test two identical frames in a single run by benefiting from the advantage of symmetry. Figure 3.1 shows a general view of the bare frames.

Figure 3.1 - General View of the Bare Frame

The specimens were tested under reversed cyclic lateral loading. Except the reference specimens, all specimens were strengthened against the lateral loads by using custom shaped high strength concrete masonry blocks. Two different concrete strength (C30 and C70) and two different block geometries were tested. In order to bond the masonry blocks to each other and to the frame members, a kind of epoxy was used. The specimens used in this experimental research are listed in Table 3.1 below.

Table 3.1 - Test Specimens

Specimen	Strengthening or Retrofitting
S1	Unstrengthened frame used as reference (lower limit)
S2	Cast-in-place R/C infilled frame used as reference (upper limit)
S3	30 MPa strength and custom shape concrete blocks
S4	30 MPa strength and rectangular shape concrete blocks
S5	70 MPa strength and custom shape concrete blocks
S6	70 MPa strength and rectangular shape concrete blocks
S4XMesh	FRCM retrofitted infill wall

For frames of specimens, continuous reinforcement was used. All reinforced concrete frames were constructed according to the standards and they do not have any structural deficiencies

3.2 Dimensions of the test specimens

All specimens were cast horizontally by using steel formworks. The specimens consist of 200x300 mm columns, T section (80x120x300 mm) beams and 400x300 mm foundation beam. The columns have a clear height of 750 mm and the specimens have a clear span of 1000 mm. All dimensions are shown in Figure 3.2.

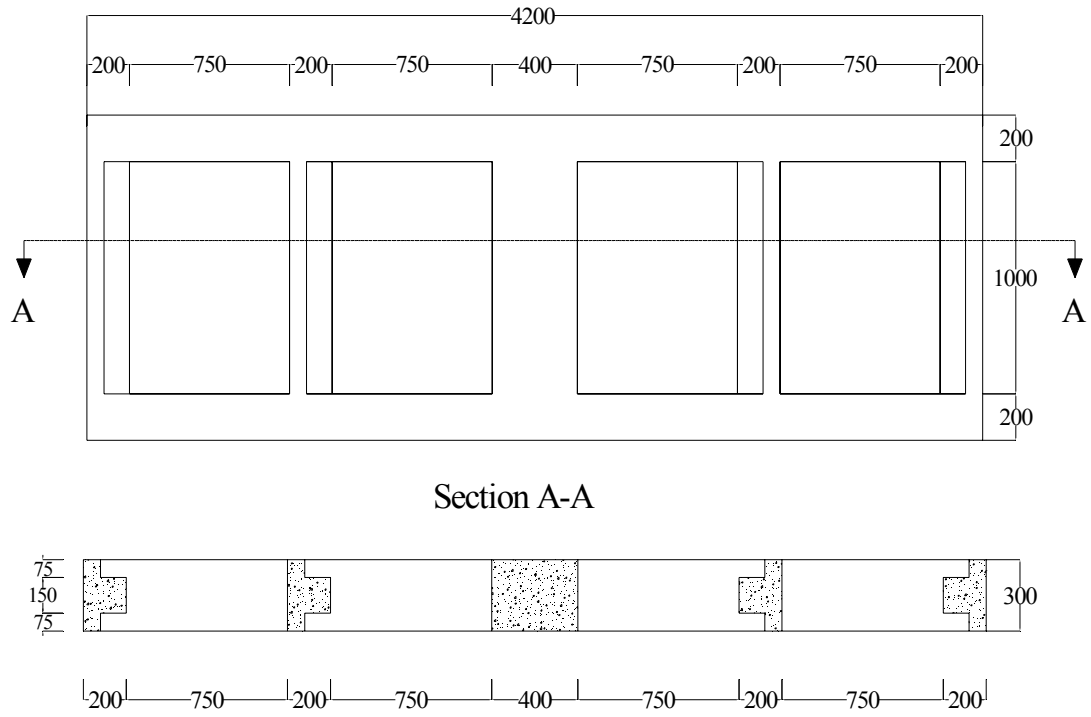

Figure 3.2 - Dimensions of the Test Specimens (dimensions in mm)

Steel formwork was used for the construction of the reinforced concrete frame. This formwork facilitated the reinforcement works and accelerated the test procedure. Figure 3.3 shows a general view of the formwork.

Figure 3.3 - General View of the Formwork

3.3 Detailing of the Frames

ϕ14 deformed bars were used as longitudinal reinforcements in the columns and foundation beam. There were 4 ϕ14 bars in each column and 6 ϕ14 bars in foundation beam. ϕ8 and ϕ14 deformed bars were used as longitudinal reinforcements in the beams. There were 4 ϕ8 and 2 ϕ14 bars in each beam. The details of the reinforcement for the frame are shown Figures 3.4 - 3.7 and properties of reinforcing bars are listed in Table 3.2.

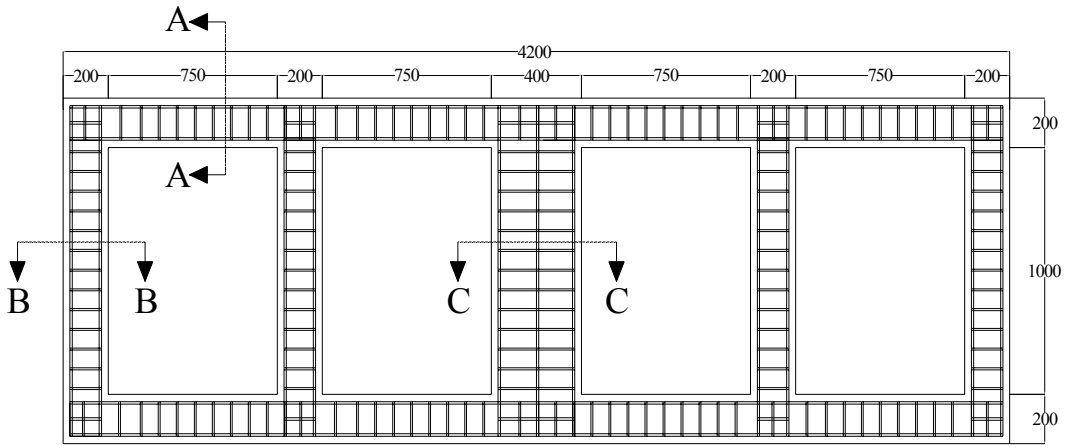

Figure 3.4 - General View of Reinforcement

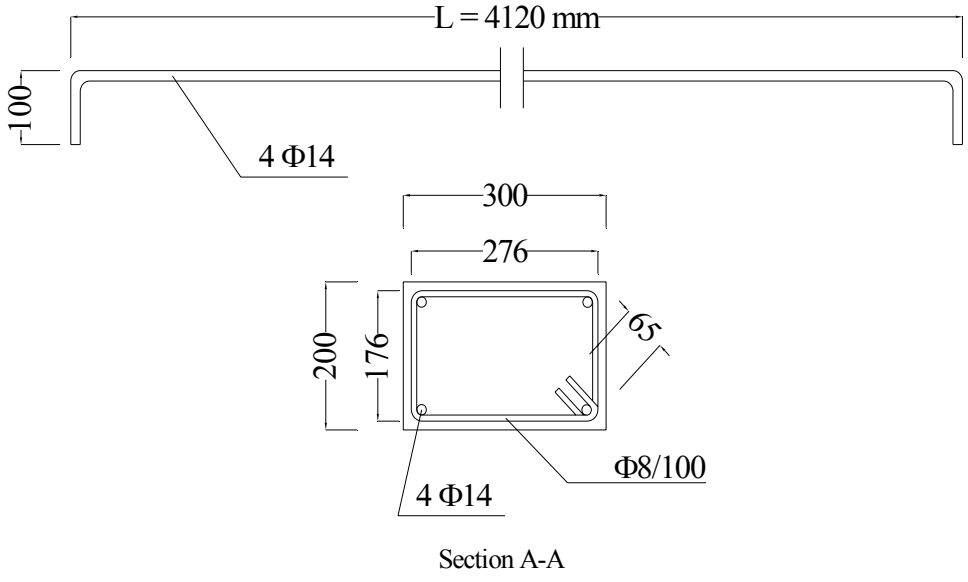

Figure 3.5 - Reinforcement Details of Columns

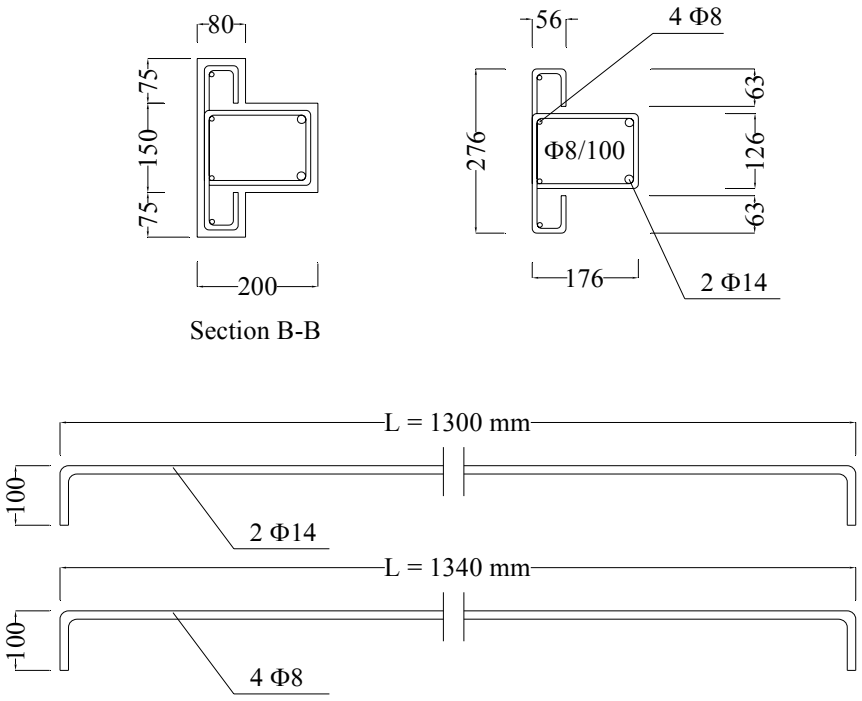

Figure 3.6- Reinforcement Details of Beams

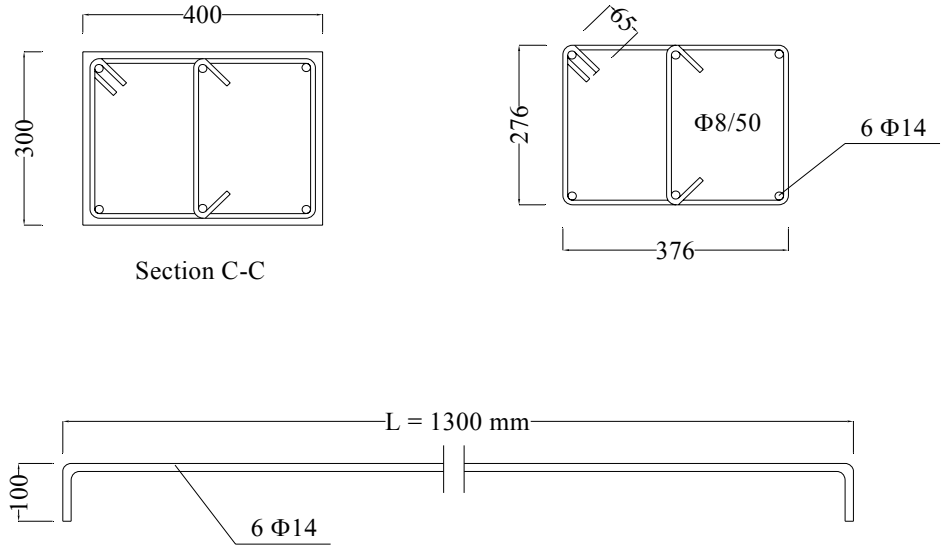

Figure 3.7 - Reinforcement Details of Foundation

Table 3.2 - Properties of Reinforcing Bars in the Frames

Bar Location	Number of Bars	Bar Diameter ϕ (mm)	Property	Yield Strength f_y (MPa)
Beam Longitudinal Bars	4 x 4	8	Deformed	420
Beam Longitudinal Bars	4 x 2	14	Deformed	420
Column Longitudinal Bars	2 x 4	14	Deformed	420
Foundation Longitudinal Bars	6	14	Deformed	420
Transverse reinforcement	-	8	Deformed	420

3.4 RC Infill

Specimen S2 was a strengthened frame with RC infills. This test frame was constructed for acting as a reference. RC infill consisted of ϕ8 deformed bars in vertical and horizontal directions. These bars were fixed with epoxy in to the frame. Deformed bars were extended about 100 mm into the beams and columns. For this, a set of holes were drilled on the inner faces of the frame members. Then, these holes were cleaned and deformed bars were inserted into epoxy injected holes. Reinforcement details for infill walls are shown in Figure 3.8. When all these works were carried out, frame was in a vertical position (Figure 3.9). After these works were completed, the frame was brought into the horizontal position to cast concrete of infills. Concrete used for infills was the same with that of the frame.

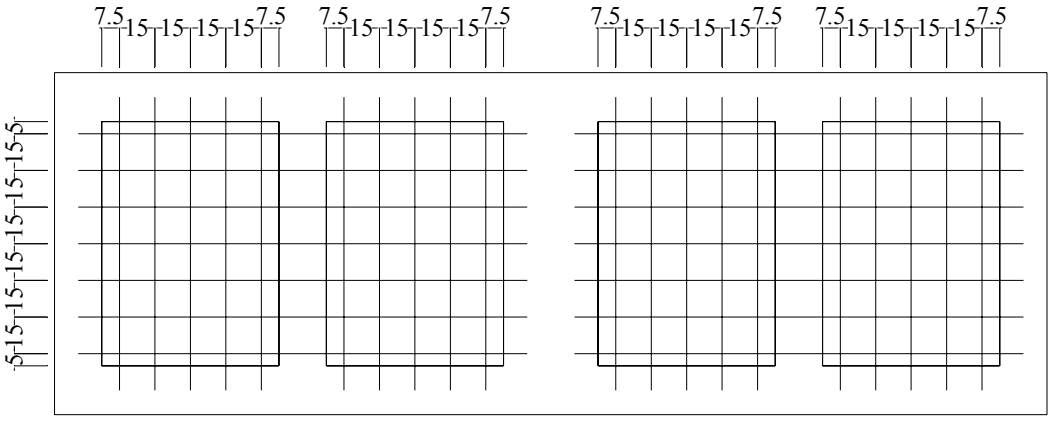

Figure 3.8 - Reinforcement Details for Infill Wall (dimensions in cm)

Figure 3.9 - Frame after Anchorage of Reinforcement

After the curing process of specimen was finished, test specimen was carried carefully and positioned to its exact location in the steel closed frame.

3.5 Concrete Blocks

This research project is a pilot study to explore the potential of using infill walls made of custom shaped and high strength concrete blocks as a simpler and more practical alternative to cast-in-place R/C panels to increase the lateral load bearing capacity of frame structures. These blocks have reasonable size and weight, so they can be carried and installed by one ordinary worker easily.

Blocks of two different geometry and two different strength levels were designed. Rectangular and S-shaped concrete blocks were tested. The thickness of both type blocks was chosen 60 mm. Details of concrete blocks are shown in Figure 3.10. Aim from custom shaped (called S-shaped) geometry is to provide better bonding and improve shear force transfer between concrete blocks. About 160 concrete blocks were used for every specimen.

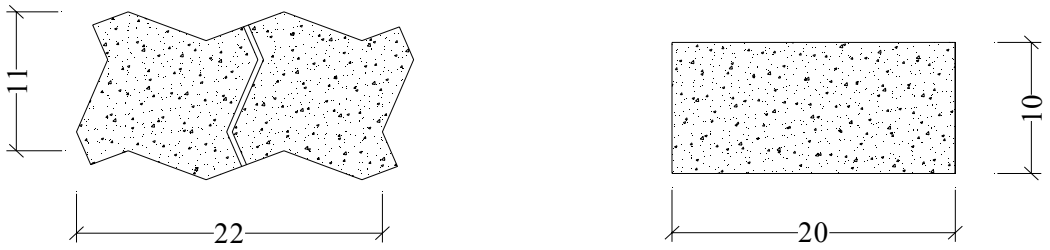

Figure 3.10 - Details of Concrete Blocks (dimensions in cm)

General view of specimens with infill wall made of rectangular and S-shaped concrete blocks are shown in Figure 3.11 and Figure 3.12.

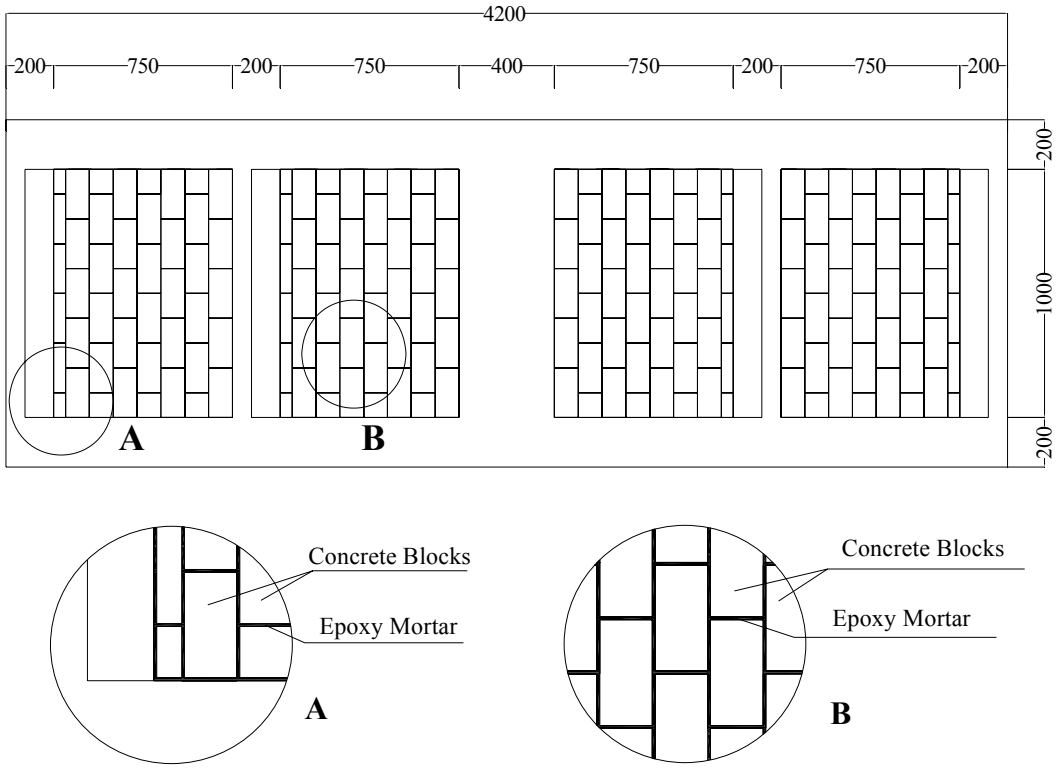

Figure 3.11 - Specimen with Infill Wall Made of Rectangular Concrete Blocks

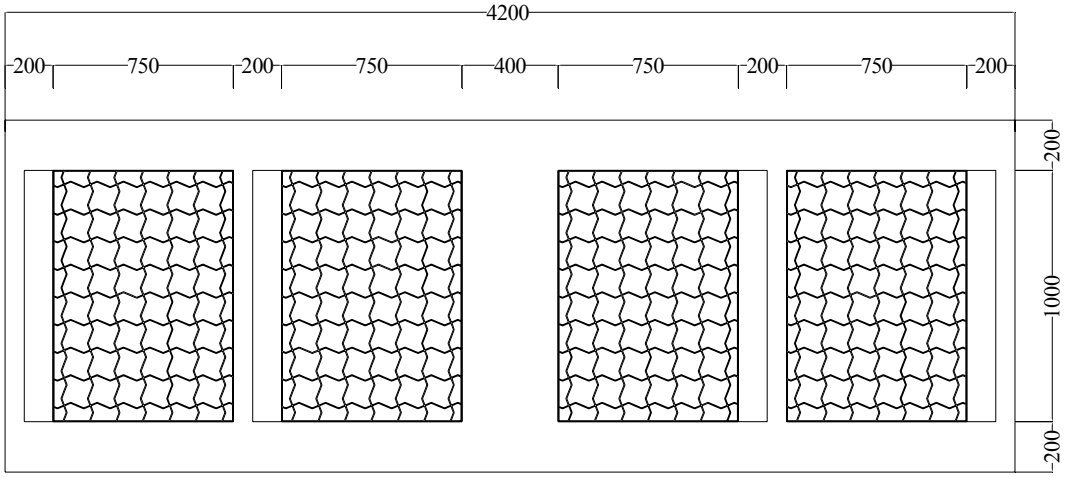

Figure 3.12 - Specimen with Infill Wall Made of S-shaped Concrete Blocks

The concrete blocks were produced from about 5 mm thick forms made of plastic. Since concrete block forms were limited, about 100 concrete blocks were casted at the same time.

Connections of concrete blocks with each other and connections of them with frame were provided by the epoxy mortar called Concresive 1406. Walls made of concrete blocks behaved monolithically by the means of this mortar.

The concrete blocks provide stiffness and strength to the frame and also increase the energy consumption capacity of the frame. Since the adhesive property of epoxy mortar is so strong that out-of-plane deformation of blocks is also prevented.

3.6 FRCM System

To increase lateral load capacity and energy dissipated capacity of moderately damaged specimen (specimen S4), FRCM (Fiber Reinforced Cementitous Matrix) method was used. This system is a kind of high performance fiber structural reinforcement system called FRP.

This system consists of a Polyparaphenylene benzobisoxazale (PBO) mesh and a stabilized inorganic matrix designed to connect the mesh with the concrete surface. Some fibers and mesh properties of this system are given in the commercial catalog by the producer as shown in Table 3.3.

Table 3.3 - Properties of Fiber Reinforced Cementitous Matrix

Mesh weight (g/m^2)	126.0
Equivalent dry fabric thickness (mm)	0.0455
Ultimate tensile stress per unit of width (kN/m)	264.0

3.6.1 Application of FRCM System

To observe the effectiveness of FRCM system on damaged structures, FRCM system was applied on damaged specimen S4.

Before application of FRCM system, dust, loose parts, etc. on infills of damaged specimen S4 were removed. Then, a pre-mixed mortar of cement called Exocem FP was applied on both surfaces of the infills. In the following day, infills were saturated with water and a kind of adhesive called X Mesh M750 was applied on the surfaces of infills with a smooth metal trowel in a layer about 2-3 mm thick. After a couple of minutes, X Mesh system was buried in it. To increase the effectiveness of X Mesh application, X Mesh was also sticked to beams and columns beside infills. The details of X Mesh are shown in Figure 3.13. Finally, a second layer of X Mesh M750 about 2-3 mm thick was applied to cover the mesh completely.

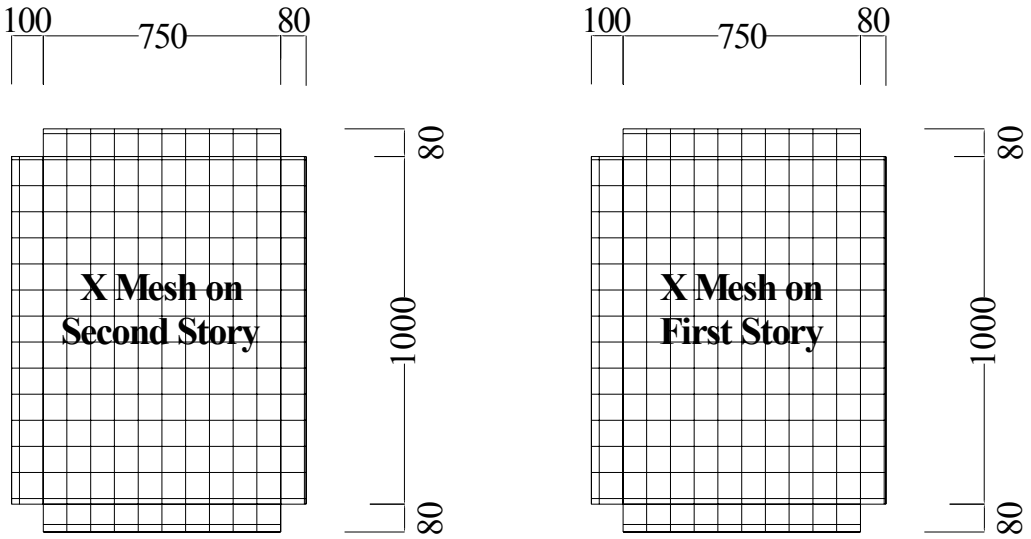

Figure 3.13 - Details of X Mesh on Infills (dimensions in mm)

3.7 Materials

3.7.1 Concrete

Ready mix concrete was used for concrete of the frames and the target compressive strength of the frame concrete was 20 MPa. Concrete of the blocks was produced in the Materials of Construction Laboratory of METU. Since concrete block forms were limited, concrete of the blocks was cast in 6 times. The target compressive strengths of the concrete blocks were 30 MPa for specimen S3 and S4 and 70 MPa for specimen S5 and S6. Mix proportions of concrete for blocks are given in Table 3.4. Materials used in the mix design are given by weight for 1 m^3 of concrete.

Table 3.4 - Mix Design of Concrete Blocks (for 1 m^3 of concrete)

	C30		C70	
	Weight (kg)	Weight (%)	Weight (kg)	Weight (%)
Cement	250	10.7	500	20.9
Fly ash	250	10.7	200	8.4
Silica fume	0	0.0	50	2.1
Water	188	8.0	175	7.3
No.1 Aggregate	742	31.6	649	27.2
No.2 Aggregate	247	10.5	216	9.0
No.3 Aggregate	247	10.5	216	9.0
No.4 Aggregate	412	17.6	360	15.1
Glenium	10	0.4	20	1.0
Total	2346	100	2387	100

Samples were taken during casting to determine the compressive strength of the concrete. The samples were kept under same conditions as the specimens. After 7 and 28 days, they were tested for axial compression. Test results for frames and concrete blocks are given in Table 3.5 and 3.6, respectively.

Table 3.5 - Cylinder Test Results for Frames

Specimen	f_{c7} (average) (kgf/cm^2)	f_{c28} (average) (kgf/cm^2)
S1	207.0	294.3
S2	230.0	276.0
S3	197.0	285.7
S4	201.0	307.0
S5	229.0	312.0
S6	147.3	254.0

Table 3.6 - Cylinder Test Results for Concrete Blocks

Cast	f_{c7} (average) (kgf/cm^2)	f_{c28} (average) (kgf/cm^2)
1	259.1	468.4
2	188.8	407.6
3	348.4	384.3
4	392.6	562.7
5	469.9	712.6
6	432.3	686.1

3.7.2 Steel

For each beam, four ϕ8 and two ϕ14, for each column, four ϕ14 deformed bars were used. In members of the frames, ϕ8 deformed bars were used as stirrups. In foundation beam, six ϕ14 deformed bars were used as longitudinal reinforcement. Some properties of reinforcing bars are given in Table 3.7.

Table 3.7 - Properties of Reinforcing Bars

Bar Diameter ϕ (mm)	Property	Yield Strength f_y (MPa)
8	Deformed	420
14	Deformed	420
14	Deformed	420
14	Deformed	420
8	Deformed	420

3.7.3 Epoxy Mortar

Concresive 1406 epoxy mortar was used for bonding the concrete blocks to each other and to frame. Concrete blocks bonded to each other with epoxy mortar were tested for axial compression. Test results showed that the bond between the blocks was so strong that failure was due to crushing of blocks (Figure 3.14). Walls made of concrete blocks behaved monolithically by the means of this mortar. Concresive 1406 is a preferred adhesive for concrete repair works, anchorage works and fitting works. The material properties of Concresive 1406 are given in the commercial catalog by the producer as presented in Table 3.8.

Figure 3.14 – Concrete Blocks After the Compression Test

Table 3.8 - Properties of Concresive 1406

Compressive Strength	75 MPa
Tensile Strength	25 MPa
Adhesion (for concrete)	3.5 MPa
Adhesion (for steel)	6.5 MPa

CHAPTER 4

TEST SETUP AND PROCEDURE

4.1 Test Setup

The test setup was built in METU Materials of Construction Laboratory. The setup includes test specimen, a steel closed frame around the specimen, loading system, linear variable displacement transducers, load cells and data acquisition system (Figure 4.1).

Figure 4.1 - Test Setup

The steel closed frame is a kind of loading frame type. In this kind of system, reactions are taken by the frame itself and no load except the weight of the equipment is transmitted to the floor or base. Steel frame also prevents the out-of-plane displacement of the specimen. Figure 4.2 shows a detailed view of the steel closed frame.

Figure 4.2 - Detailed View of the Steel Closed Frame

Since the specimens were tested horizontally, reinforced concrete frames were restrained from both of the end sides of the frames. Steel plates were used to restrain the specimens in closed steel frame. A sketch of the test set up is shown in Figure 4.3 and Figure 4.4.

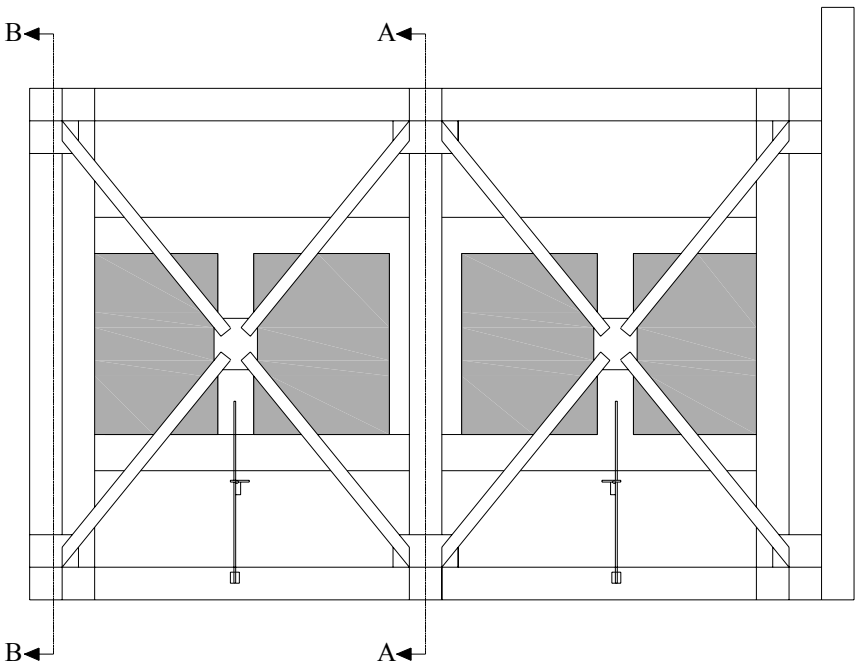

Figure 4.3 - Sketch of the Test Setup

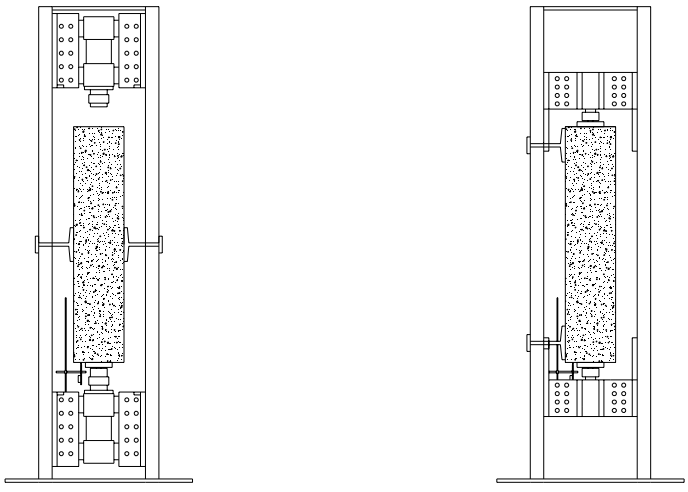

Section A-A Section B-B

Figure 4.4 - Sketch of the Test Setup (Section A-A and B-B)

4.2 Loading System

The loading system attached to the steel closed frame consisted of a load cell, a hydraulic jack and adaptors for connecting the load cell and the hydraulic jack. A photograph of the loading system is given in Figure 4.5. Reversed cyclic lateral loading was applied by two hydraulic jack, both of them were capable of only 500kN in compression. One of them was located at the top and middle of the steel closed frame and the other was located at the bottom and again middle of the steel frame.

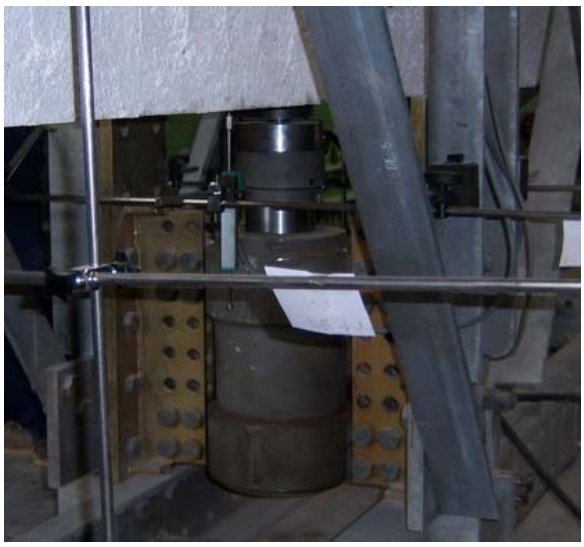

Figure 4.5 - Loading System

The hysteretic loading for modeling ground motion effect was applied at the foundation level, so each of the reinforced concrete frames always takes half of the load. Load sharing between the floor levels is given in Figure 4.6.

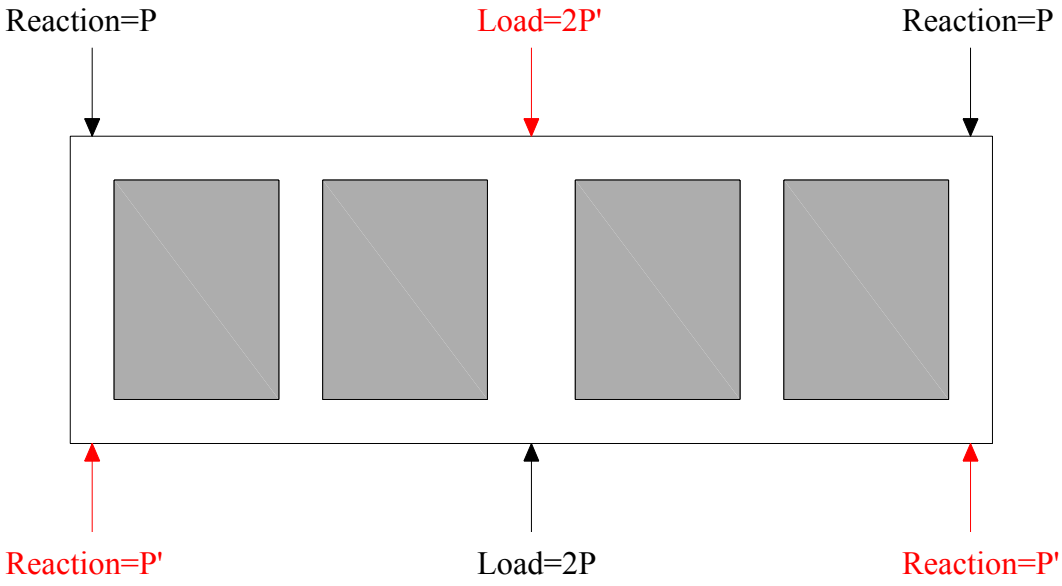

Figure 4.6 - Load Sharing Between the Floor Levels

The load was applied to the frames in two directions. Firstly, load was applied from the bottom of the frame then, from the top of the frame. The axis of the pump was aligned to the centroid of the foundation beam. Steel plates were used to distribute the load to the foundation beam uniformly.

4.3 Instrumentation

During the test, the load was recorded by load cells. In order to record deformations, linear variable displacement transducers (LVDT) were used. The positions of the LVDTs and load cells are shown in Figure 4.7. All data were collected in a personal computer.

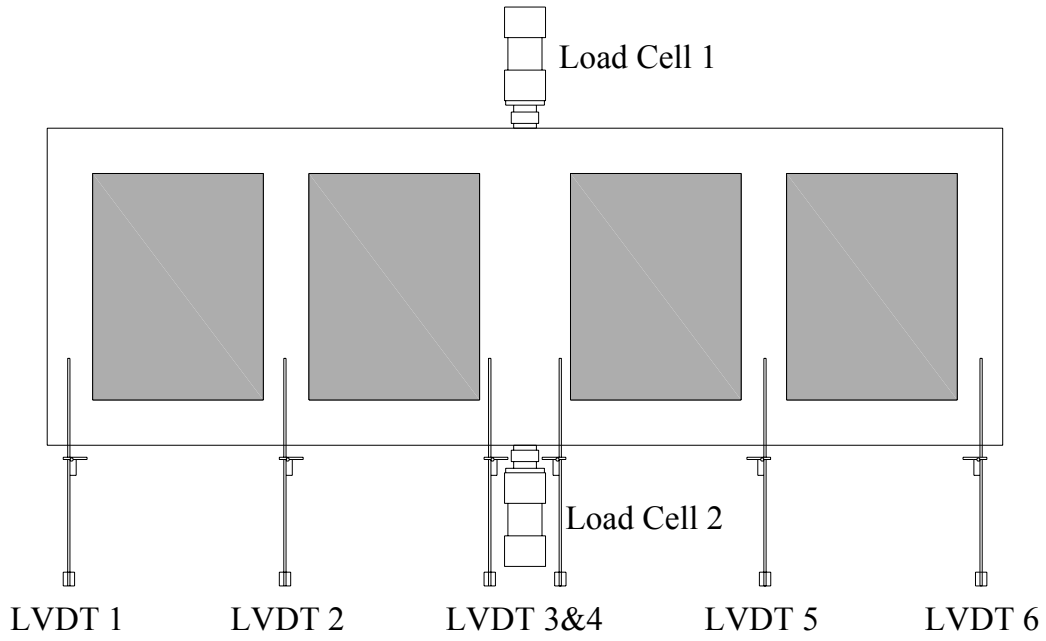

Figure 4.7 - Positions of the LVDTs and Load cells

4.3.1 LVDTs

To measure the deformations of the specimens, LVDTs (linear variable displacement transducers) were used. The LVDT is an instrument that produces an electrical voltage proportional to the displacement of a movable magnetic core. 50 mm, 100 mm and 150 mm measurement capacity LVDTs were used during the tests.

4.3.2 Load Cells

Two load cells were used to measure the load. These load cells have a measurement capacity of up to 500 kN in compression.

4.3.3 Data Acquisition System

Data acquisition system consists of a data logger unit, a personal computer and software. Voltage outputs from the LVDTs and load cells were fed into this system, from which all signals were directed to PC.

4.4 Test Procedure

After the curing process of specimen was finished, test specimen was carried carefully and positioned to its exact location in the steel closed frame. In order to prevent unexpected situations due to eccentricity, alignments and horizontality of specimen was controlled. Then, specimen was tightly fixed to its final location by fastening to the steel frame by steel plates located at the corners of the frame. After the location of the specimen was completed, displacement transducers (LVDTs) were mounted onto the test specimen and their connections to the data acquisition system were established. The calibration of the transducers was re-checked. Before the experiments, concrete cylinder tests were performed to get the compressive strength of the test specimen.

For modeling ground motion effect, all specimens were tested under reversed cyclic lateral loading. Load level was increased gradually at each cycle. During the tests, cracks formed due to loading were observed, marked and necessary notes and also photographs were taken.

CHAPTER 5

TEST RESULTS

5.1 General

In this chapter, test results and experimental observations of the specimens are presented in detail. Photographs are also used for interpreting the critical observations during the tests. In the explanations section, upward cycle term is used for the loading from bottom and downward cycle term is used for the loading from top. The directions are shown in Figure 5.1. For each specimen, the loading history and lateral load-displacement curves are given.

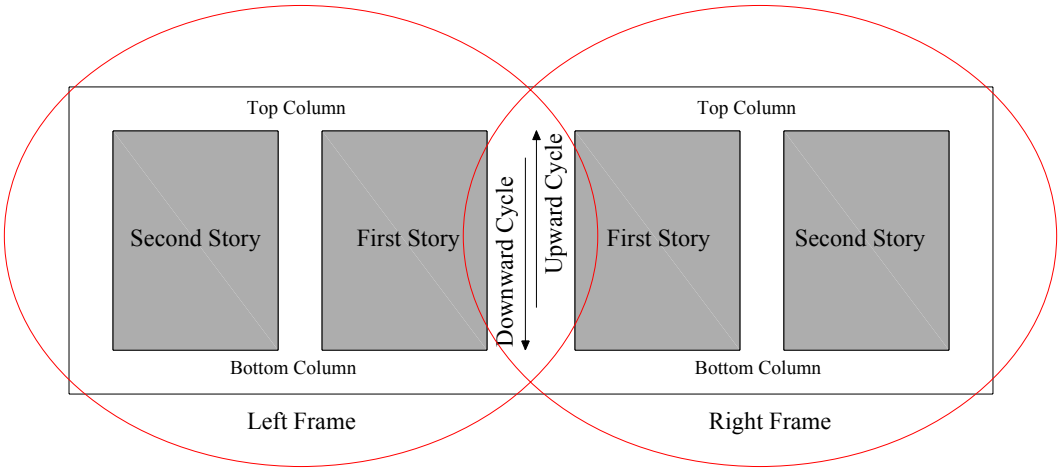

Figure 5.1 - Directions and Names Used for Describing the Observations

5.2 Specimen S1

The specimen S1 was the unstrengthened frame used as reference and represented the present state of a typical frame in an existing building. The test results of this specimen would serve as a reference for the behaviour and capacity of the specimens strengthened by custom shaped high strength concrete masonry blocks.

Specimen S1 was subjected to lateral loading history presented in Figure 5.2. For this specimen, maximum upward and downward loads were 60.1 kN and 64.99 kN, respectively. In Figure 5.3 and Figure 5.4, lateral load-displacement curves are presented for second story and first story, respectively. In order to obtain information about relative displacement between two successive floors, first story and second story drift ratio of the specimen were also drawn in Figure 5.5 and Figure 5.6.

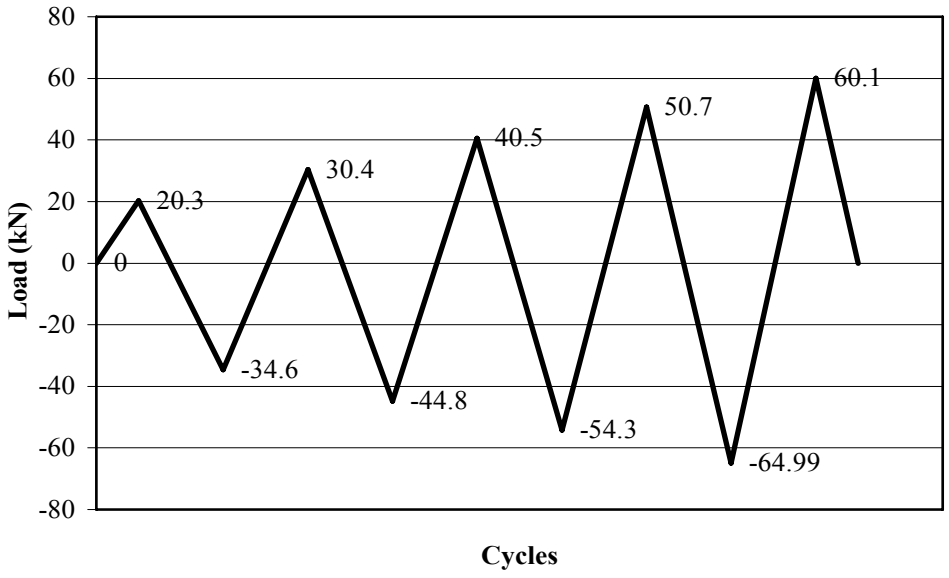

Figure 5.2 - Loading History of Specimen S1

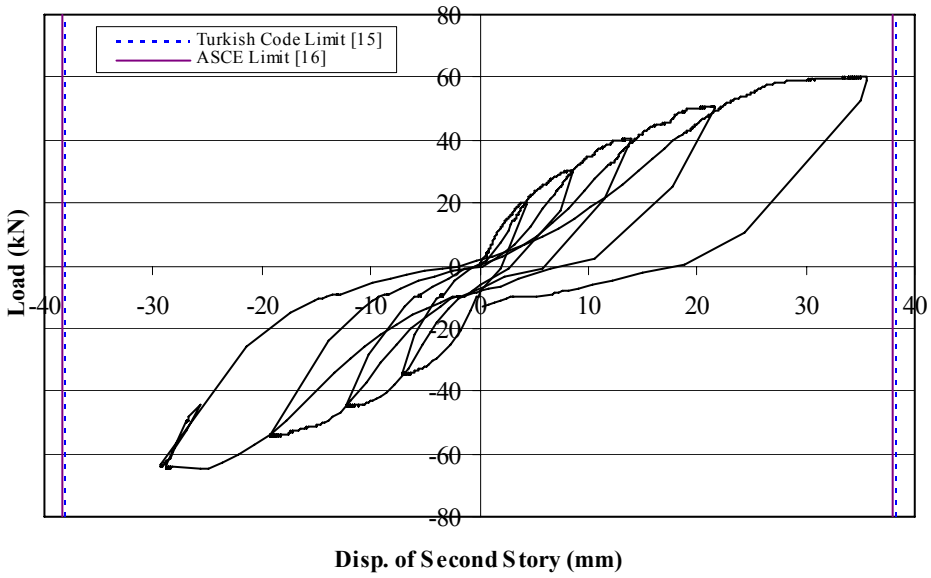

Figure 5.3 - Load – Second Story Level Displacement Curve, Specimen S1

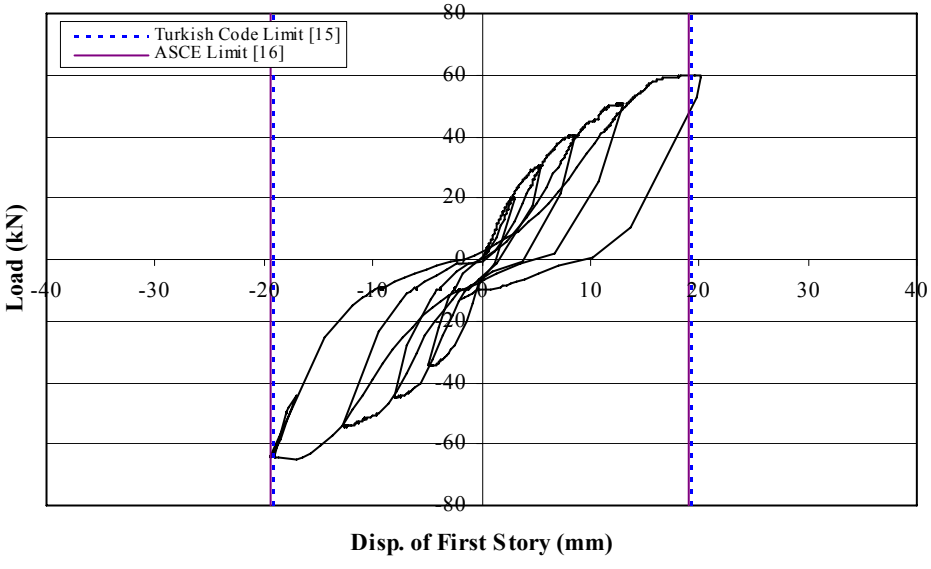

Figure 5.4 - Load – First Story Level Displacement Curve, Specimen S1

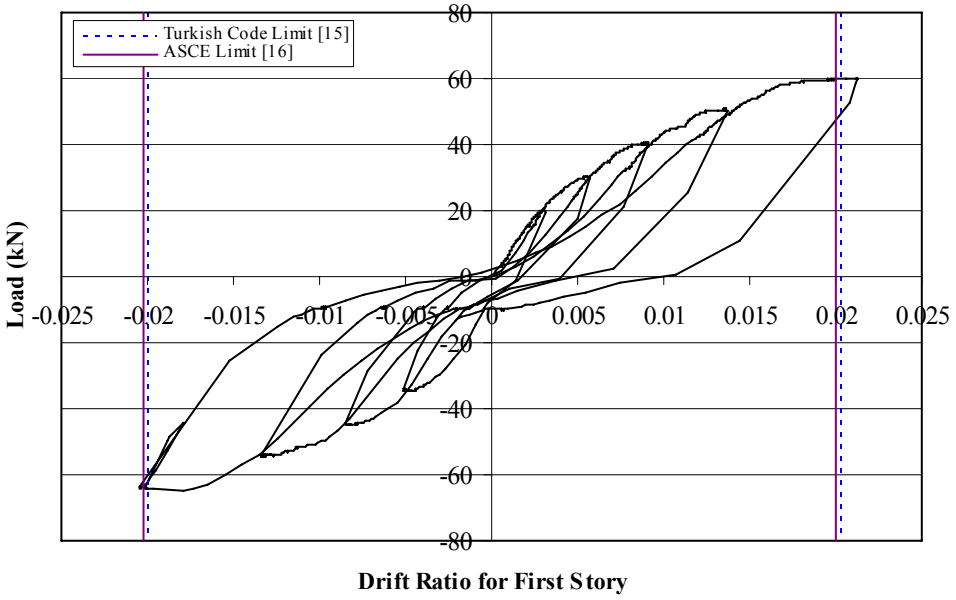

Figure 5.5 - Load – First Story Drift Ratio Curve, Specimen S1

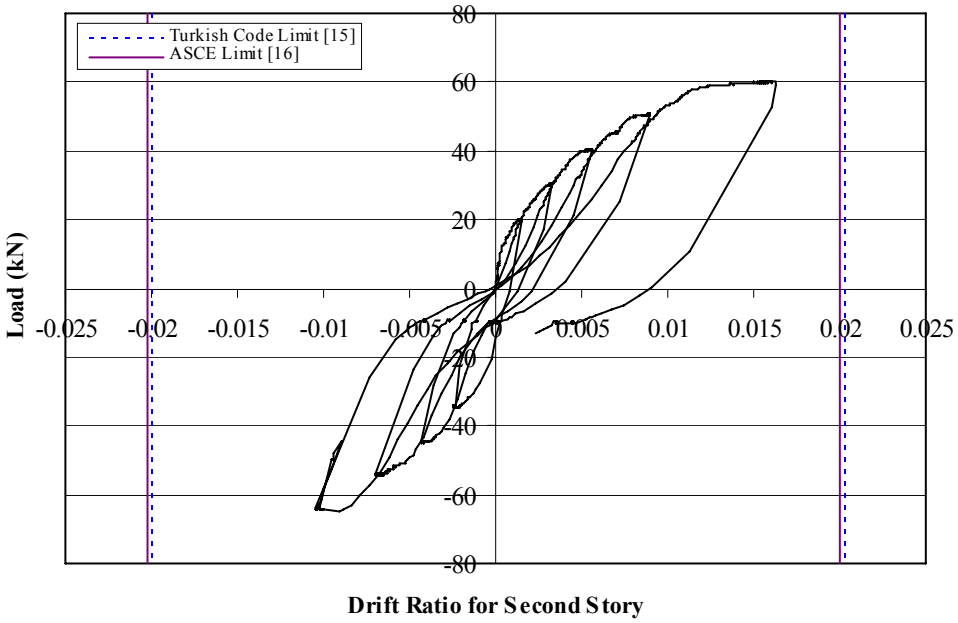

Figure 5.6 - Load – Second Story Drift Ratio Curve, Specimen S1

Important observations during the test are as follows:

- In the first upward half cycle, hairline cracks were formed at the column-foundation beam joints (Figure 5.7). In the next load stage, similar cracks were observed at the column-first story beam joint as shown in Figure 5.8.

Figure 5.7 - Column-Foundation Joint Crack

Figure 5.8 - Column-First Story Beam Joint Crack

- In the second cycle, new cracks appeared at the base of the first story columns and cracks at the joints widened. At this cycle, the maximum load of 44.8 kN was recorded.
- In the third upward half cycle, first cracks were formed at the second story top column-beam joints of frames as shown in Figure 5.9. In the downward half cycle, similar cracks were formed at the opposite joints. In this cycle, second story level displacements reached 14 mm and 19 mm for both half cycles.

Figure 5.9 - Column-Beam Joint Crack at the Second Story Level

- In the fourth cycle, new cracks occurred at the column-beam joints (Figure 5.10). For this full cycle, column bottom cracks reached a width of 4 mm. In this cycle, maximum forward load was recorded and second story level displacement reached 26 mm.

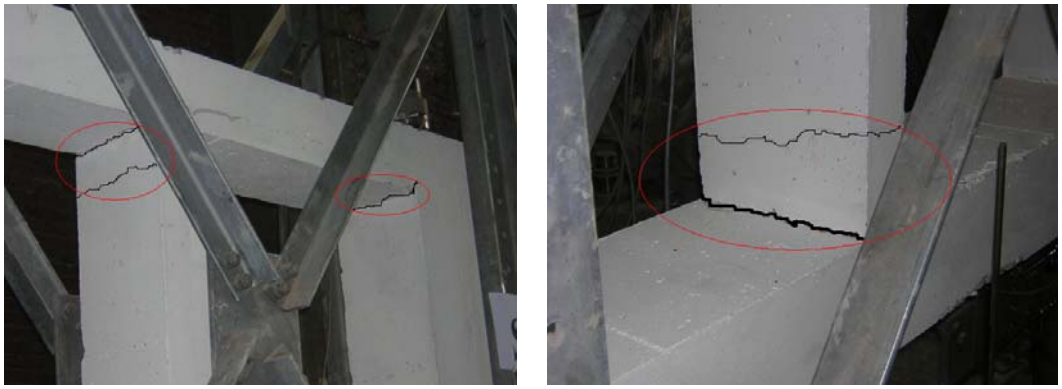

Figure 5.10 - Column-Beam Joint Cracks in the Fourth Cycle

- In the fifth upward cycle, the crushing of columns accelerated. At this cycle, the maximum load of 60.1 kN was recorded. In the fifth downward cycle, the frame could not take any further load due to crushing of the columns. Hence, the test was terminated. The front view photograph of Specimen S1 after the test is given in Figure 5.11.

Figure 5.11 - Specimen S1 After the Test

5.3 Specimen S2

The specimen S2 was the cast-in-place R/C infilled frame used as reference also. This specimen was constructed for comparison. The test results of specimen S2 will be upper limits for this research.

Specimen S2 was subjected to lateral loading history presented in Figure 5.12. For this specimen, maximum upward and downward loads were 262 kN and 276.4 kN, respectively. In Figure 5.13 and Figure 5.14, lateral load-displacement curves are presented for second story and first story, respectively. First story and second story drift ratio of the specimen were also drawn in Figure 5.15 and Figure 5.16.

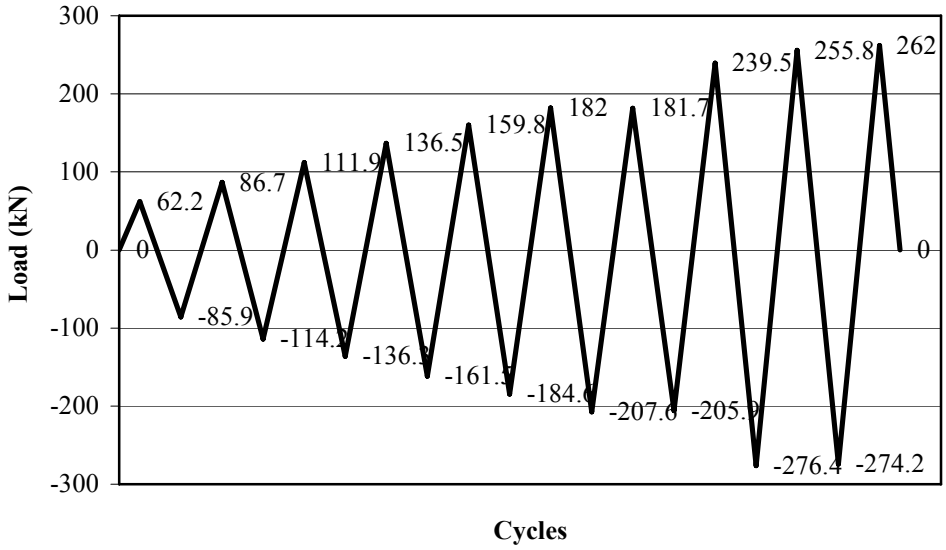

Figure 5.12 - Loading History of Specimen S2

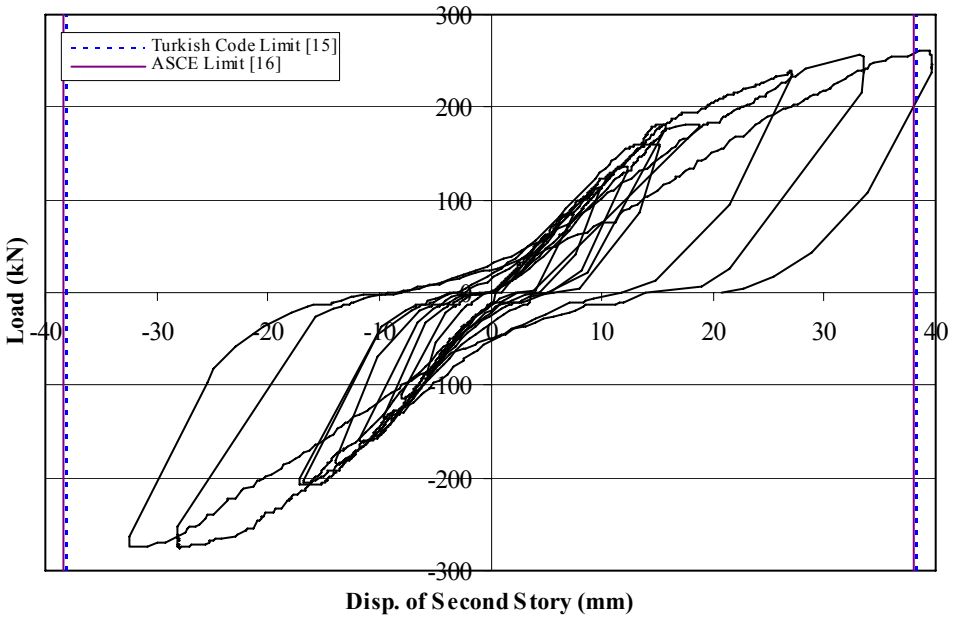

Figure 5.13 - Load - Second Story Level Displacement Curve, Specimen S2

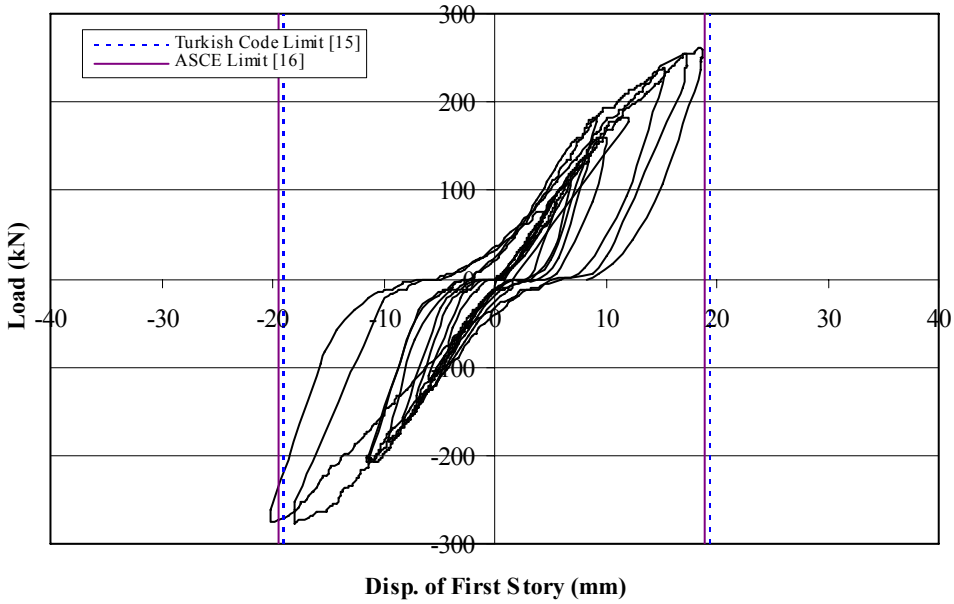

Figure 5.14 - Load - First Story Level Displacement Curve, Specimen S2

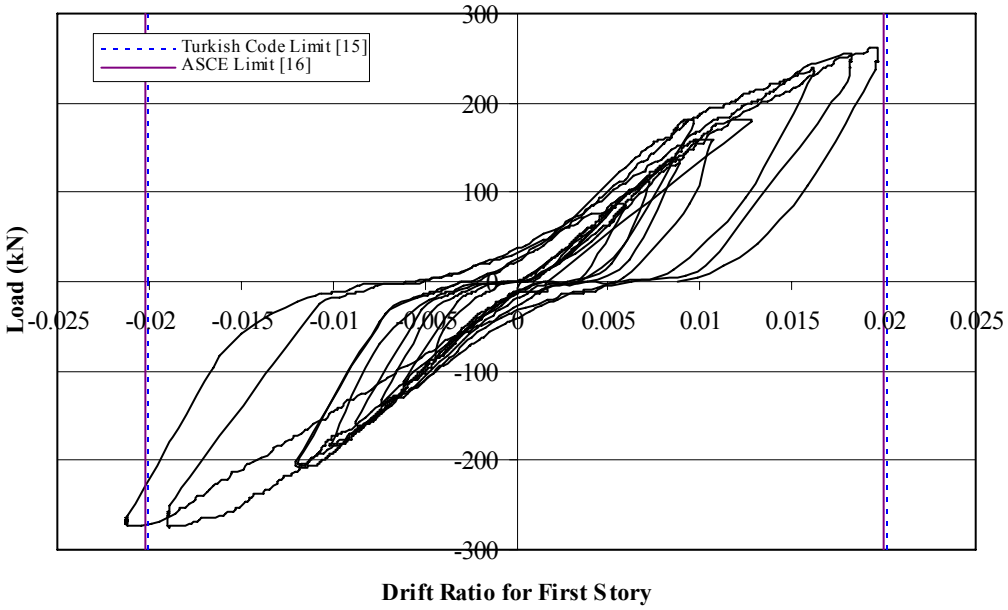

Figure 5.15 - Load - First Story Drift Ratio Curve, Specimen S2

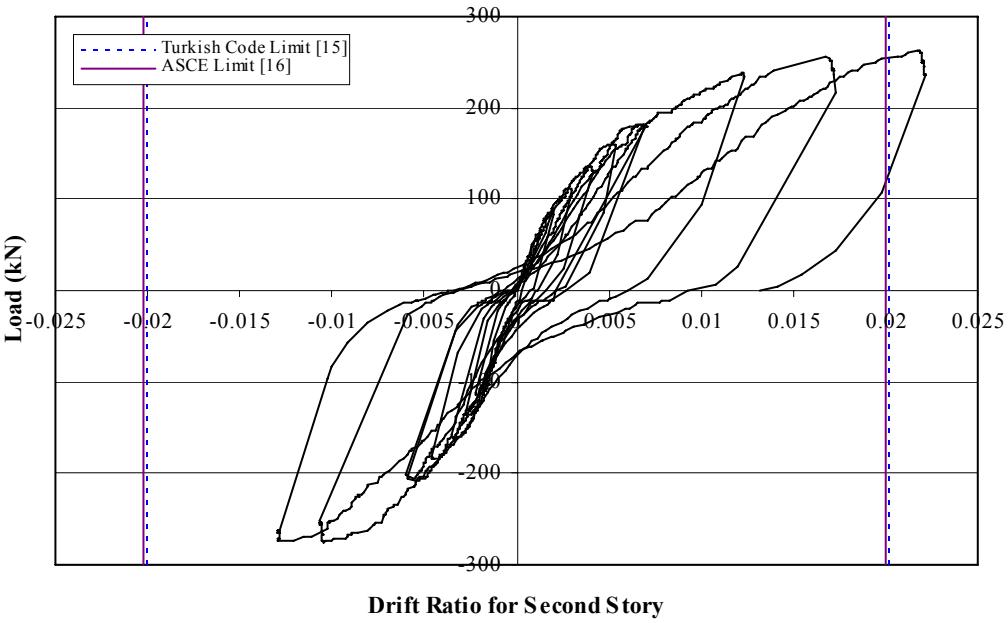

Figure 5.16 - Load - Second Story Drift Ratio Curve, Specimen S2

Important observations during the test are as follows:

- In the first loading cycle, no cracking has occurred.
- In the second upward half cycle, hairline cracks were observed at the base of the top columns. In the next load stage, similar cracks developed on the symmetric columns.
- In the third upward half cycle, first crack was observed on the first story infills. In the downward half cycle, a hairline crack was formed on the first story beam of the left frame and diagonal cracks on the first story infill of the both frames increased in number and length (Figure 5.17)

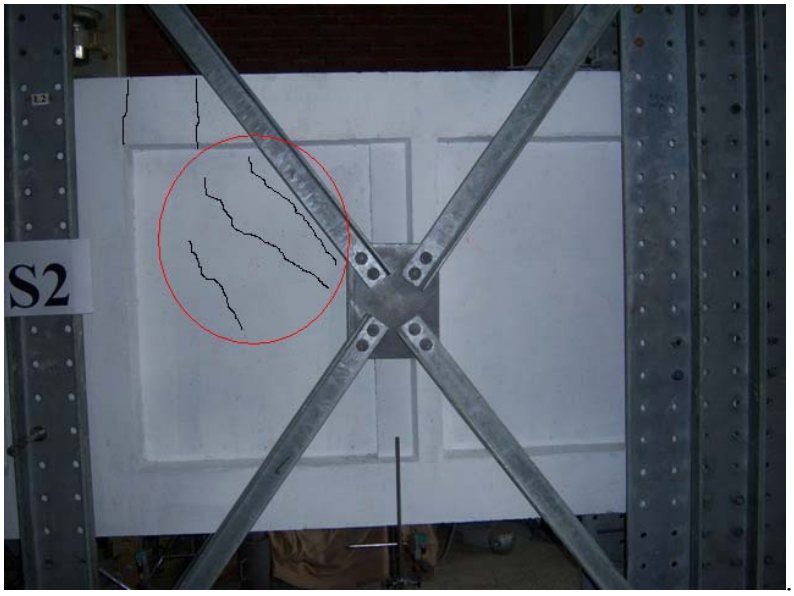

Figure 5.17 – Diagonal Cracks on the First Story Infill Wall

- In the fifth half cycle, Hairline cracks appeared on the second story infill walls. In this cycle, second story level displacements reached 16 mm and 19 mm for both half cycles. At this cycle, the maximum lateral load was 184.6 kN.

- Column-foundation joint cracks increased in number in the following three cycles. Diagonal cracks increased and formed X marks on the infills. New cracks were observed on the first story column mid-height. In the eighth cycle, the maximum load of the test was recorded as 276.4 kN. The view of the specimen after the eighth cycle is shown in Figure 5.18.

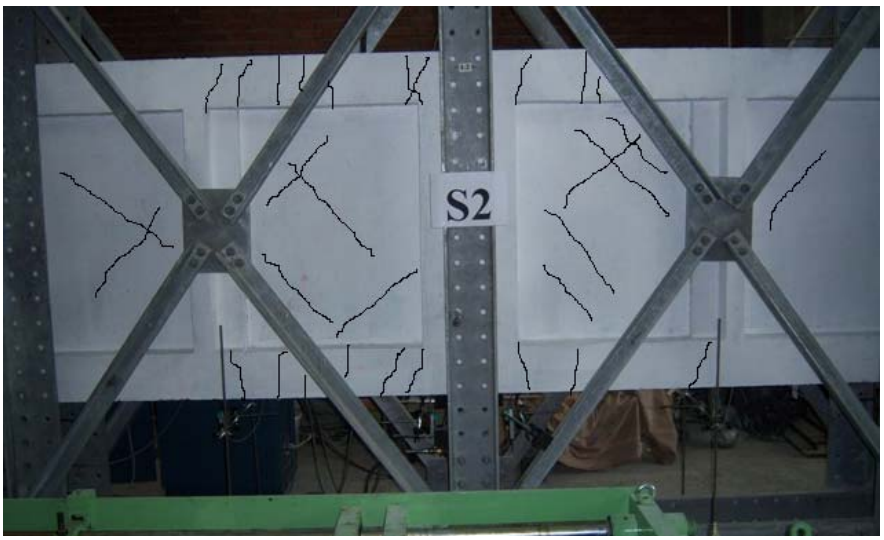

Figure 5.18 – Specimen at the End of the Eighth Cycle

- In the ninth upward half cycle, flexural crack width on the foundation beam-column joints approximated as 5 mm as shown in Figure 5.19. New cracks were observed on the first and second story infill walls. Second story level displacement reached 28 mm in this cycle.

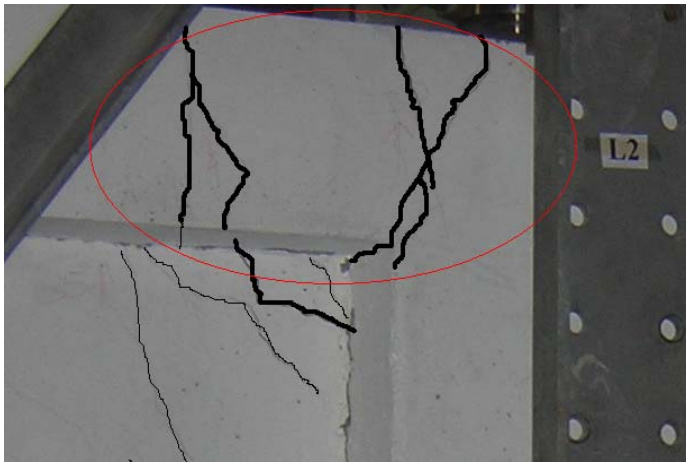

Figure 5.19 – Foundation Beam-Column Joint Cracks

- In the tenth upward half cycle, due to excessive deformations, the loading was stopped at 262.0 kN. The final view of the specimen at the end of the test is shown in Figure 5.20.

Figure 5.20 – Specimen at the End of the Test

5.4 Specimen S3

Specimen S3 was the strengthened frame with infill wall made of 30 MPa strength and custom shape concrete blocks. The reason why custom shaped (called S-shaped) geometry was used is to provide better bonding and improve shear force transfer between concrete blocks.

Specimen S3 was subjected to lateral loading history presented in Figure 5.21. For this specimen, maximum upward and downward loads were 185.6 kN and 206.8 kN, respectively. In Figure 5.22 and Figure 5.23, lateral load-displacement curves are presented for second story and first story, respectively. First story and second story drift ratio of the specimen were also drawn in Figure 5.24 and Figure 5.25.

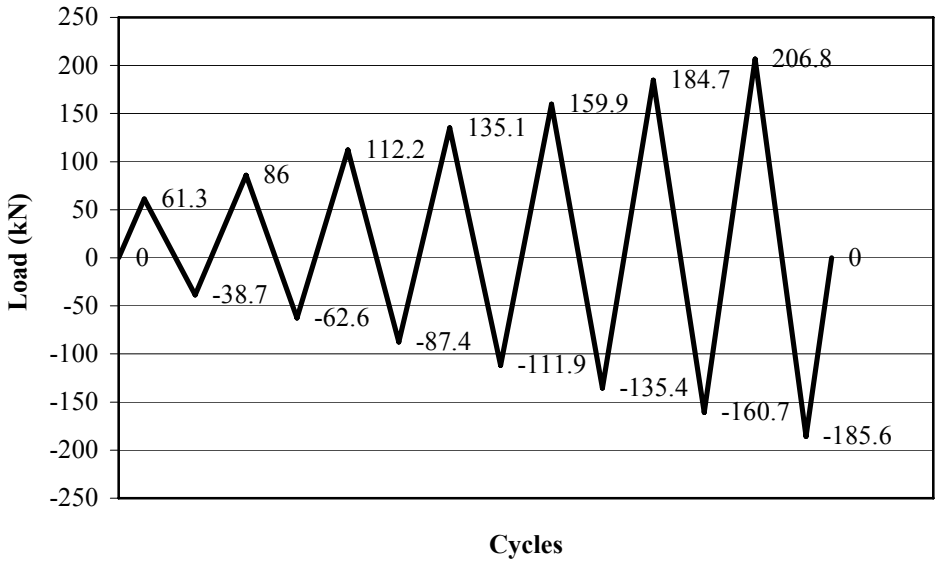

Figure 5.21 - Loading History of Specimen S3

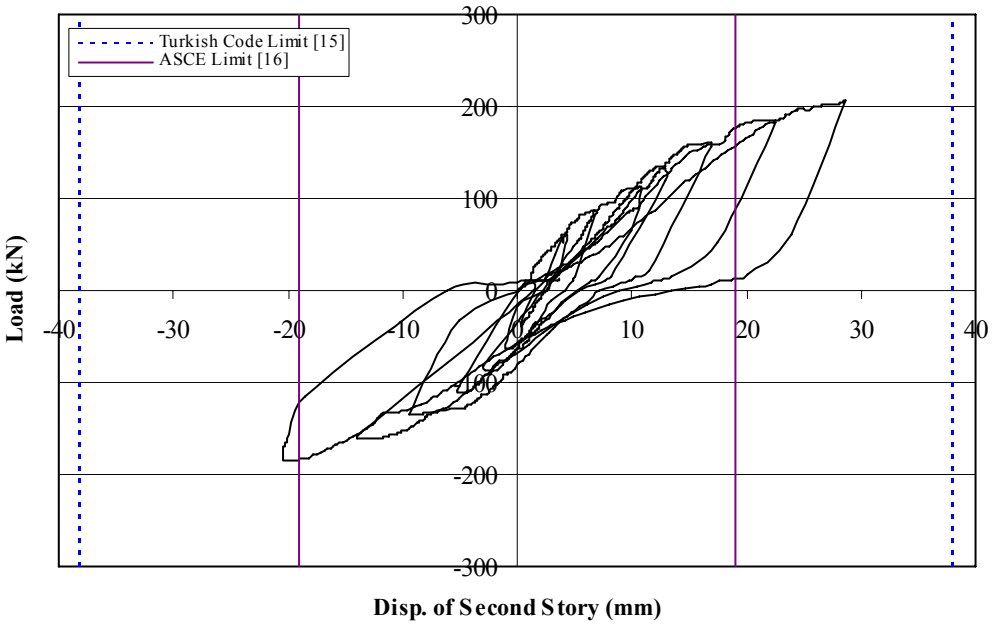

Figure 5.22 - Load – Second Story Level Displacement Curve, Specimen S3

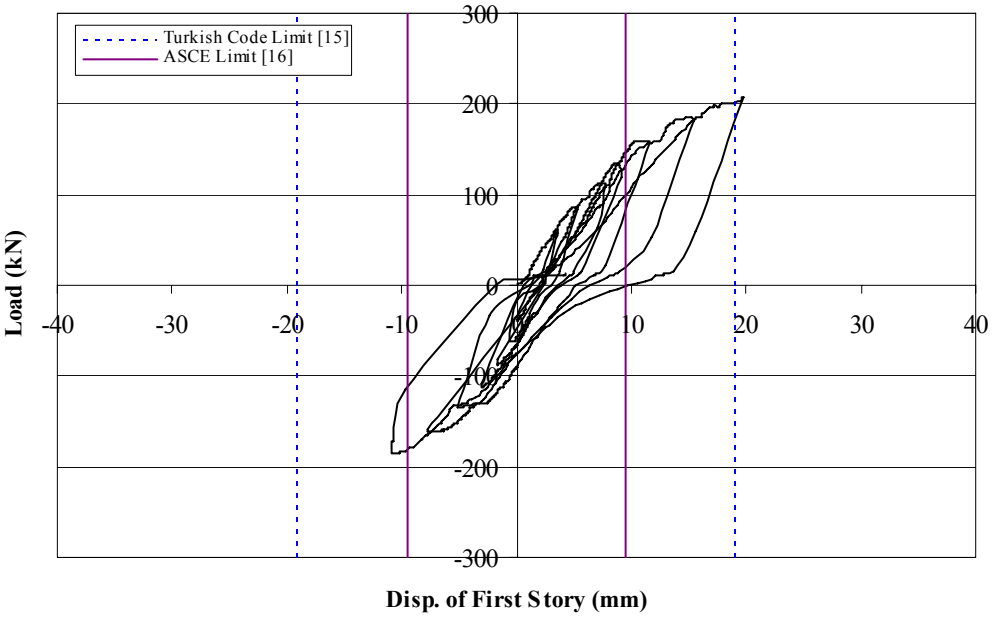

Figure 5.23 - Load – First Story Level Displacement Curve, Specimen S3

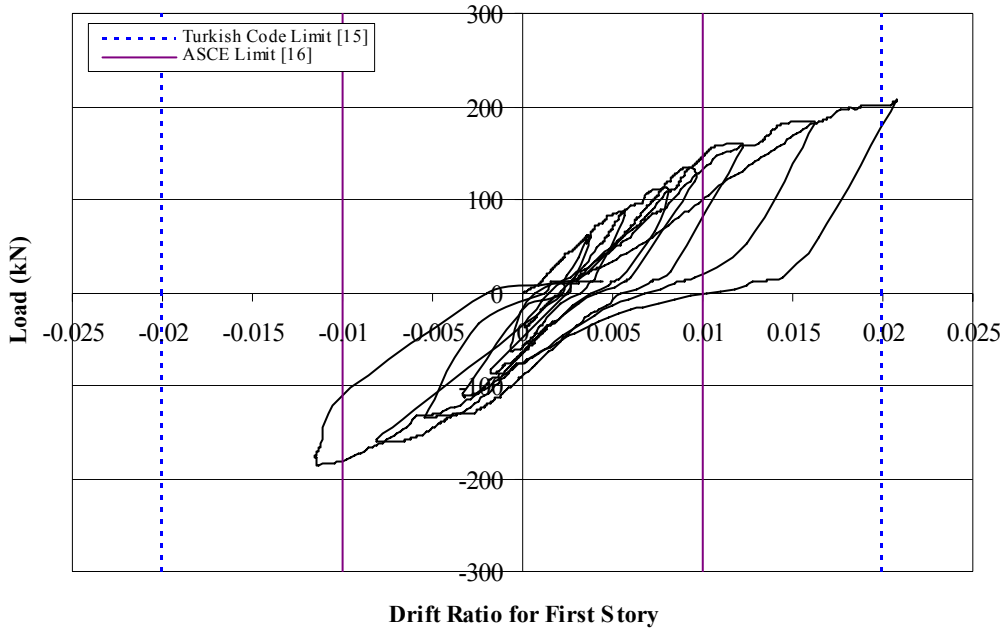

Figure 5.24 - Load – First Story Drift Ratio Curve, Specimen S3

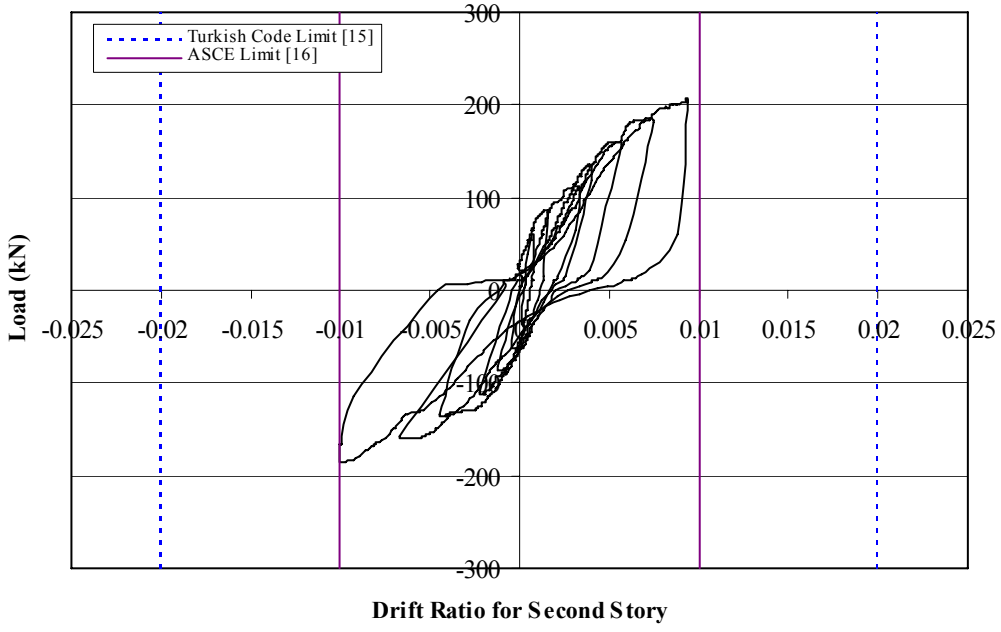

Figure 5.25 - Load – Second Story Drift Ratio Curve, Specimen S3

Important observations during the test are as follows:

- In the first loading cycle, no cracking has occurred.
- In the second downward half cycle, hairline cracks appeared at the base of the bottom column (Figure 5.26). In the next load stage, this was the second upward half cycle, similar cracks developed at the opposite column. At this cycle, the maximum load of 86.0 kN was recorded.

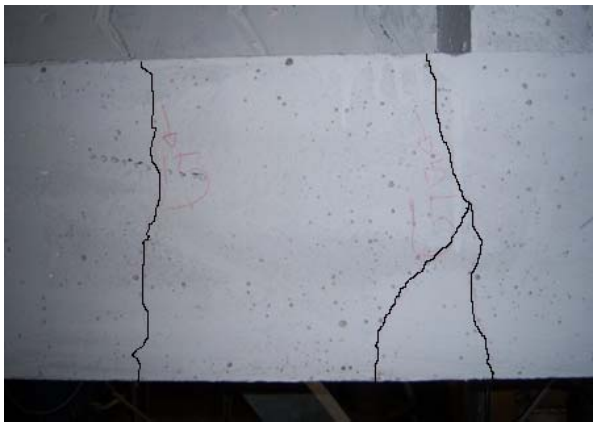

Figure 5.26 - Hairline Cracks on the Column

- Diagonal cracks were observed on the first story infills in the third downward half cycle. Column cracks also widened in this cycle.
- The crack width on the first story infills approximated as 1 mm in the fourth downward half cycle (Figure 5.27). New diagonal cracks were formed on the first story infill walls. Maximum lateral load of 135.1 kN was observed in the fourth cycle.

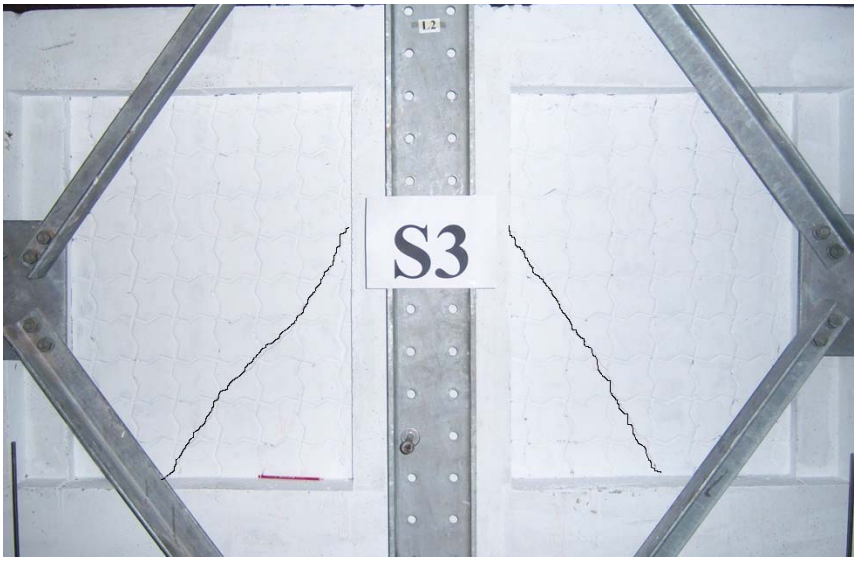

Figure 5.27 - Diagonal Cracks on the First Story Infills

- In the fifth downward half cycle, hairline cracks were observed on the first story beams. The diagonal cracks on the first story infill walls narrowed down and sometimes diminished while unloading and reloading the system. Separation of the first story infills along the column edges started in the upward half cycle.
- Diagonal cracks were formed on the second story infill of right frame in the sixth downward half cycle. Cracks formed X marks on the infill. Some diagonal cracks grew as wide as 3 mm and as long as 350 mm. Large cracks were observed on the base of the columns.
- In the seventh downward half cycle, diagonal crack width on the second story infills of both frames approximated as 4 mm. The number of cracks on the first story columns increased so much. The maximum lateral load of the test was recorded as 206.8 kN. In the upward cycle, both columns developed many cracks again and their deformation was noticeable. Due to excessive damage, the experiment was ended at the end of this cycle. The final view of the specimen from the front is given in Figure 5.28.

Figure 5.28 - Specimen S3 at the End of the Test

5.5 Specimen S4

Specimen S4 was the strengthened frame with infill wall made of 30 MPa strength and rectangular shape concrete blocks. Construction and application of these blocks was easier and more practical than that of S-shaped blocks.

Specimen S4 was subjected to lateral loading history presented in Figure 5.29. For this specimen, maximum upward and downward loads were 182.0 kN and 205.3 kN, respectively. In Figure 5.30 and Figure 5.31, lateral load-displacement curves are presented for second story and first story, respectively.

First story and second story drift ratio of the specimen were also drawn in Figure 5.32 and Figure 5.33.

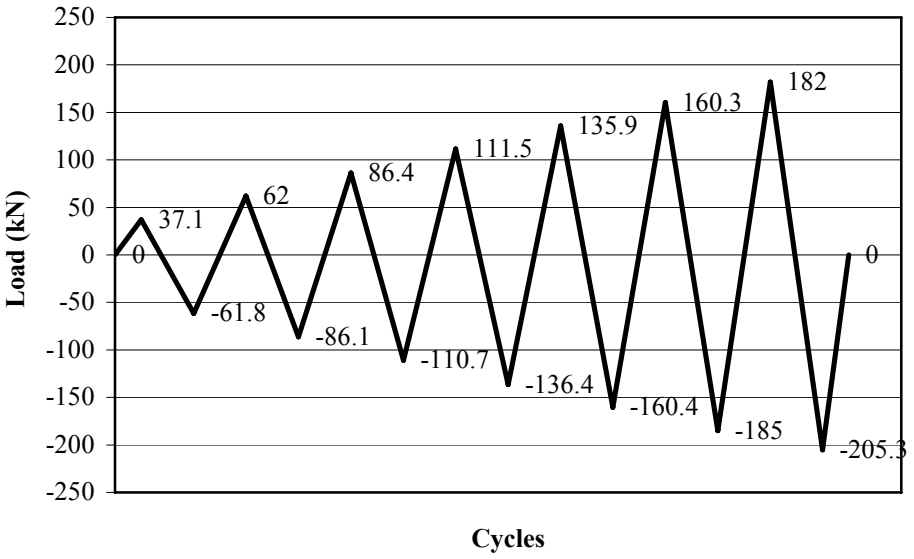

Figure 5.29 - Loading History of Specimen S4

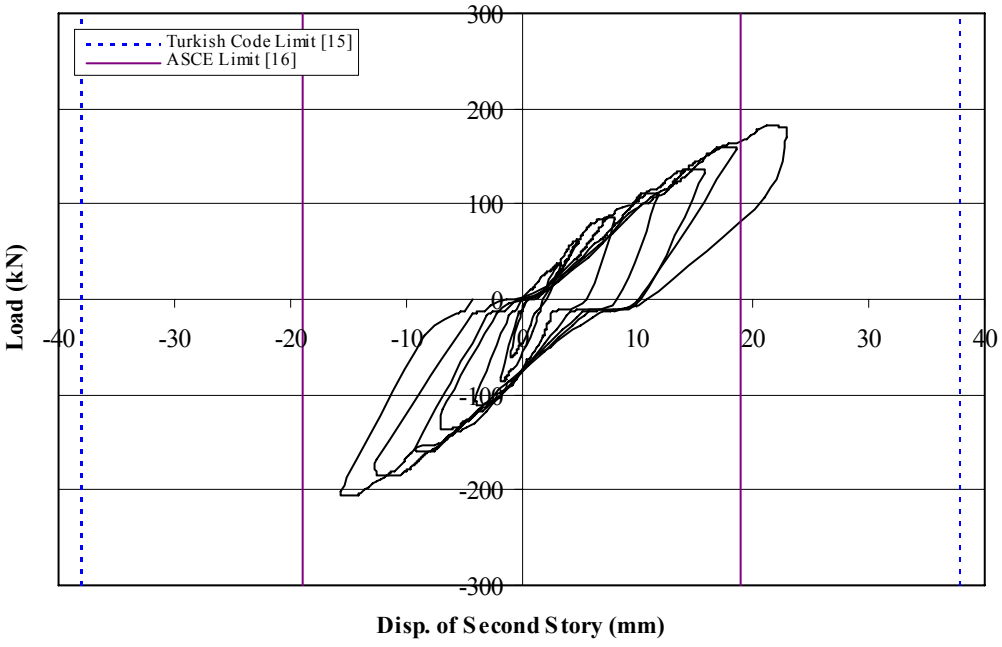

Figure 5.30 - Load – Second Story Level Displacement Curve, Specimen S4

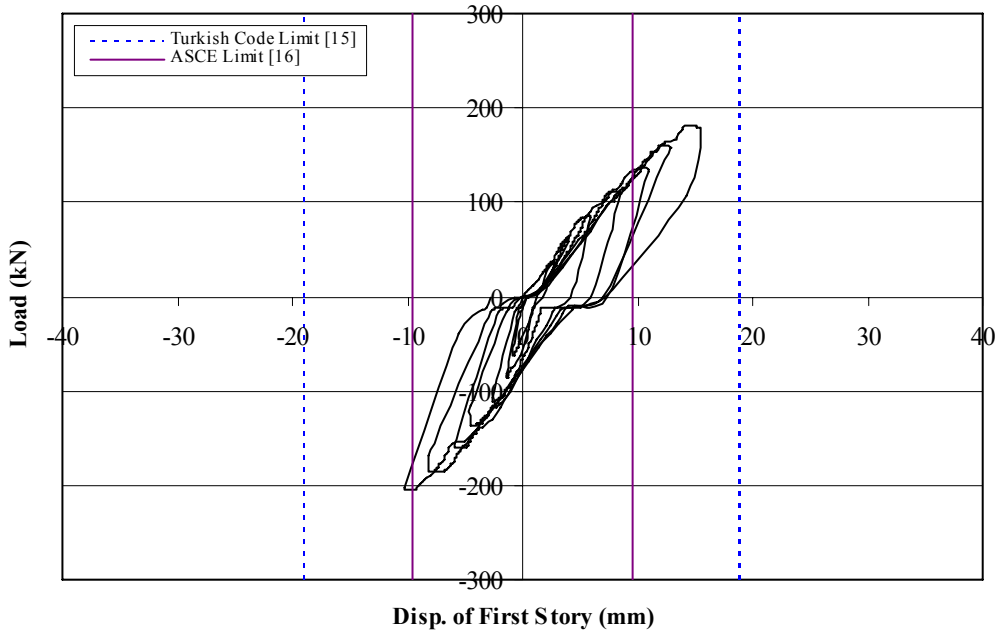

Figure 5.31 - Load – First Story Level Displacement Curve, Specimen S4

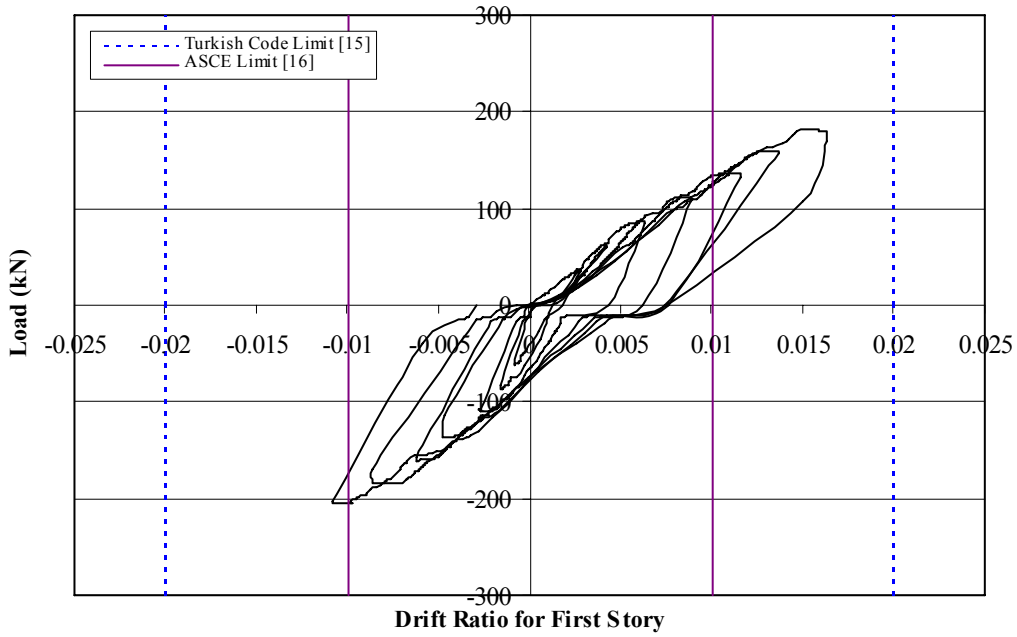

Figure 5.32 - Load – First Story Drift Ratio Curve, Specimen S4

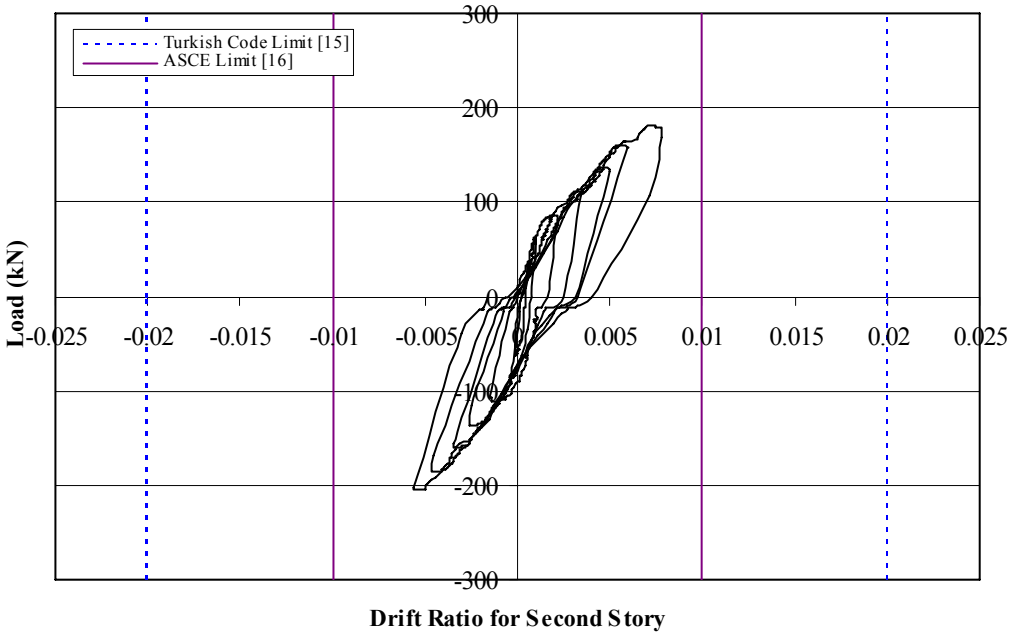

Figure 5.33 - Load – Second Story Drift Ratio Curve, Specimen S4

Important observations during the test are as follows:

- In the first two loading cycle, no cracking has occurred.
- In the third upward half cycle, hairline cracks started to form at the base of the lower column and on the first story infill wall of the right frame. In the next load stage, similar cracks developed on the symmetric infill. Diagonal crack shapes on the first story infill of the left frame may be seen in Figure 5.34. At this cycle, the maximum load of 110.7 kN was recorded.

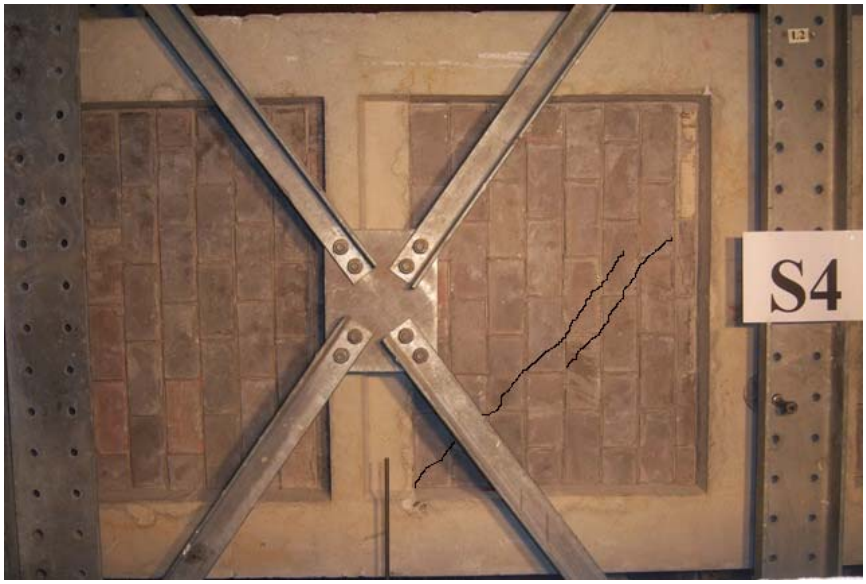

Figure 5.34 - Diagonal Cracks in the Third Cycle

- New diagonal cracks appeared on the first story infills in the fourth upward half cycle. Hairline cracks formed on the second story infill wall of the right frame. Formed cracks widened especially for the right frame. New cracks were observed on the first story column mid-height. In the downward half cycle, diagonal cracks on the first story infill of the left frame increased in number and length. Hairline cracks appeared on the second story infill wall of the left frame also.
- In the fifth upward half cycle, crack width on the first story infills approximated as 1 mm. In this cycle, new cracks were observed on the first story infills. At this cycle, the maximum lateral load was 160.4 kN.
- Column-foundation joint cracks increased in number in the sixth upward half cycle. Some diagonal cracks grew as wide as 2 mm (Figure 5.35). In the next load stage, cracks formed at the beam-column joints and on the second story columns of the left frame. Diagonal crack width on the second story infills approximated as 1 mm.

Figure 5.35 - Cracking on the Infill in the Six Cycle

- In the seventh upward half cycle, new cracks were observed on the first story beams and at the second story beam-column joints. Diagonal cracks increased and formed X marks on the infills. Crack width on the beam-column joints approximated as 1 mm. In the seventh backward half cycle, due to excessive deformations, the loading was stopped at 205.3 kN. The final view of the specimen at the end of the test is shown in Figure 5.36.

Figure 5.36 - Final View of the Specimen S4

5.6 Specimen S5

Specimen S5 was the strengthened frame with infill wall made of 70 MPa strength and custom shape concrete blocks. The reason why 70 MPa strength blocks were used for infill is to investigate how strength of the infill affects the capacity of the frame.

Specimen S5 was subjected to lateral loading history presented in Figure 5.37. For this specimen, maximum upward and downward loads were 184.7 kN and 203.5 kN, respectively. In Figure 5.38 and Figure 5.39, lateral load-displacement curves are presented for second story and first story, respectively.

First story and second story drift ratio of the specimen were also drawn in Figure 5.40 and Figure 5.41.

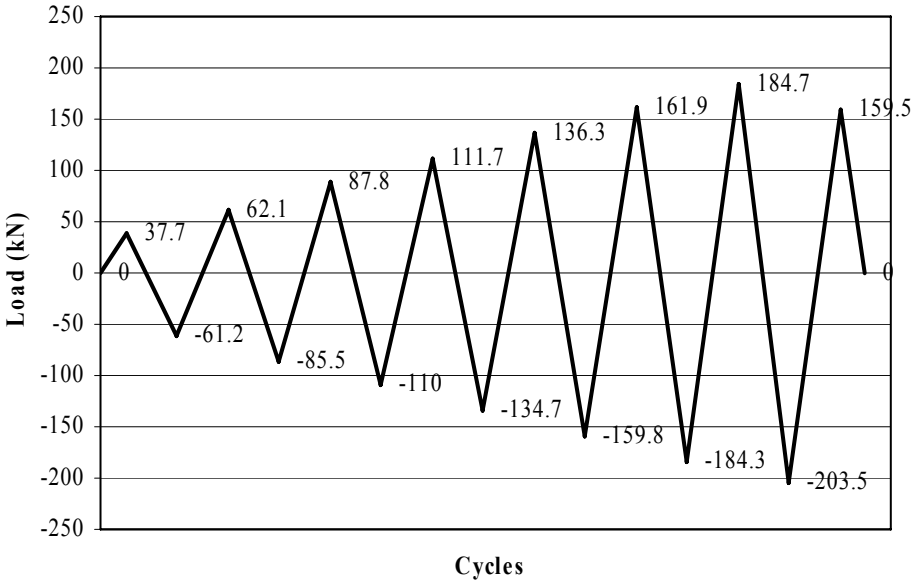

Figure 5.37 - Loading History of Specimen S5

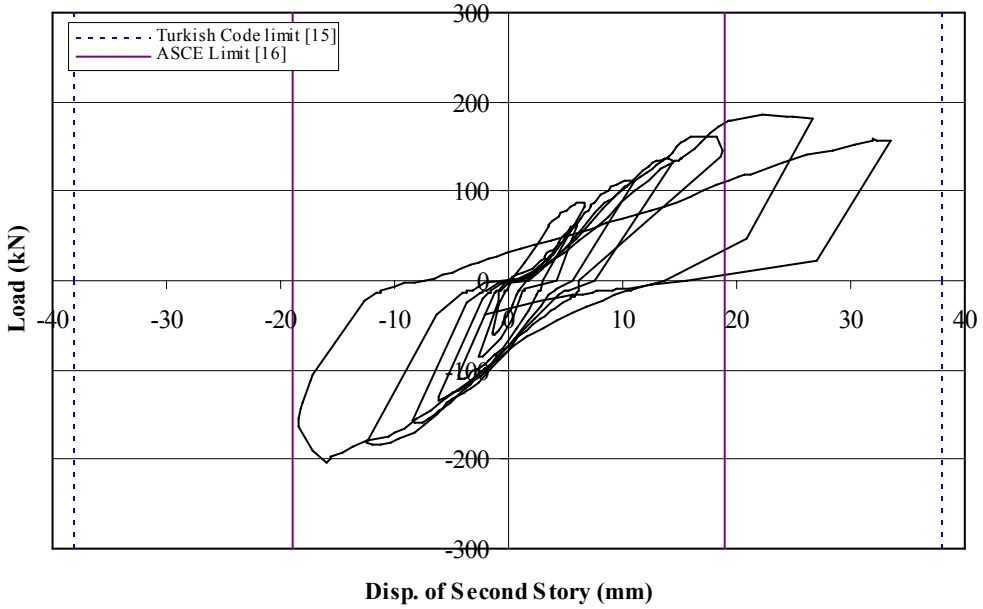

Figure 5.38 - Load - Second Story Level Displacement Curve, Specimen S5

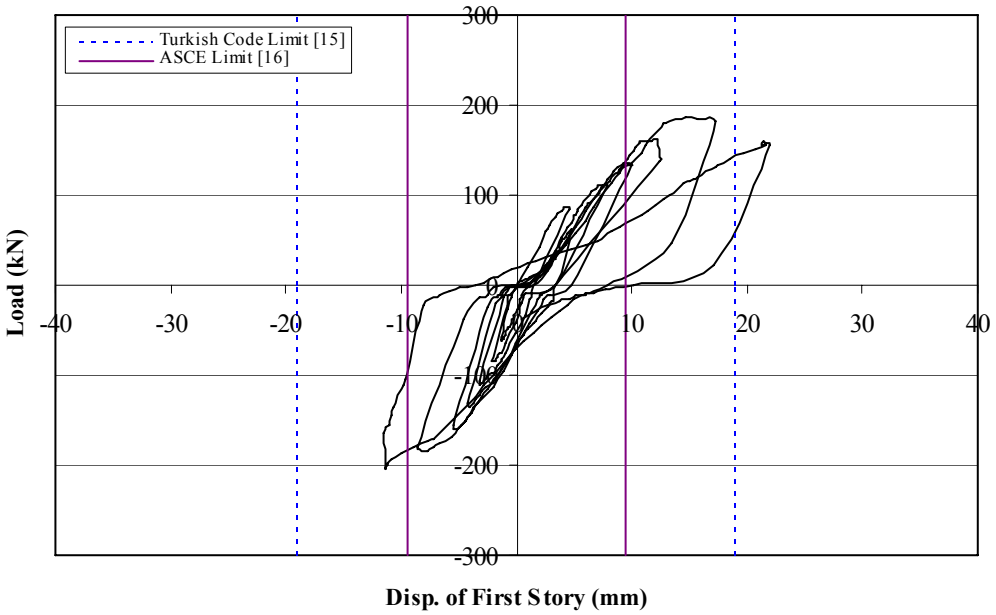

Figure 5.39 - Load - First Story Level Displacement Curve, Specimen S5

Figure 5.40 - Load - First Story Drift Ratio Curve, Specimen S5

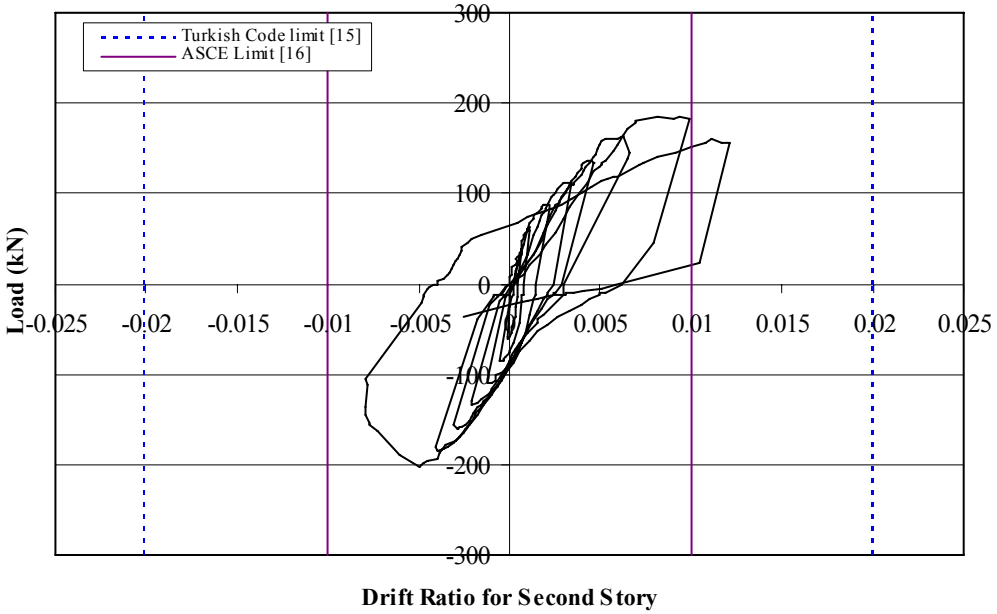

Figure 5.41 - Load - Second Story Drift Ratio Curve, Specimen S5

Experimental observations for this specimen are given below:

- In the first two loading cycle, no cracks were observed on the frame or infills.
- In the third upward half cycle, first hairline crack was observed at the top column-foundation joint of the right frame. Same type of crack was observed at the bottom column-foundation joint of the left frame in the third downward cycle.
- Hairline cracks formed on the first story infills near the top column-foundation joints in the fourth upward half cycle (Figure 5.42). No new cracks were observed on the symmetric frames but the existing cracks widened in the next load stage.

Figure 5.42 - Hairline Crack on the First Story Infill

- In the fifth upward half cycle, some diagonal cracks on the first story infill of the right frame grew as wide as 2 mm. In the downward half cycle, the existing cracks increased in number and length. First hairline crack appeared on the second story infill of the left frame and also, new cracks formed on the first story beam of the right frame in this cycle (Figure 5.43).

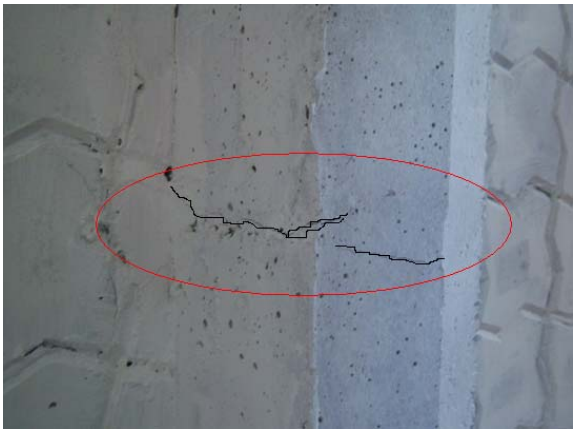

Figure 5.43 - Cracks on the First Story beam of the Right Frame

- In the sixth upward half cycle, cracks on the first story infill of the left frame widened and partial separation between the second story concrete blocks was observed (Figure 5.44). Crushing began at the supports of the left frame (Figure 5.44). In the sixth downward half cycle, first crack formed on the second story infill of the right frame. New diagonal cracks were observed on the second story infill of the left frame.

Figure 5.44 - Separation Between Blocks (left) and Cracks on the Support (right)

- In the seventh upward half cycle, diagonal crack widths on the first and second story infills of the left frame approximated as 6 mm and cracks formed X marks on the infills. In the seventh downward half cycle, second story infill of the left frame was damaged seriously so the test was terminated. The maximum lateral load of 203.5 kN was recorded at this stage. Front view of Specimen 5 after the test is given in Figure 5.45.

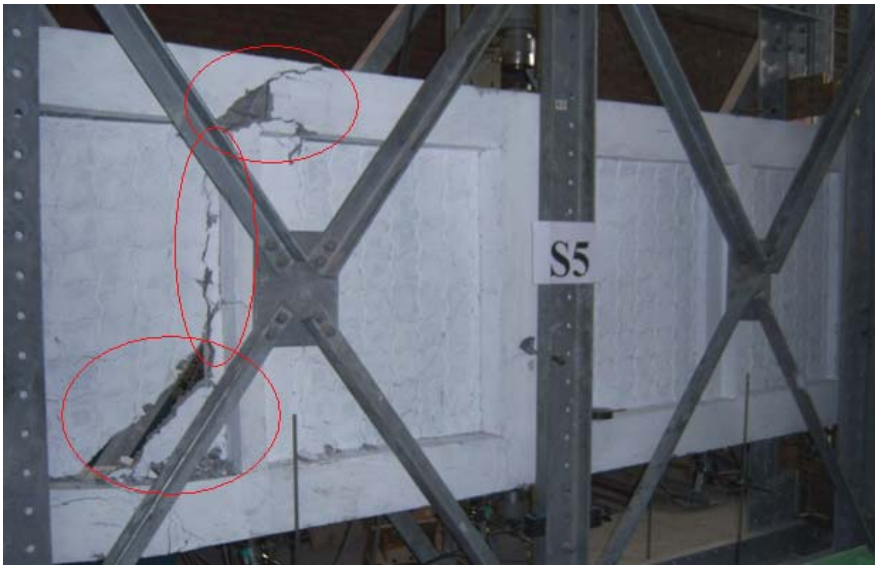

Figure 5.45 - Front View of Specimen S5 after the Test

5.7 Specimen S6

Specimen S6 was the strengthened frame with infill wall made of 70 MPa strength and rectangular shape concrete blocks.

Specimen S6 was subjected to lateral loading history presented in Figure 5.46. For this specimen, maximum upward and downward loads were 186.6 kN and 185.5 kN,

respectively. In Figure 5.47 and Figure 5.48, lateral load-displacement curves are presented for second story and first story, respectively.

First story and second story drift ratio of the specimen were also drawn in Figure 5.49 and Figure 5.50.

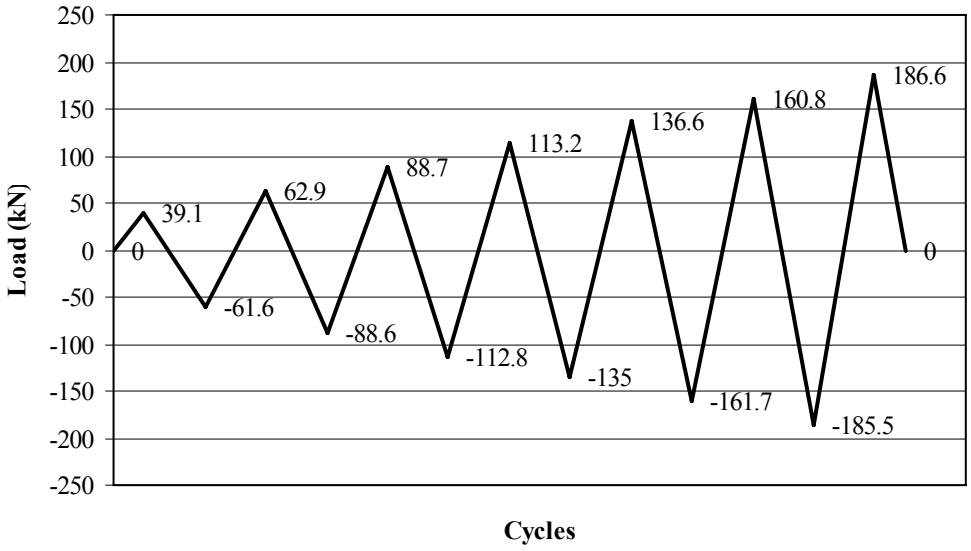

Figure 5.46 - Loading History of Specimen S6

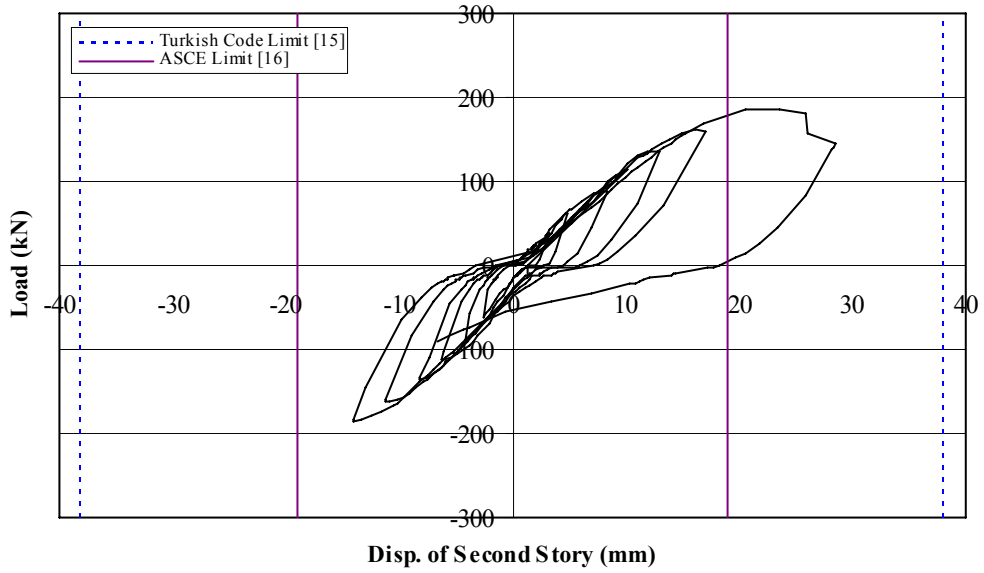

Figure 5.47 - Load – Second Story Level Displacement Curve, Specimen S6

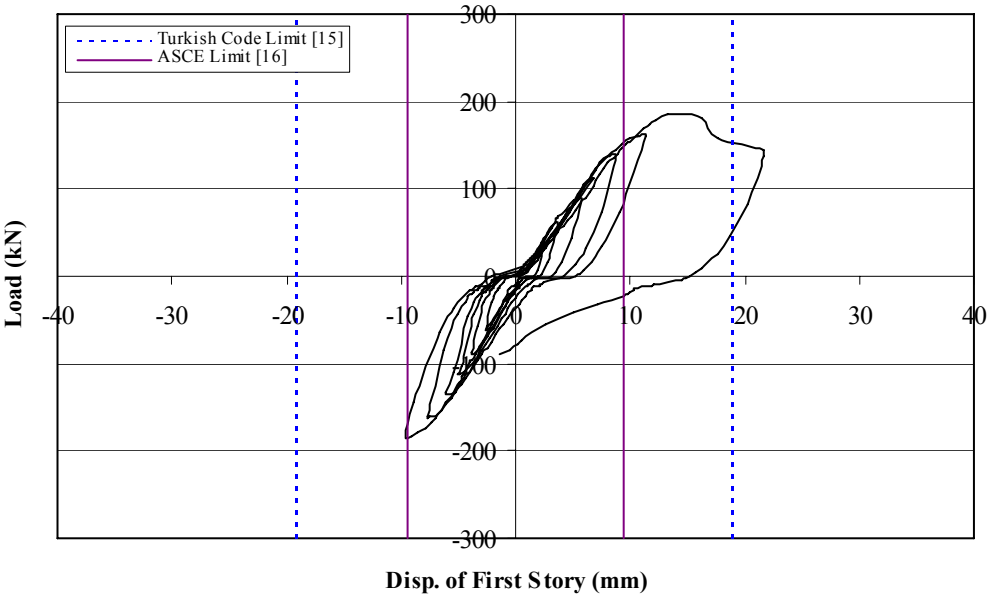

Figure 5.48 - Load – First Story Level Displacement Curve, Specimen S6

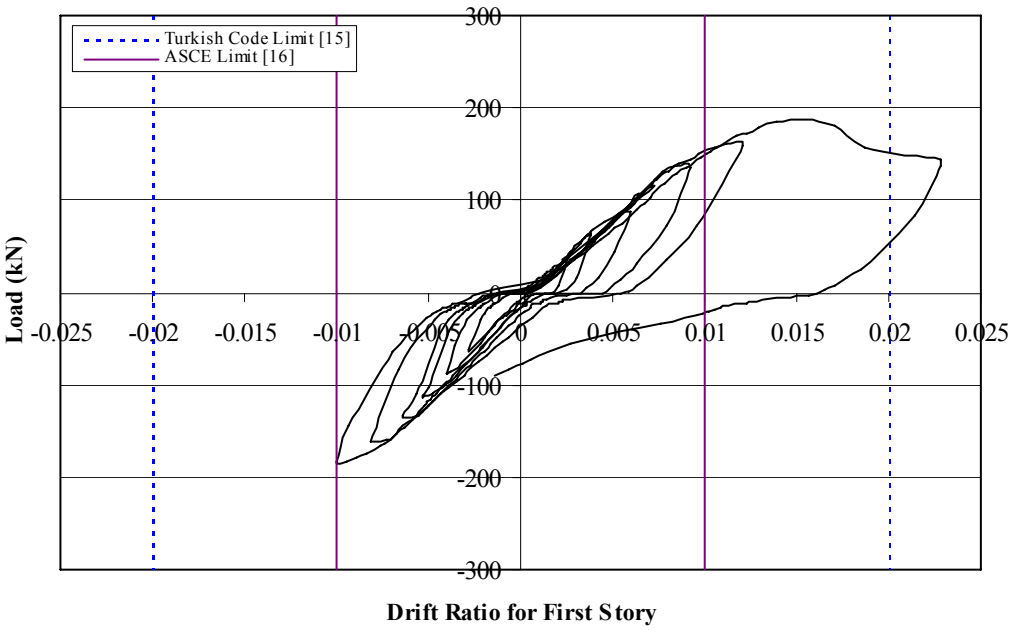

Figure 5.49 - Load – First Story Drift Ratio Curve, Specimen S6

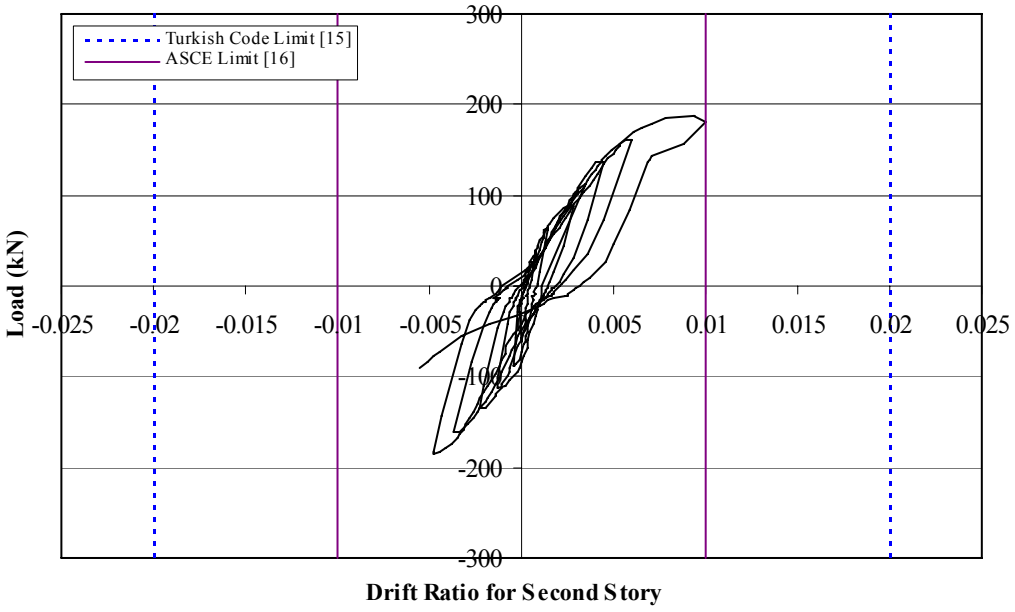

Figure 5.50 - Load – Second Story Drift Ratio Curve, Specimen S6

Experimental observations for this specimen are given below:

- In the first two loading cycle, no cracks were observed on the frame or infills.
- Hairline cracks was formed at the base of the top columns of the both frames in the third upward half cycle, also first diagonal hairline crack appeared on the first story infills near the top column-foundation joint (Figure 5.51). Symmetric cracks were observed in the downward half cycle.

Figure 5.51 – Cracks on the Column (right) and on the First Story Infill Wall (left)

- In the fourth cycle, new cracks were formed at the top column-foundation joints. Another diagonal crack was observed on the first story infills.
- In the fifth upward half cycle, the existing cracks on the first story infill grew larger. Hairline cracks were formed at the first story column-beam joints of the both frames. First cracks were observed on the second story infill of the right frame as shown in Figure 5.52. In the downward half cycle, symmetric cracks were formed on the second story infill wall of the right frame.

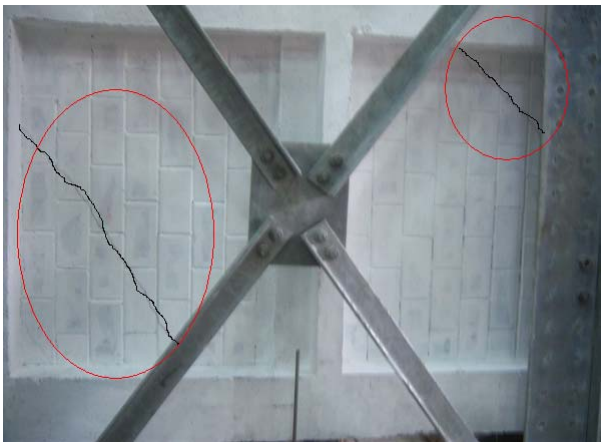

Figure 5.52 – Cracks on the First and Second Story Infill Walls of the Right Frame

- New cracks were observed on the first and second story infills of the left frame in the sixth upward half cycle. Number of cracks on the first story top columns increased (Figure 5.53). In addition, cracks were formed on the first story beams of frames. In the downward cycle, same types of cracks were observed on the symmetric columns.

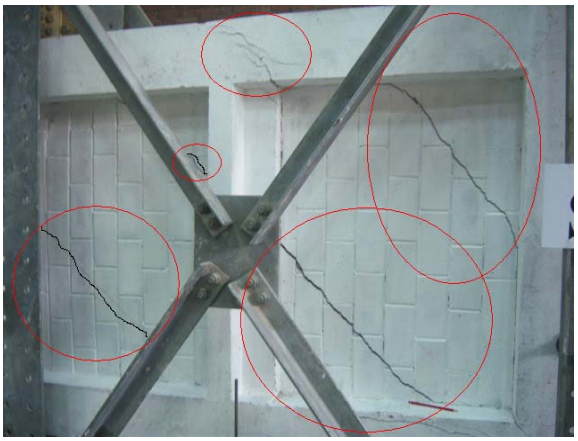

Figure 5.53 – Specimen at the End of the Sixth Cycle

- In the seventh cycle, many new cracks were formed on the infills of the both frames. Diagonal crack widths on the first story infill wall of the left frame approximated as 20 mm. Second story infill wall of the left frame partially separated from the frame and bottom column-foundation joint of the left frame damaged seriously. Therefore, the specimen could not carry any further load and hence, the test was terminated. Photograph of the specimen is given in Figure 5.54. The maximum lateral load of 186.6 kN was recorded at this stage.

Figure 5.54 - Front View of Specimen S6 after the Test

CHAPTER 6

EVALUATION OF THE TEST RESULTS

6.1 General

In this chapter, test results are evaluated considering strength, stiffness and energy dissipation.

6.2 Response Envelopes

Response-envelope curves are produced by connecting the peak points of each upward and downward cycles of the load-displacement curves. Response envelope curves of the specimens are given in Figure 6.1.

As it can be seen in Figure 6.1, the performances of the specimens strengthened with concrete blocks were considerably superior to the reference specimen S1, but the reference specimen S2, cast-in-place R/C infilled frame showed the best performance. All specimens behaved nearly the same both in the upward and downward cycles. Response envelopes for specimens S5 and S6 followed a very similar trend in upward cycles. As the result of this, concrete block geometry did not affect the lateral load carrying capacities of frames.

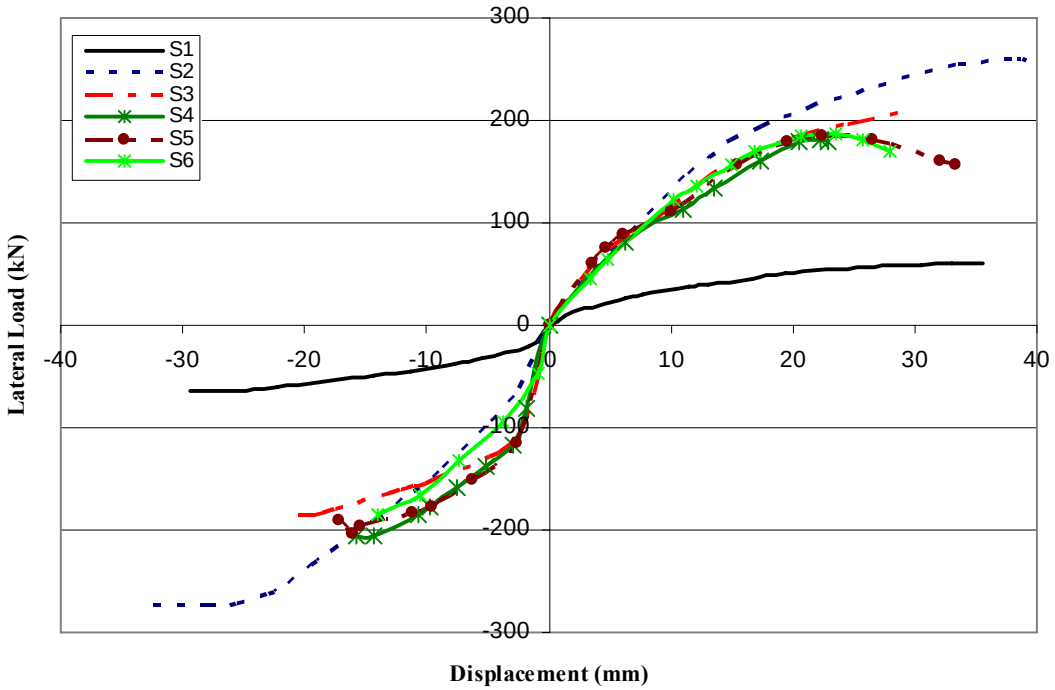

Figure 6.1 – Response Envelope Curves of the Specimens

6.3 Strength

Strength is one of the most important parameters that determine how effective the strengthening technique. Increasing lateral load carrying capacity of frame is generally one of the initial goals for strengthening. For each specimen, the maximum values of lateral loads are presented in Table 6.1.

When response envelope curves and lateral load carrying capacities of specimens were examined carefully, it can be clearly seen that concrete blocks significantly increased the lateral load carrying capacities of the bare frame but this increase was not as much as that in specimen S2.

As it can be seen in Table 6.1, specimens S3, S4, S5 and S6 have nearly the same lateral load carrying capacities. Therefore, it can be said that the concrete block strength did not affect the test results, but fundamentally, this result was not correct. Because failure of specimens S3 and S4 was due to damaging of infill wall but failure of specimens S5 and S6 was due to damaging of frame seriously. That is, capacity of frame determined the level of failure.

Table 6.1 – Lateral Load Carrying Capacities of the Specimens

Specimen	Maximum upward load (kN)	Displacement at max. Load (mm)	Maximum downward load (kN)	Displacement at max. Load (mm)
S1	60.1	35.6	65.0	25.6
S2	262.0	39.2	276.4	28.0
S3	185.6	20.4	206.8	28.7
S4	182.0	22.2	205.3	15.0
S5	184.7	22.4	203.5	16.1
S6	186.6	23.6	185.5	14.1

6.4 Stiffness

Resistance of the structures against the imposed displacements is called stiffness. Inadequate lateral stiffness is one of the major causes of damage in reinforced concrete buildings. Structures should have adequate stiffness in order to control structural damage.

Stiffness of the first cycle was designated as initial slope. The initial slopes of the specimens are given in Table 6.2.

In Table 6.2, it can be seen that all strengthened specimens had higher initial slope value than the reference specimens S1 and S2. Although it was estimated that specimens S5 and S6 would have the highest initial slope values, specimen S3 and S4 had the highest ones. This can be owing to the lower concrete compressive strength of these frames and the quality of the workmanship in the construction of the infill walls, which can play an important role in the displacement history in early cycles.

Table 6.2 – Initial Slope of Test Specimens

Specimen	Initial Slope (kN/mm)	Ratio of Initial Stiffness to that of Reference Specimen
S1	6.97	-
S2	16.19	2.32
S3	21.58	3.10
S4	21.09	3.03
S5	18.84	2.70
S6	19.03	2.73

By plotting the stiffness in each cycle, stiffness degradation curve of a specimen is obtained. Stiffness degradation curves for specimens are given in Figure 6.2 with the same scale.

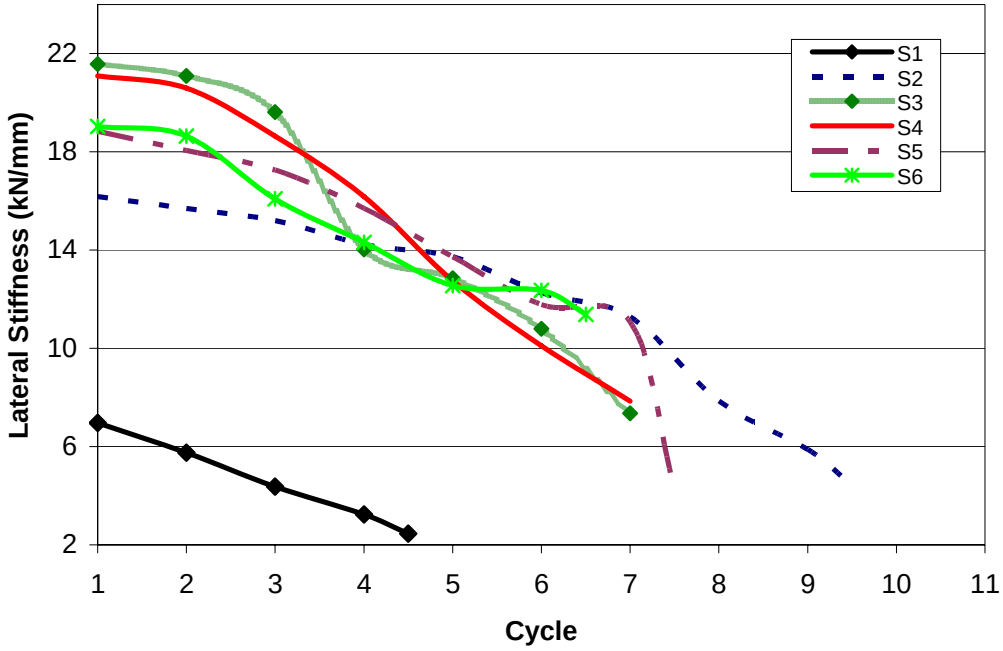

Figure 6.2 - Stiffness Degradation Curves for Specimens

6.5 Energy Dissipation

One of the primary aims for the strengthening is to increase the energy dissipation in a structure. The energy dissipation in the tested frames was evaluated by calculating the area enclosed by the hysteretic loops from load-displacement graphs for each cycle during the test. Cumulative energy dissipation curves of the specimens are presented in Figure 6.3. The results of the energy dissipation calculations for each specimen are given in Table 6.3.

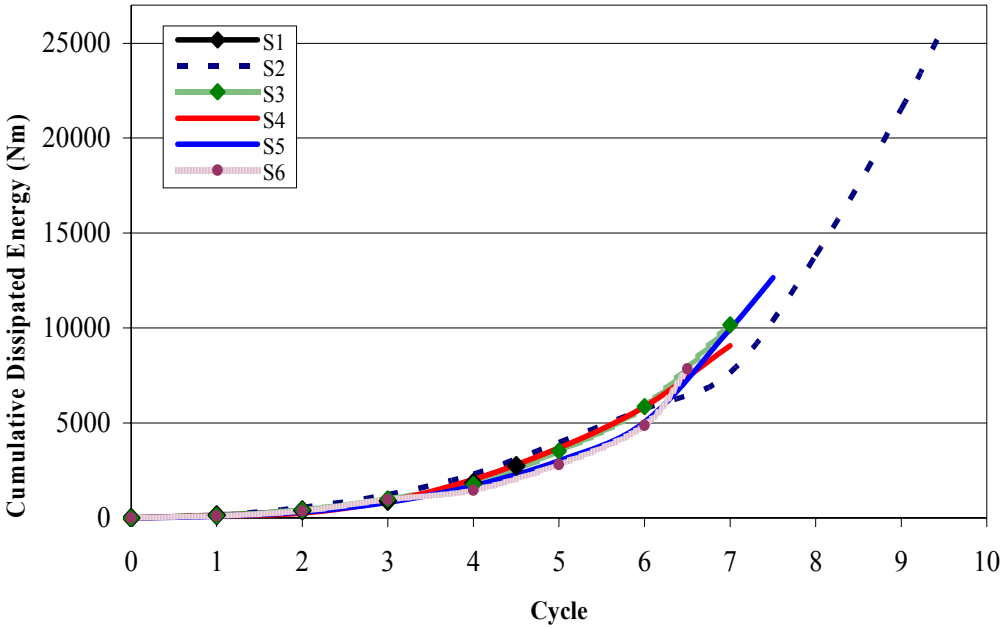

Figure 6.3 - Cumulative Energy Dissipation for Specimens

Table 6.3 – Total Dissipated Energy for Test Specimens

Specimen	Dissipated Energy ($N_x m$)	Ratio of total energy to that of Reference Specimen
S1	2729	-
S2	25934	9.5
S3	10162	3.7
S4	9081	3.3
S5	12645	4.6
S6	7846	2.9

Test results showed that the increase in the cumulative dissipated energy values of the strengthened specimen with respect to reference specimen S1 varied between ~200% and ~400% which means that the proposed method improves the energy dissipation characteristics of the specimens. The highest energy was dissipated by reference specimen S2. This was due to high energy dissipated capacity of R/C infilled wall and perfect bond between infill wall and frame.

Since the concrete compressive strength of frame was lower than other frames, specimen S6 dissipated less energy.

6.6 Summary

When test results are analyzed, using high strength concrete masonry blocks to increase the lateral load bearing capacity of frame structures can be a simpler and more practical alternative to cast-in-place R/C panels. Although specimen S2 (cast-in-place R/C infilled frame) has the highest energy consumption capacity, specimens strengthened with concrete blocks can dissipate 2.9 to 4.6 times more energy than an unstrengthened frame.

Test results given in Table 6.4 display the all improvement in behaviour.

Table 6.4 – Summary of the Test Results

Specimen	Frame f_c (kgf/cm^2)	Infill Wall f_c (kgf/cm^2)	Upward Loading			Downward Loading			Initial Slope (kN/mm)	Cumulative Dissipated Energy (Nxm)
			Max. Load (kN)	1st St. Drift Ratio D1/h1	2nd St. Drift Ratio (D2-D1)/h2	Max. Load (kN)	1st St. Drift Ratio D1/h1	2nd St. Drift Ratio (D2-D1)/h2		
S1	294.3	-	60.1	0.021	0.016	65.0	0.018	0.009	6.97	2729
S2	276.0	~276.0	262.0	0.020	0.022	276.4	0.019	0.010	16.19	25934
S3	285.7	~435.0	185.6	0.012	0.010	206.8	0.021	0.009	21.58	10162
S4	307.0	~395.0	182.0	0.015	0.007	205.3	0.010	0.005	21.09	9081
S5	312.0	~635.0	184.7	0.017	0.009	203.5	0.012	0.005	18.84	12645
S6	254.0	~620.0	186.6	0.015	0.009	185.5	0.010	0.005	19.03	7846

CHAPTER 7

ANALYTICAL STUDIES

7.1 General

The experimental test results were also supported analytically. It is not easy to model the behaviour of the reinforced concrete frames strengthened by custom shaped high strength concrete masonry blocks in the analytical models. In recent years, the use of finite element analysis has increased due to progressing knowledge and capabilities of computer software and hardware. ANSYS version 10 was used to determine the load displacement behaviour of test specimens by using nonlinear push over analysis.

The objective of this study was to investigate and evaluate the use of the finite element method for the analysis of reinforced concrete frames strengthened by custom shaped high strength concrete masonry blocks.

7.2 Previous Studies

Wolanski [17] investigated and evaluated the use of the finite element method for the analysis of reinforced and prestressed concrete beams. To meet this goal, he used the following procedure:

- Literature review was conducted to evaluate previous experimental and analytical procedures related to reinforced concrete components.
- Calibration model using a commercial finite element analysis package (ANSYS, SAS 2003) was set up and evaluated using experimental data.

- A mild-steel reinforced concrete beam with flexural and shear reinforcement was analyzed to failure and compared to experimental results to calibrate the parameters in ANSYS (SAS 2003) for later analyses.

The following conclusions were obtained from this analitical research:

- Deflections and stresses at the centerline along with initial and progressive cracking of the finite element model compared well to experimental data obtained from a reinforced concrete beam.
- The failure mechanism of a reinforced concrete beam was modeled quite well using FEA, and the failure load predicted was very close to the failure load measured during experimental testing.
- Deflections and stresses at the zero deflection point and decompression were modeled well using a finite element package.

Kachlakev and Miller [18] prepared a report about finite element modeling of reinforced concrete structures strengthened with FRP laminates. Using the ANSYS program (ANSYS 1998) finite element method (FEM) models were developed to simulate the behavior of four full-size beams from linear through nonlinear response and up to failure. Comparisons were made for load-strain plots at selected locations on the beams; load-deflection plots at midspan; first cracking loads; loads at failure; and crack patterns at failure. The models were subsequently expanded to encompass the linear behavior of the Horsetail Creek Bridge. The study compared strains from the FEM analysis with measured strains from load tests.

The report stated the following conclusions according to the research results:

- The general behavior of the finite element models represented by the load-deflection plots at midspan showed good agreement with the test data from the full-scale beam tests. However, the finite element models showed slightly more stiffness than the test data in both the linear and nonlinear ranges.

- The load-strain plots for selected locations from the finite element analysis showed fair agreement with the test data. For the load-tensile strain plots for the main steel reinforcing at midspan, the strains from the finite element analysis and the experimental data correlated well in the linear range, and the trends in the nonlinear range were generally comparable.
- The final loads from the finite element analyses were lower than the ultimate loads from the experimental results by 5% - 24%.
- The load carrying capacity of the Flexure/Shear strengthened beam predicted by the finite element analysis was higher than that of the Control Beam by 105%.
- The crack patterns at the final loads from the finite element models corresponded well with the observed failure modes of the experimental beams.

This report also recommended finite element modeling procedure for reinforced concrete beams. These recommendations were listed below.

- The symmetry of the beams should be used to reduce computational time and computer disk space requirements.
- A steel plate needs to be included in the models at the support locations to represent the actual support condition in the full-size beams.
- For nonlinear analysis of a reinforced concrete beam, the total load applied to a model must be divided into a number of load steps.

Dede [19] made a research to model reinforced concrete frame experiments in which the loads were applied in a reversed-cyclic manner. Comparisons between the results of experiment and the results of analysis were made. For the modeling purposes, ANSYS finite element software which has a type of element that assumes full bond between steel and concrete and can model failure in tri-axial stress rule was used.

The main conclusions obtained from this research were:

- The behavior of the finite element models represented by the load-deflection plots showed good agreement with the experiment results data. However, it was observed that ANSYS analysis stopped after the load carrying capacity of the system was reached.
- The crack patterns of finite element models also showed good agreement with the experiment results.

7.3 ANSYS Finite Element Model

An eight-node solid element, Solid65, is used to model the concrete, mortar and the concrete masonry blocks. The solid element has eight nodes with three degrees of freedom at each node - translations in the nodal x, y, and z directions. The element is capable of plastic deformation, cracking in three orthogonal directions, and crushing [20]. The geometry and node locations for this element type are shown in Fig 7.1.

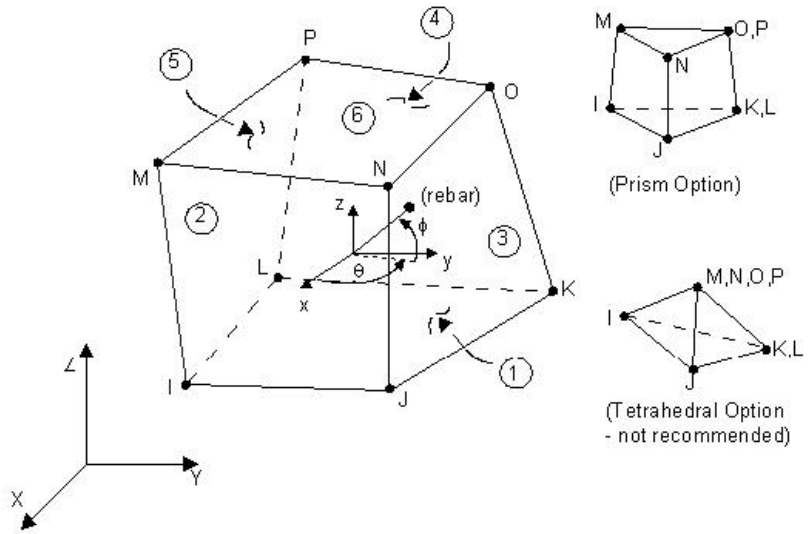

Figure 7.1 - Solid65 - 3D Reinforced Concrete Solid

7.3.1 Real Constants

The real constants for the frame models are shown in Table 7.1. Since only one element was used for modeling, real constants were used for the Solid65 element. It requires real constants for rebar, since smeared model was used for the reinforcements. Also, values of Material Number, Volume Ratio and Orientation Angles are required. The material number refers to the type of material for the reinforcement. The volume ratio refers to the ratio of steel to concrete in the element. The orientation angles refer to the orientation of the reinforcement in the smeared model. ANSYS allows the user to enter three rebar materials in the concrete. Each material corresponds to x, y, and z directions in the element (Figure 7.1).

Table 7.1 - Real Constants For Frame Model

Real Constant Set	Element Type	Constants				
1	Solid 65		Material Number	Volume Ratio	Orientation Angle	Orientation Angle
		Rebar 1	2	0.103	90	0
		Rebar 2	2	0.028	0	0
		Rebar 3	2	0.017	0	90
2	Solid 65		Material Number	Volume Ratio	Orientation Angle	Orientation Angle
		Rebar 1	2	0.028	0	0
		Rebar 2	0	0	0	0
		Rebar 3	0	0	0	0
3	Solid 65		Material Number	Volume Ratio	Orientation Angle	Orientation Angle
		Rebar 1	2	0.017	0	90
		Rebar 2	0	0	0	0
		Rebar 3	0	0	0	0
4	Solid 65		Material Number	Volume Ratio	Orientation Angle	Orientation Angle
		Rebar 1	0	0	0	0
		Rebar 2	0	0	0	0
		Rebar 3	0	0	0	0
5	Solid 65		Material Number	Volume Ratio	Orientation Angle	Orientation Angle
		Rebar 1	2	0.034	0	0
		Rebar 2	2	0.028	90	0
		Rebar 3	2	0.017	0	90
6	Solid 65		Material Number	Volume Ratio	Orientation Angle	Orientation Angle
		Rebar 1	2	0.017	0	0
		Rebar 2	2	0.017	0	90
		Rebar 3	0	0	0	0
7	Solid 65		Material Number	Volume Ratio	Orientation Angle	Orientation Angle
		Rebar 1	2	0.028	90	0
		Rebar 2	2	0.017	0	90
		Rebar 3	0	0	0	0
8	Solid 65		Material Number	Volume Ratio	Orientation Angle	Orientation Angle
		Rebar 1	2	0.028	90	0
		Rebar 2	0	0	0	0
		Rebar 3	0	0	0	0
9	Solid 65		Material Number	Volume Ratio	Orientation Angle	Orientation Angle
		Rebar 1	2	0.103	0	0
		Rebar 2	2	0.028	90	0
		Rebar 3	2	0.017	0	90

The real constants for the frame members are shown in Figure 7.2. Since the model was symmetric on the x-y plane, half of the members were used for modeling.

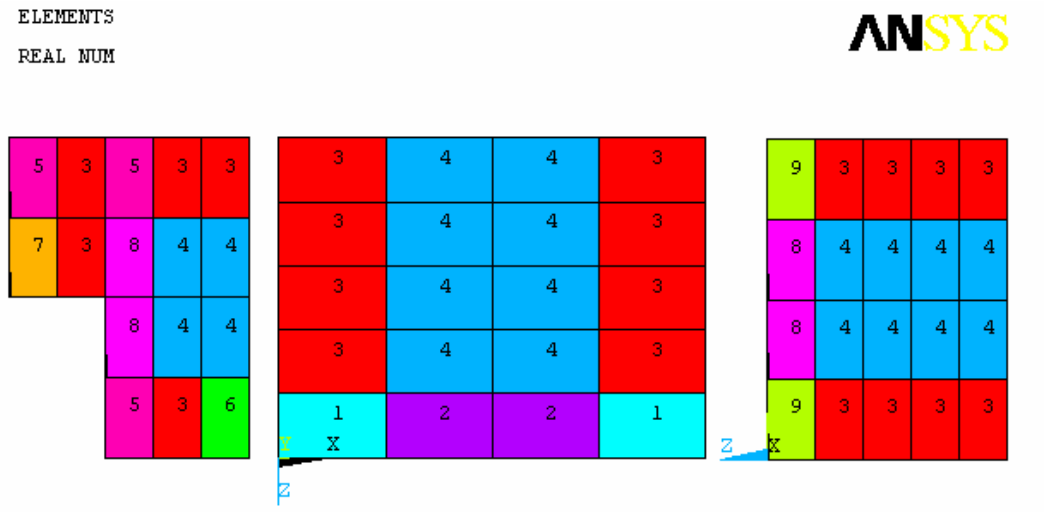

Figure 7.2 - Real Constants for Beams, Columns and Foundation Beam

7.3.2 Material Properties

Since concrete deforms plastically, both linear elastic properties and plastic properties were defined. In the linear region, the concrete was treated as linear isotropic so only Young's modulus and Poisson's ratio were used. For the nonlinear region, multilinear isotropic model was used. Parameters needed to define the material models are given in Table 7.2.

Table 7.2 - Material Models For the Calibration Model

Material Number: 1 (C20), 3 (C30), 4 (C70)

Material Properties

Linear Isotropic			
Material Num.	1 (C20)	3 (C30)	4 (C70)
EX (MPa)	1.91×10^4	2.86×10^4	6.67×10^4
PRXY	0.2	0.2	0.2

Multilinear Isotropic						
Material Num.	1 (C20)		3 (C30)		4 (C70)	
	Strain	Stress (MPa)	Strain	Stress (MPa)	Strain	Stress (MPa)
Point 1	19×10^{-5}	3.62	19×10^{-5}	5.43	19×10^{-5}	12.67
Point 2	57×10^{-5}	9.80	57×10^{-5}	14.70	57×10^{-5}	34.20
Point 3	15×10^{-4}	18.90	15×10^{-4}	28.30	15×10^{-4}	66.00
Point 4	17×10^{-4}	19.60	17×10^{-4}	29.40	17×10^{-4}	68.50
Point 5	20×10^{-4}	20.00	20×10^{-4}	30.00	20×10^{-4}	70.00
Point 6	38×10^{-4}	13.40	38×10^{-4}	12.50	30×10^{-4}	14.50

Concrete			
Material Num.	1 (C20)	3 (C30)	4 (C70)
ShrCf-Op	0.5	0.5	0.5
ShrCf-Cl	1	1	1
UnTensSt (MPa)	3	4.5	10.5
UnCompSt	-1	-1	-1
BiCompSt	0	0	0
HydroPrs	0	0	0
BiCompSt	0	0	0
UnTensSt	0	0	0
TenCrFac	0	0	0

Material Number: 2

Linear Isotropic	
EX (MPa)	20×10^4
PRXY	0.3

Bilinear Isotropic	
Yield Stss (MPa)	420
Mod	0

The multilinear isotropic material uses the von Mises failure criterion. Modified Kent and Parker unconfined concrete model was used to define the stress and strain curve of concrete. EX is the modulus of elasticity of the concrete, and PRXY is the Poisson's ratio.

Implementation of the Willam and Warnke (1974) material model in ANSYS requires that different constants be defined. These 9 constants are:

1. Shear transfer coefficients for an open crack;
2. Shear transfer coefficients for a closed crack;
3. Uniaxial tensile cracking stress;
4. Uniaxial crushing stress (positive);
5. Biaxial crushing stress (positive);
6. Ambient hydrostatic stress state for use with constants 7 and 8;
7. Biaxial crushing stress (positive) under the ambient hydrostatic stress state
8. Uniaxial crushing stress (positive) under the ambient hydrostatic stress state
9. Stiffness multiplier for cracked tensile condition.

Typical shear transfer coefficients range from 0.0 to 1.0, with 0.0 representing a smooth crack (complete loss of shear transfer) and 1.0 representing a rough crack (no loss of shear transfer).

The uniaxial crushing stress in this model was based on the uniaxial unconfined compressive strength. It was entered as -1 to turn off the crushing capability of the concrete element as suggested by past researchers. Convergence problems have been repeated when the crushing capability was turned on.

Although smeared model was used for the reinforcements, material properties of steel were also required. It was assumed to be bilinear isotropic. Bilinear isotropic material is also based on the von Mises failure criteria. The bilinear model requires the yield stress, as well as the hardening modulus of the steel to be defined.

7.3.3 Modeling

Frames, walls and concrete blocks were modeled as volumes. By taking advantage of the symmetry of the specimens, half of the full specimen was used for modeling. This approach reduced computational time and computer disk space requirements significantly.

The combined volumes of the frame and concrete blocks are shown in Figure 7.3. Since wall made of concrete blocks behaved monolithically by the means of epoxy mortar, blocks were not modeled separately and only a wall was modeled for the all blocks bonded to each other.

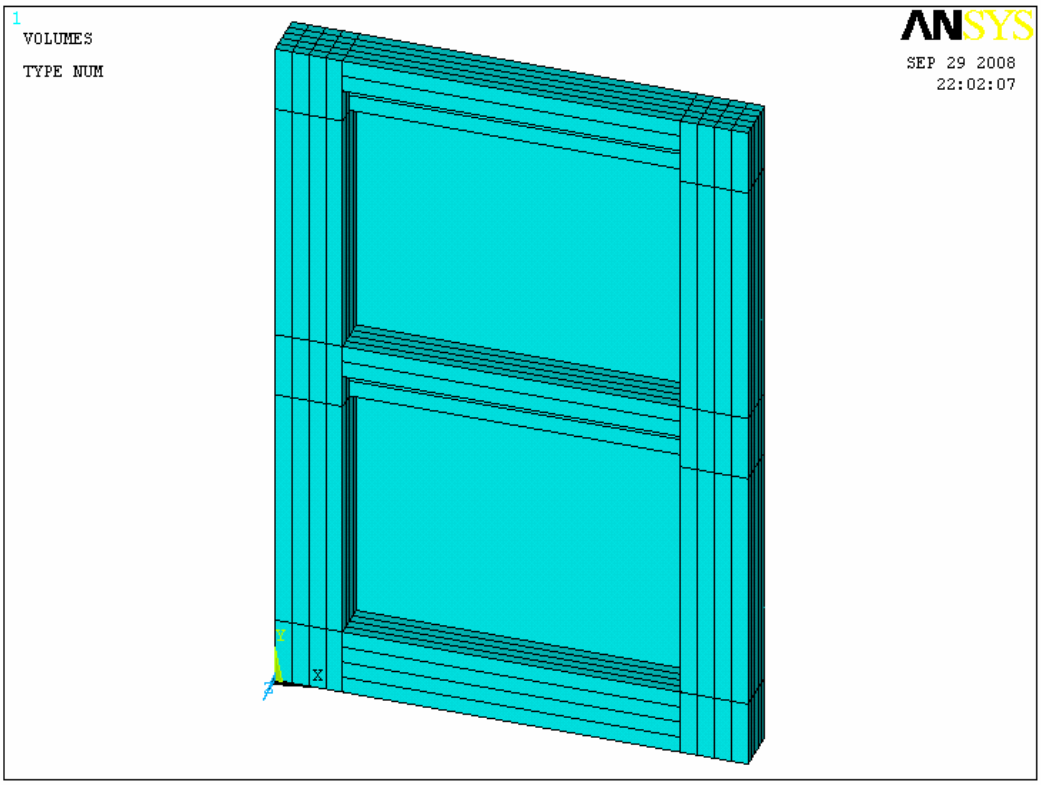

Figure 7.3 - Volumes Created in ANSYS

7.3.4 Meshing

To obtain good results from the Solid65 element, the use of a rectangular mesh is recommended. Therefore, the mesh was set up such that rectangular elements were created (Figure 7.4). The volume sweep command was used to mesh the walls and concrete blocks. This properly sets the width and length of elements in the walls to be consistent with the elements and nodes in the concrete portions of the model.

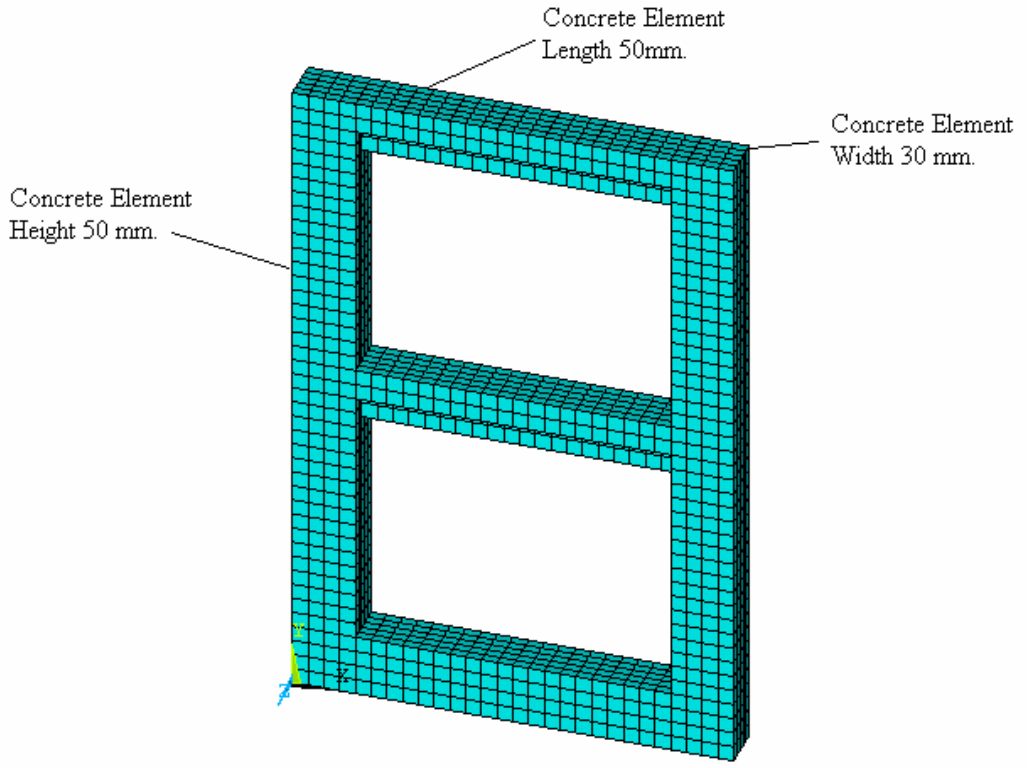

Figure 7.4 - Mesh of the Concrete

7.3.5 Loads and Boundary Conditions

In order to constrain the model, displacement boundary conditions are needed. To ensure that the model acts the same way as the experimental specimen, boundary conditions need to be applied at points of symmetry, and where the supports and loadings exist.

Since the model was symmetric on the x-y plane, half of the full specimen was used for modeling. To model the symmetry, nodes on this plane were constrained in the perpendicular direction. So, these nodes had a degree of freedom constraint UZ = 0.

The boundary conditions for symmetry and the points of supports are shown in Figure 7.5.

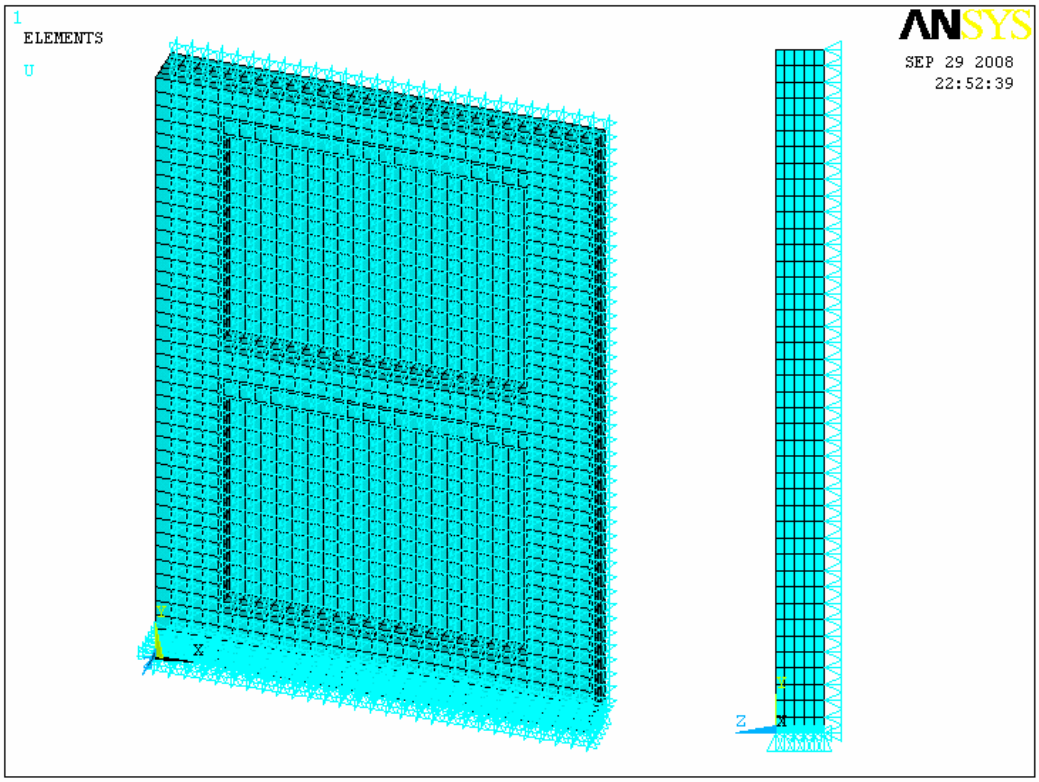

Figure 7.5 - Boundary Conditions for Supports and Planes of Symmetry

7.3.6 Analysis Type And Process

The finite element model for this analysis was a frame under static loading. For the purposes of this model, the Static analysis type was utilized.

The Restart command was utilized to restart an analysis after the initial run or load step has been completed, so the cracks formed on the specimen could be investigated regularly.

The Newton-Raphson method of analysis was used to compute the nonlinear response. The application of the loads up to failure was done incrementally as required by the Newton-Raphson procedure. After each load increment was applied, the restart option was used to go to the next step after convergence.

7.3.7 Results

The goal of the comparison of the FE models and the strengthened frames is to ensure that the elements, material properties, real constants and convergence criteria are adequate to model the response of the member. The cracking patterns and load vs. deflection curve for all frames were obtained for comparison.

The cracking pattern(s) in the frame can be obtained using the Crack/Crushing plot option in ANSYS.

7.3.7.1 Specimen S1 (Reference-Lower Limit)

The cracking patterns in Specimen S1 for different load values can be seen in Figures 7.6, 7.7, 7.8.

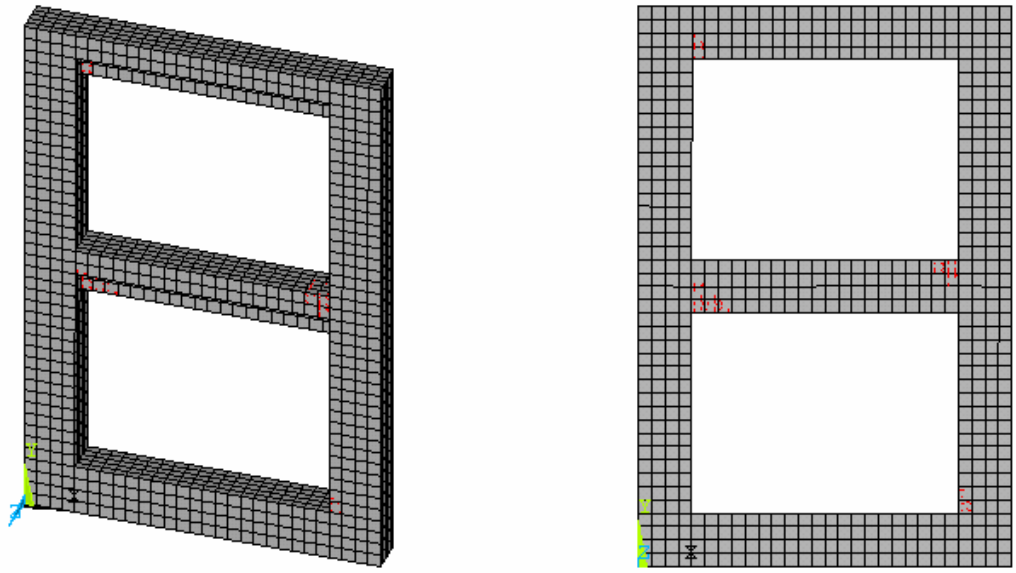

Figure 7.6 - Cracking at 20.0 kN

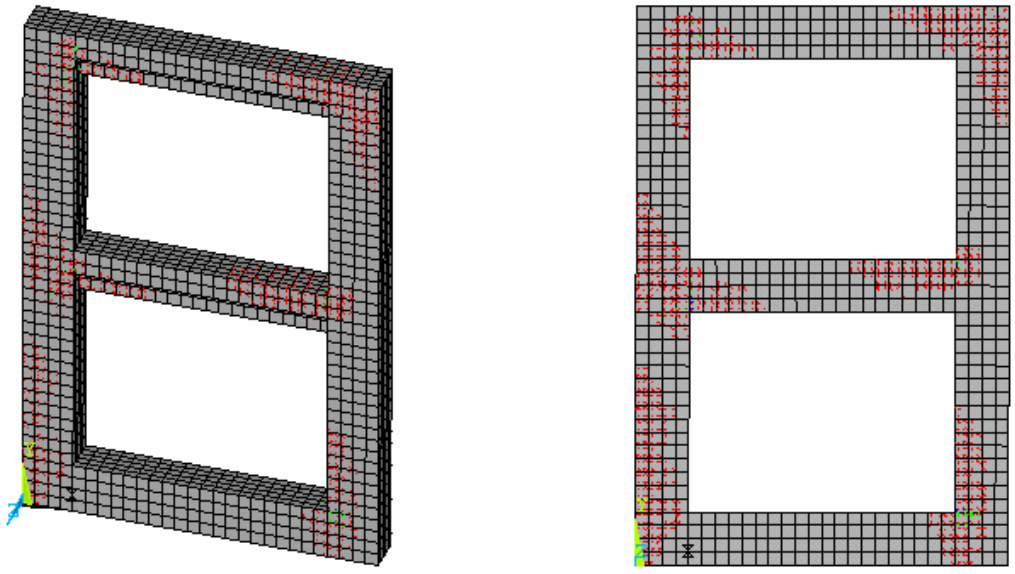

Figure 7.7 - Cracking at 40.0 kN

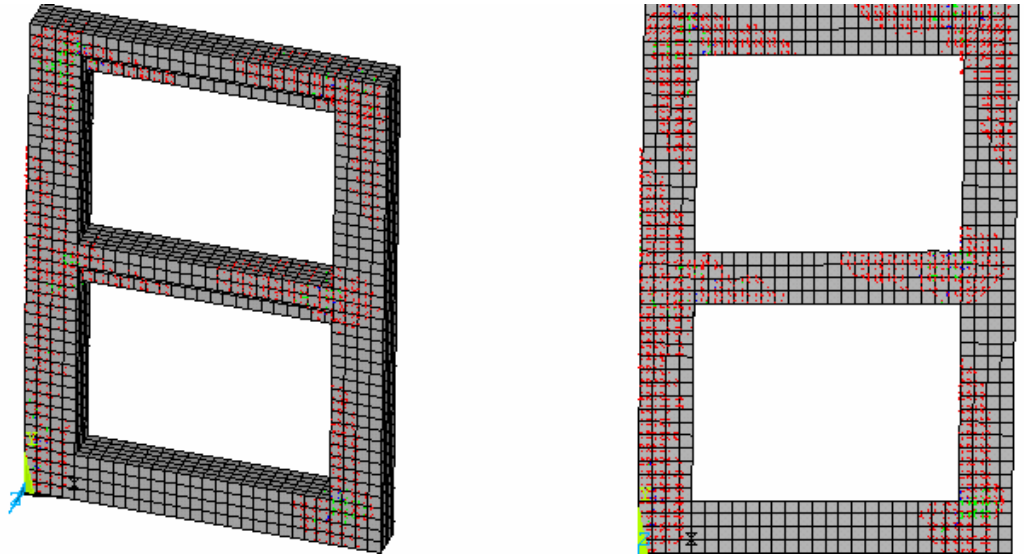

Figure 7.8 - Cracking at Maximum Load Carrying Capacity (69.5 kN)

The full nonlinear load-displacement response can be seen in Figure 7.9. The entire load-deformation response of the model produced compares well with the response from test frame. This gave confidence in the use of ANSYS and the model developed.

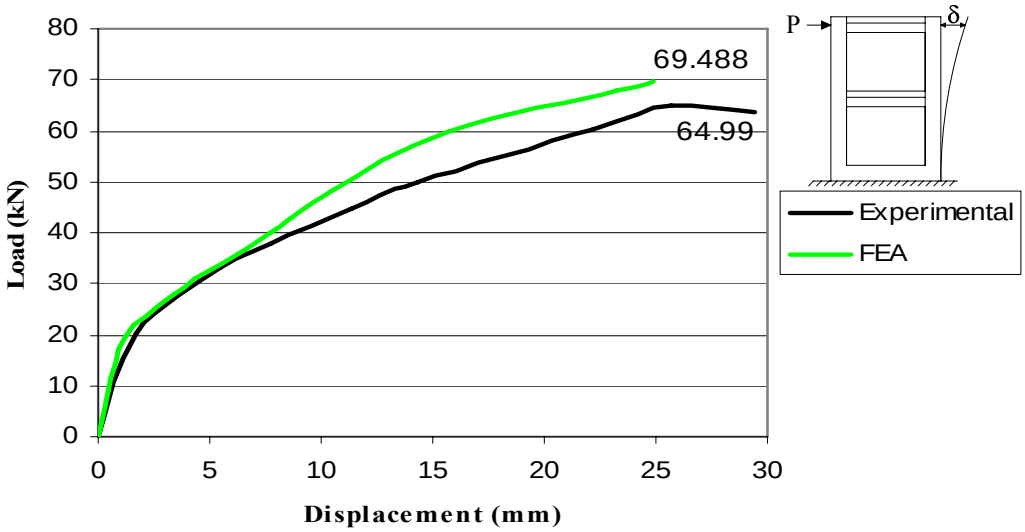

Figure 7.9 - Load vs. Displacement Curve Comparison of ANSYS and Experiment

The principal stresses for Specimen S1 are shown in Figure 7.10.

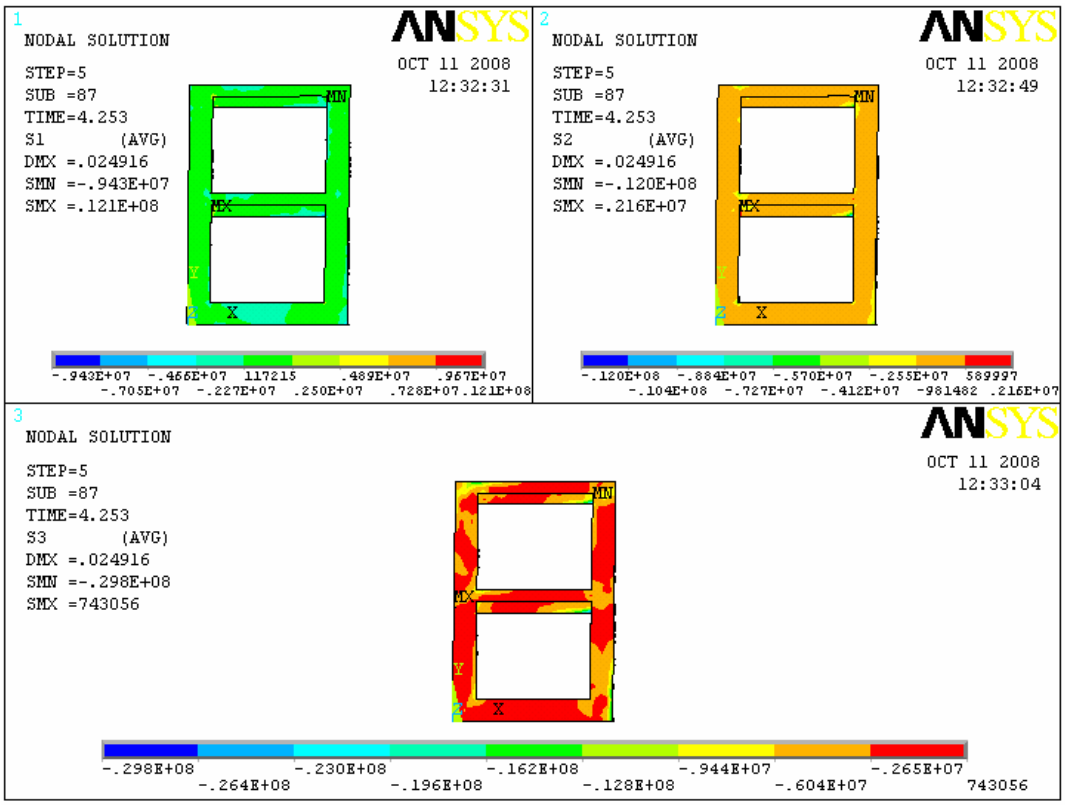

Figure 7.10 - Principal Stresses (N/m^2)

7.3.7.2 Specimen S2 (Reference-Upper Limit)

Since this specimen was cast-in-place R/C infilled frame used as reference, it also required real constants for reinforcement infilled wall. The real constants for the infilled wall are shown in Table 7.3. The real constants for the frames were also used.

Table 7.3 - Real Constants For Infill Wall

Real Constant Set	Element Type	Constants				
			Material Number	Volume Ratio	Orientation Angle	Orientation Angle
10	Solid 65	Rebar 1	2	0.0084	90	0
		Rebar 2	2	0.0042	0	0
		Rebar 3	0	0	0	0

The cracking patterns in Specimen 2 for different load values can be seen in Figures 7.11, 7.12, 7.13, 7.14.

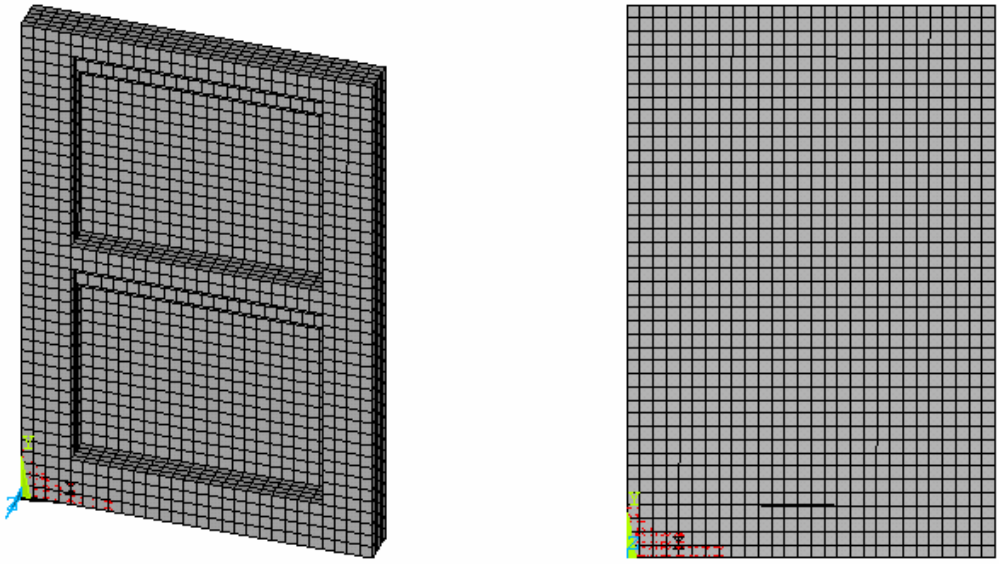

Figure 7.11 - Cracking at 80.0 kN

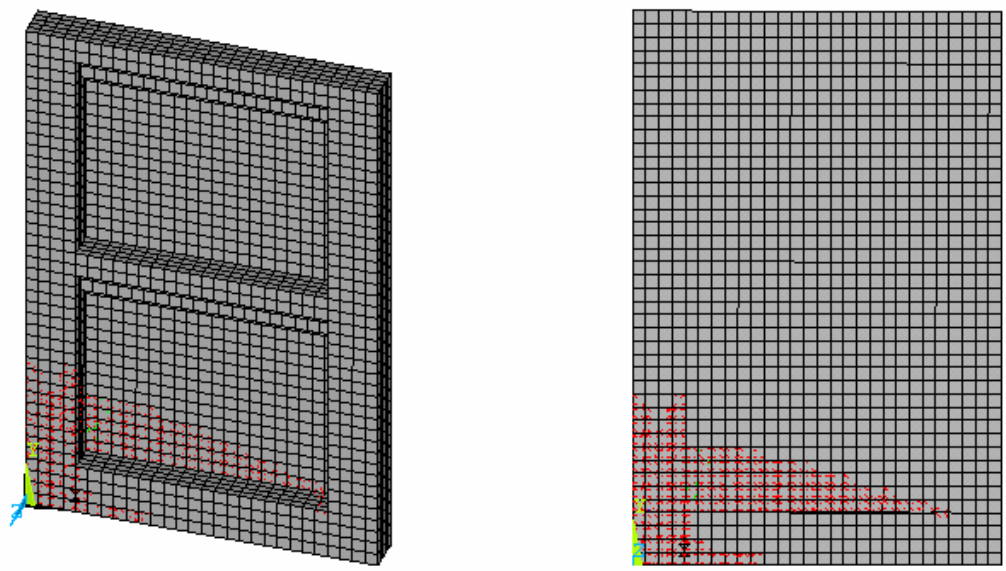

Figure 7.12 - Cracking at 100.0 kN

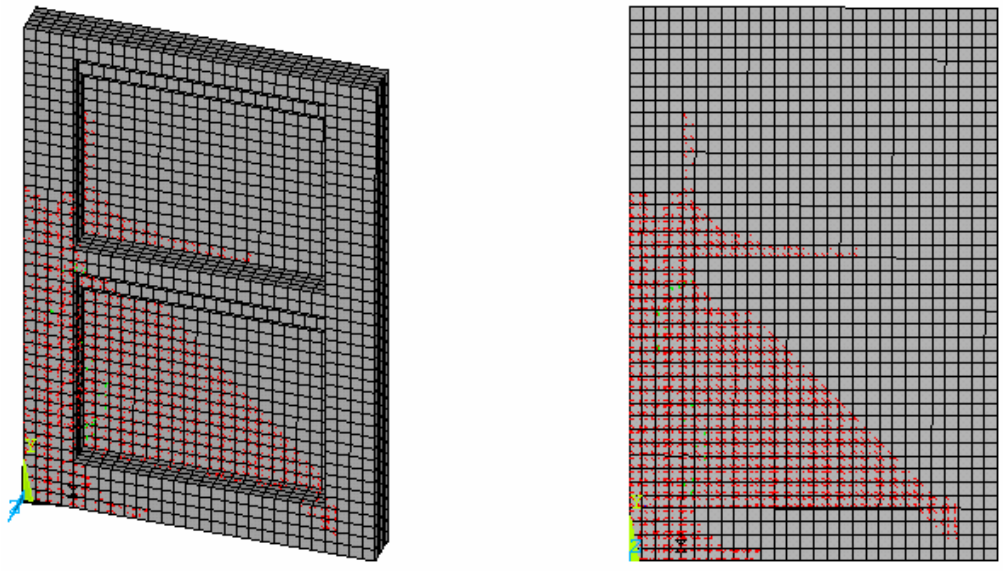

Figure 7.13 - Cracking at 130.0 kN

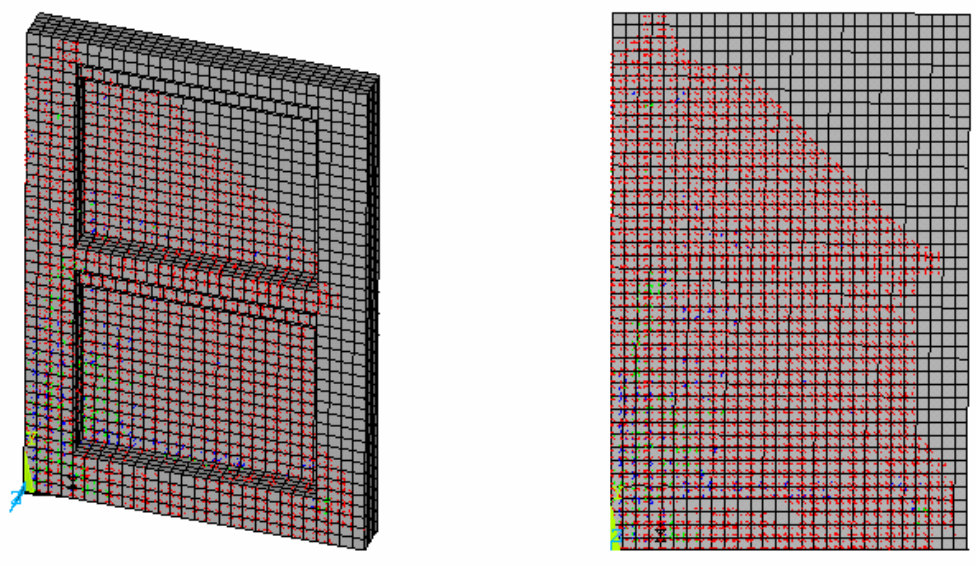

Figure 7.14 - Cracking at Maximum Load Carrying Capacity (294.8 kN)

The full nonlinear load-displacement response for specimen S2 can be seen in Figure 7.15. For comparison, first order elastic analysis was also carried out for this model.

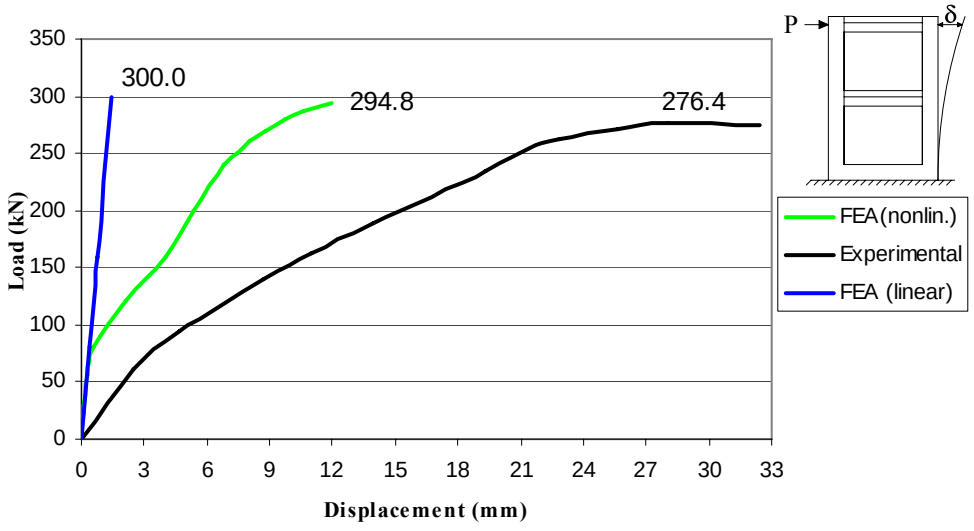

Figure 7.15 - Load vs. Displacement Curve for ANSYS Model

The principal stresses for Specimen S2 are shown in Figure 7.16.

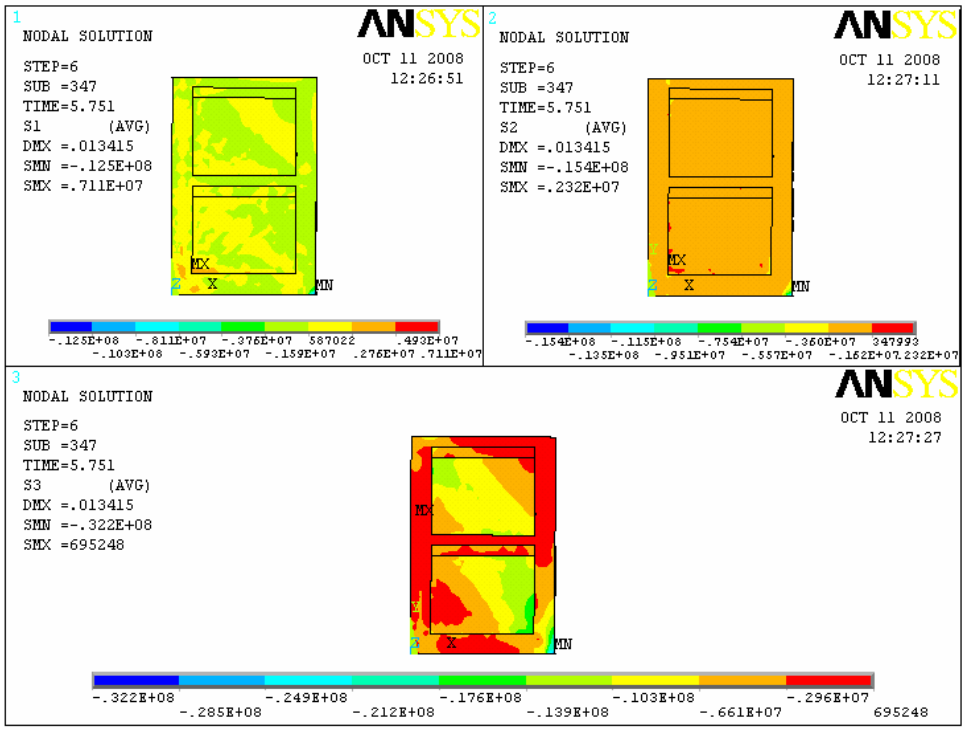

Figure 7.16 - Principal Stresses (N/m^2)

7.3.7.3 Specimen S3 and S4

Observations during the test and test results showed that the concrete block geometry was not an important parameter, because epoxy mortar supplied required adherence to blocks to behave a monolithical wall during the test. So blocks were not modeled separately and only a wall was modeled for the all blocks bonded to each other and also one model was formed for both Specimen 3 and Specimen 4.

The cracking patterns in strengthened frame with infill wall made of 30 MPa strength concrete blocks for different load values can be seen in Figures 7.17, 7.18, 7.19, 7.20.

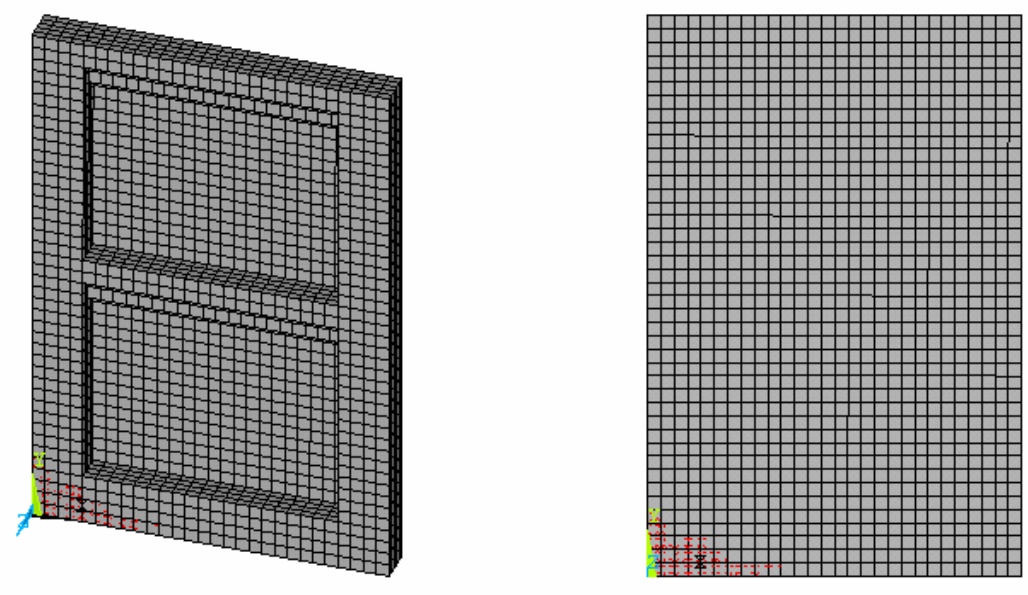

Figure 7.17 - Cracking at 90.0 kN

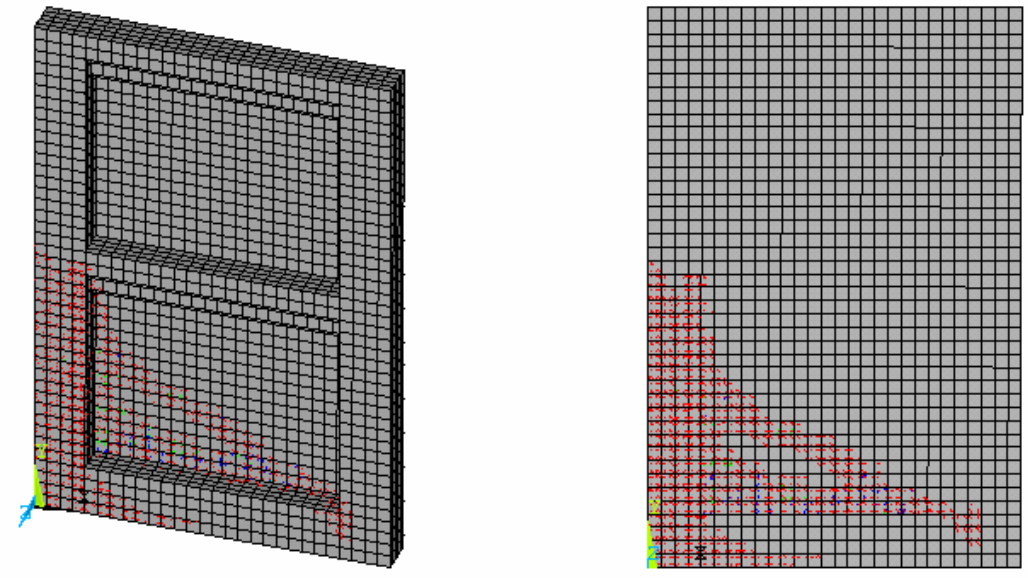

Figure 7.18 - Cracking at 106.0 kN

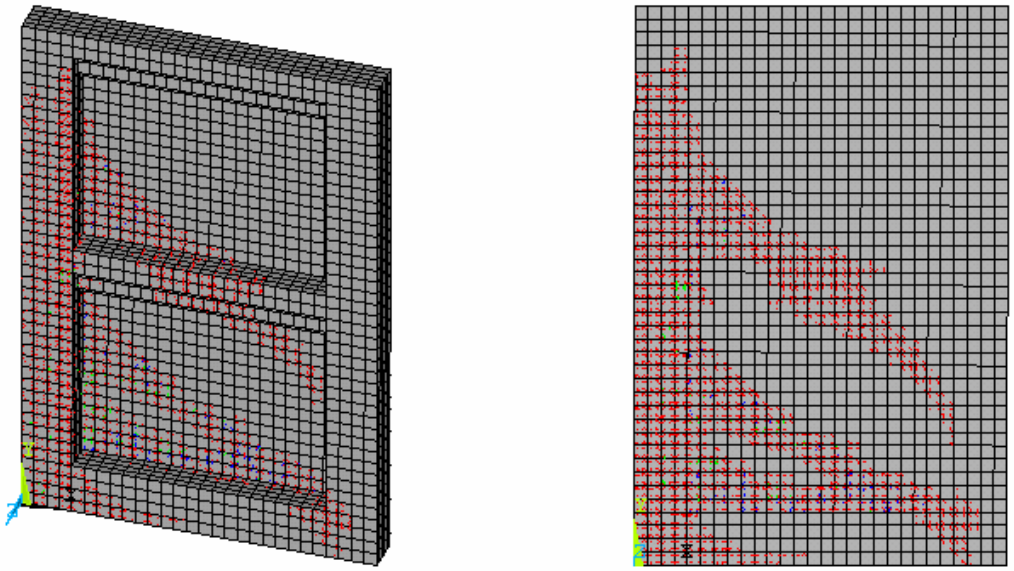

Figure 7.19 - Cracking at 160.0 kN

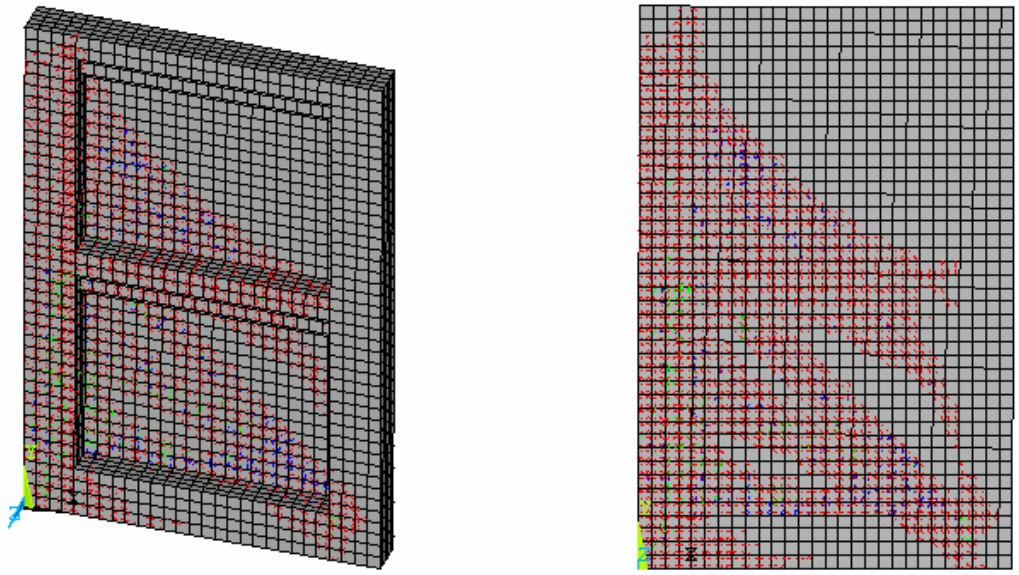

Figure 7.20 - Cracking at Maximum Load Carrying Capacity (230.0 kN)

The full nonlinear load-displacement response for specimen can be seen in Figure 7.21.

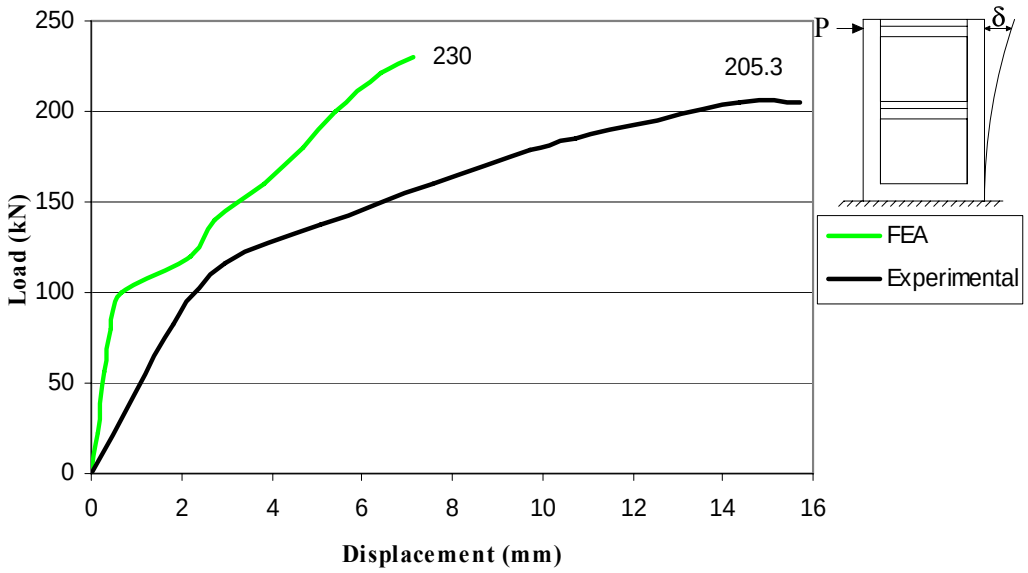

Figure 7.21 - Load vs. Displacement Curve for ANSYS Model

The principal stresses for Specimen are shown in Figure 7.22.

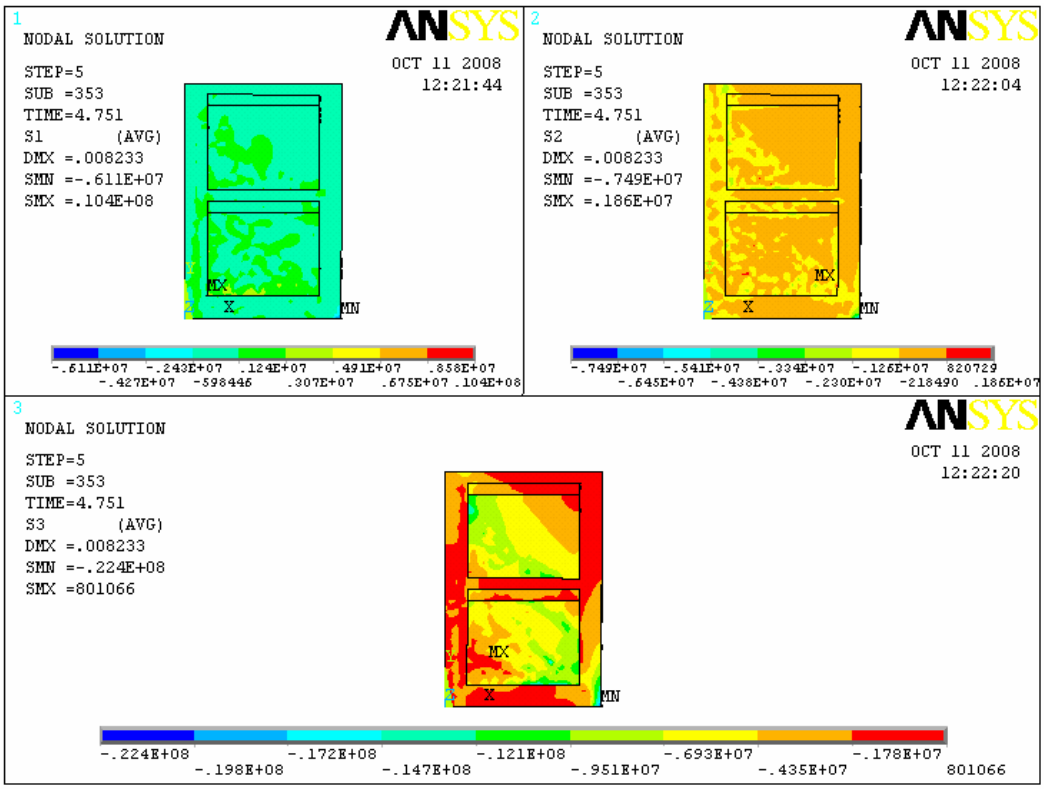

Figure 7.22 - Principal Stresses (N/m^2)

7.3.7.4 Specimen S5 and S6

Since wall made of concrete blocks behaved monolithically by the means of epoxy mortar, blocks were not modeled separately and only a wall was modeled for the all blocks bonded to each other.

The cracking patterns in strengthened frame with infill wall made of 70 MPa strength concrete blocks for different load values can be seen in Figures 7.23, 7.24, 7.25, 7.26.

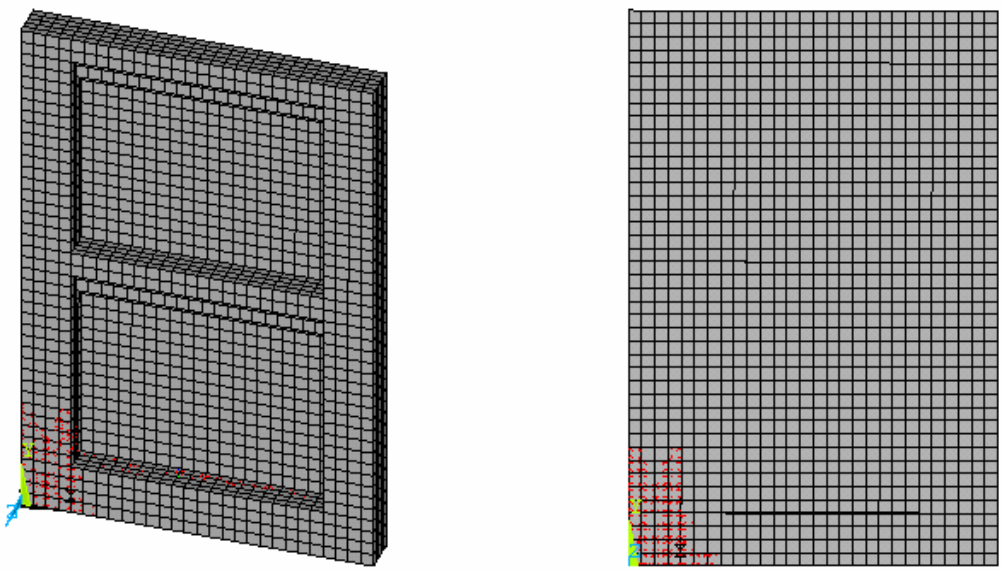

Figure 7.23 - Cracking at 100.0 kN

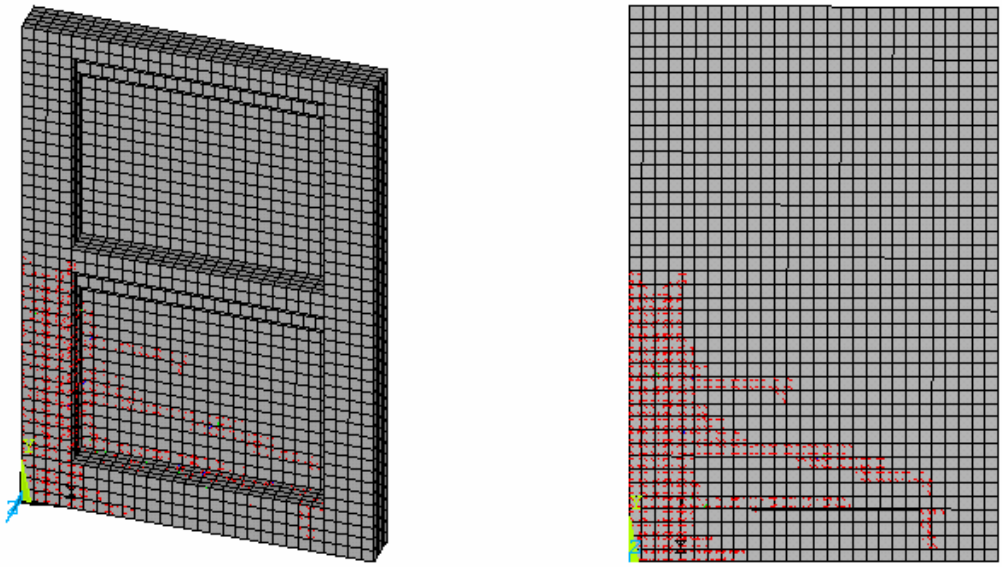

Figure 7.24 - Cracking at 130.4 kN

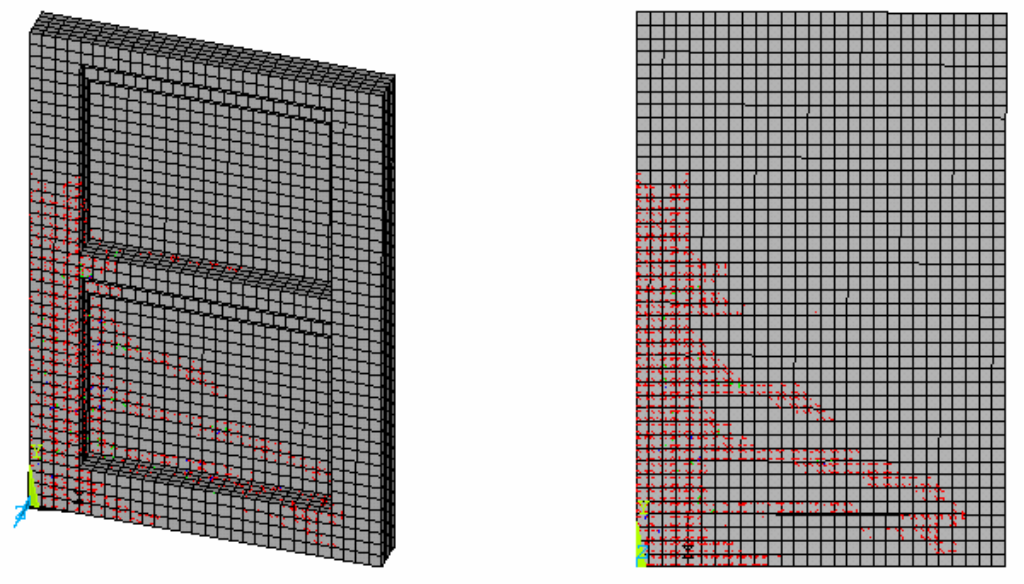

Figure 7.25 - Cracking at 190.0 kN

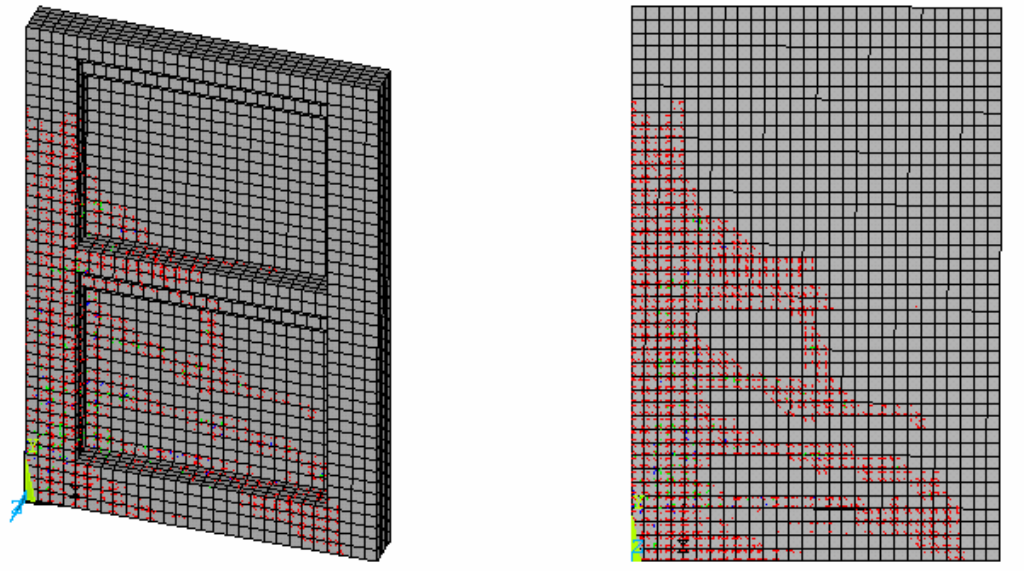

Figure 7.26 - Cracking at Maximum Load Carrying Capacity (233.5 kN)

The full nonlinear load-displacement response for Specimen S5 and S6 can be seen in Figure 7.27.

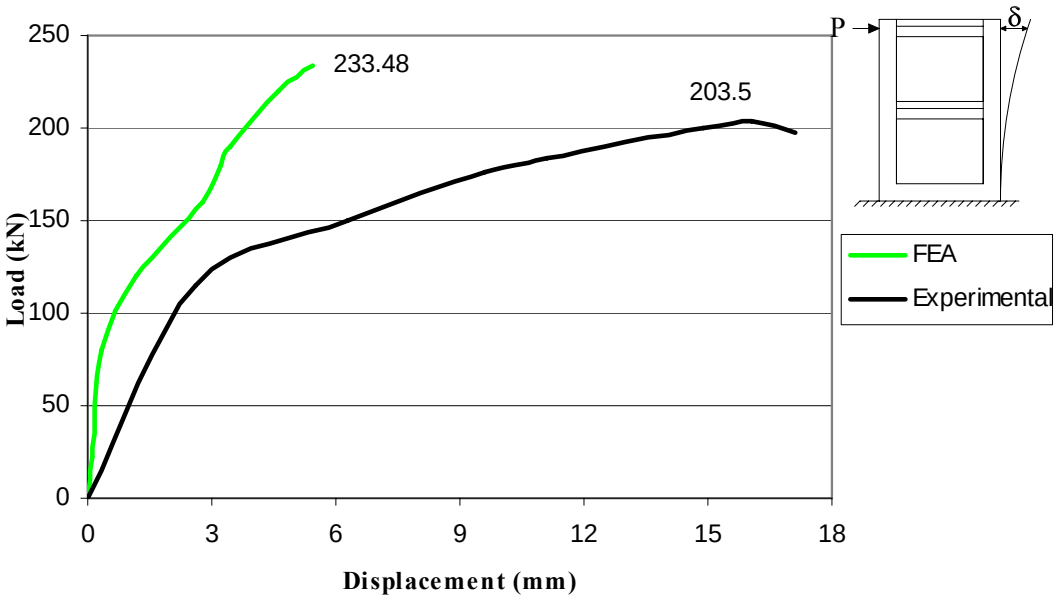

Figure 7.27 - Load vs. Displacement Curve for ANSYS Model

The principal stresses for specimen are shown in Figure 7.28.

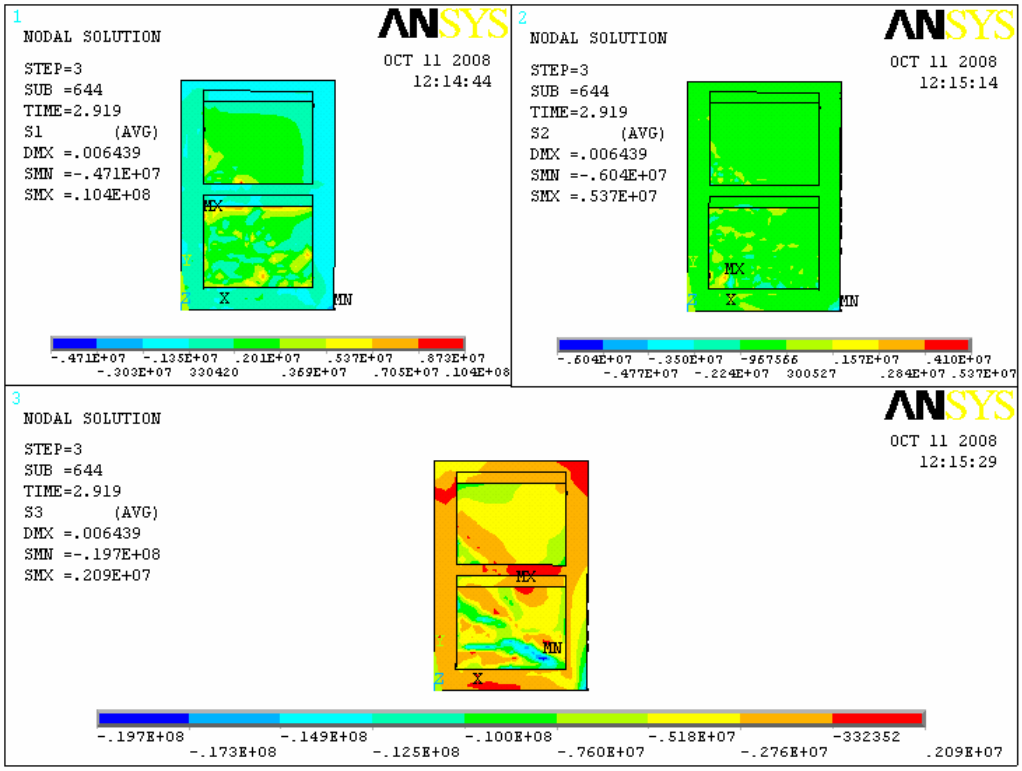

Figure 7.28 - Principal Stresses (N/m^2)

The following conclusions were drawn from this analitical research:

- Load-displacement behavior of the finite element model at second story level is in good agreement with the test results obtained in the test of bare frame (Specimen S1).
- Maximum lateral load capacities of the models are close to those measured during experimental testing
- FE models are slightly stiffer than the actual test specimens.

CHAPTER 8

SUMMARY AND CONCLUSIONS

8.1 Summary

A good percentage of the existing buildings in Turkey have a reinforced concrete frame structural system and can be classified as low to medium rise structures. They are also known to have inadequate seismic performance since many of these buildings lack sufficient lateral stiffness, ductility and strength.

For many structures, improving these deficiencies by means of some rehabilitation techniques prior to earthquakes is extensively used in practice. However, the cost of such rehabilitation projects is a major problem for great many owners due to economical condition. Also the production phase of these projects is slow, dirty, destructive and disruptive to occupants. To overcome these problems, structurally effective, practically applicable and economical seismic retrofitting techniques have been developed for years in Turkey and several countries. This study is one of these research projects sponsored by TUBITAK

In this study, six one-bay, two-story reinforced concrete frames are used in order to test the potential of using infill walls made of custom shaped and high strength concrete blocks to increase the lateral load bearing capacity of frame structures. Effect of concrete block geometry and block strength is investigated. In this study, one of the tested specimens was also retrofitted with FRCM (Fiber Reinforced Cementitous Matrix). Thus, the effectiveness of FRCM system on damaged structures is also investigated.

The test results are evaluated considering strength, stiffness, and energy dissipation characteristics. In an accompanying analytical study, finite element program ANSYS version 10 is used to determine the load-displacement behavior of test specimens by using nonlinear push over analysis.

8.2 Conclusions

The following conclusions are drawn based on the data obtained from experimental and analytical studies.

- Strengthening of reinforced concrete frames by custom shaped high strength concrete masonry blocks is found to be a simple, practical and effective method.

- The seismic rehabilitation technique developed to be an alternative to cast-in-place R/C panels increased the lateral load capacity and rigidity as well as improving the seismic behavior of the test frames. However, the relative improvement is not as high as those in the cast-in-place R/C infilled frame

- Test results show that the increase in the strength values of the strengthened specimen with respect to reference specimen S1 varied between 1.90 times and 2.20 times.

- The increase in the initial stiffness of the strengthened frames varied between 2.70 times and 3.10 times with respect to the reference frame.

- The increase in the energy dissipation capacities of the strengthened frames varied between 2.90 times and 4.60 times compared to 9.5 times in the case of cast-in-place R/C panels.

- The highest energy is dissipated by reference specimen S2 (cast-in-place R/C infilled frame). This is due to high energy dissipation capacity of R/C infilled wall and perfect bond between infill wall and the frame.

- Test results show that concrete block geometry do not affect the lateral load carrying capacities of frames since the walls made of concrete blocks behave as a monolithic block due to high adhesive strength of the epoxy based mortar.

- During the tests, it is observed that the specimens dissipate more energy when damage occurs in the infill wall and the frame almost simultaneously. If the frame members especially column-beam joints are damaged seriously before the infills, specimens dissipate less energy than expected. Hence, the properties of the test frame as well as the concrete blocks are important in the effectiveness of this method. Before the application of the strengthening technique, rehabilitation of the column-beam joints which are known to have inadequate seismic capacity may be required.

- Strengthening of reinforced concrete frames by high strength concrete masonry blocks can be an effective method since it would not require evacuation of the building and would be applicable without causing too much disturbance to the occupants.

- Analytical studies show that the load-displacement plot at second story is in good agreement with the test data from the full-scale bare frame (S1) test.

- Analytical studies show that the maximum lateral load capacities obtained from the finite element models are close to the maximum load measured during experimental testing. However, the load-displacement plots for the strengthened frame models did not show such a good agreement with the test results. The finite element models are stiffer than the actual structure in both the linear and the nonlinear ranges.

8.3 Recommendations

- The effect of axial load in the columns of the test frames is ignored in this study. This way, less favorable condition is created for the frame system. However, in real life frame structures the columns are normally subjected to serious compressive loads due to heavy self-weight of the R/C structure. Therefore, it would be nice to conduct the same tests one more time under axial loads.

- Multi-story multi-bay frames should be constructed and tested to obtain more realistic test results.

REFERENCES

[1] Bai Jong-Wha and Hueste Mary Beth. “Seismic Rehabilitation For Reinforced Concrete Building Structures”, Consequence-Based Engineering (CBE) Institute Final Report, Texas A&M University, 2003.

[2] Türk M., Ersoy U., Ozcebe G. “Seismic Rehabilitation of RC Frames With RC İnfill Walls”, Fifth national conference on earthquake engineering, Istanbul, 2003.

[3] Ohkubo, M. “ Current Japanese System on Seismic Capacity and Retrofit Techniques For Existing Reinforced Concrete Buildings and Post-Earthquake Damage Inspection and Restoration Techniques”, University of California, San Diego Structural Systems Research Project, California, 1991.

[4] Ersoy U., Uzsoy S., “The Behavior and Strength of Infilled Specimens”, Report No. MAG-205, TUBITAK, Ankara, Turkey, 1971, In Turkish.

[5] Govindan P., Lakshmipathy M., Santhakumar A. R. “Ductility of Infilled Frames”. Journal of the American Concrete Institute, 1986; 83: 567-576.

[6] Phan T.L., Cheok S.G., Todd R.D., “Strengthening Methodology for Lightly Reinforced Concrete Specimens, Recommended Guidelines for Strengthening with Infill Walls”, Building and Fire Research Laboratory National Institute of Standards and Technology, Gaithersburg, MD, July 1995.

[7] Frosch, R., “Seismic Rehabilitation Using Precast Infill Walls” PhD. Thesis, University of Texas, Department of Civil Eng., Texas, 1996.

[8] Erdem İ., Akyuz U., Ersoy U., Ozcebe G. "An Experimental Study On Two Different Strengthening Techniques For RC Frames", Engineering Structures, 2006; 28: 1843-1851.

[9] Süsoy, M. "Seismic Strengthening of Masonry Infilled Reinforced Concrete Frames With Precast Concrete Panels", A Master of Science Thesis in Civil Engineering, Middle East Technical University, Ankara, 2004.

[10] Baran, M. "Precast Concrete Panel Reinforced Infill Walls for Seismic Strengthening of Reinforced Concrete Framed Structures", A Doctor of Philosophy Thesis in Civil Engineering, Middle East Technical University, Ankara, 2005.

[11] Kesner K., Billington S. L. "Investigation of Infill Panels Made from Engineered Cementitious Composites for Seismic Strengthening and Retrofit". Journal of Structural Engineering, 2005, 131: 1712-1720.

[12] Kara, M. E. "Strengthening of Non-Ductile Reinforced Concrete Frames By Reinforced Concrete Partial Infills", A Doctor of Philosophy Thesis in Civil Engineering, Gazi University, Ankara, 2006.

[13] Yüksel E., Ilki A., Erol G., Demir C., Karadoğan H. F. "Seismic Retrofit of Infilled Reinforced Concrete Frames with CFRP Composites". Advances in Earthquake Engineering for Urban Risk Reduction, Netherlands, 2006; 285-300.

[14] Garevski M., Hristovski V., Stojmanovska M. "Shaking Table Tests of Scaled RC Frame Models for Investigation of Validity and Applicability of Different Retrofitting Techniques". Advances in Earthquake Engineering for Urban Risk Reduction, Netherlands, 2006; 441-453.

[15] ABYYHY-Turkish Seismic Code, Ministry of Public Work and Settlement, Government of Republic of Turkey, Ankara, 2007.

[16] ASCE, American Society of Civil Engineers, Minimum Design Loads for Buildings and Other Structures (ASCE 7-05), Reston, Virginia, 2006.

[17] Wolanski, A. J. "Flexural Behavior of Reinforced and Prestressed Concrete Beams Using Finite Element Analysis". Degree of Master of Science, Faculty of Graduate School, Marquette University, Wisconsin, 2004.

[18] Kachlakev D., Miller T., Yim S., Chansawat K., Potisuk T. "Finite Element Modeling of Reinforced Concrete Structures Strengthened With FRP Laminates" Technical Report, No. SPR 316, Corvallis, Oregon, 2001.

[19] Dede, F. T. "Nonlinear Finite Element Analysis of Reinforced Concrete Frames Subjected to Reversed-Cyclic Loading Using ANSYS Software". A Master of Science Thesis in Civil Engineering, Selcuk University, Konya, 2006.

[20] ANSYS User's Manual 10.0: ANSYS Structural Analysis Guide.

APPENDIX A

FRCM SYSTEM

FRCM (Fiber Reinforced Cementitous Matrix) is a kind of high performance fiber structural reinforcement systems. This system consists of a Polyparaphenylene benzobisoxazale (PBO) mesh and a stabilized inorganic matrix designed to connect the mesh with the concrete surface.

FRCM system is applied to reinforced concrete structures in seismic zones for increasing resistance to shear stress and tensile stress.

To observe the effectiveness of FRCM system on damaged structures, FRCM system was applied on damaged specimen S4 and this specimen called 4-X-Mesh was tested under reversed cyclic lateral loading.

Specimen 4-X-Mesh was subjected to lateral loading history presented in Figure A.1. For this specimen, maximum upward and downward loads were 219.5 kN and 231.6 kN, respectively. In Figure A.2 and Figure A.3, lateral load-displacement curves are presented for second story and first story, respectively.

First story and second story drift ratio of the specimen were also drawn in Figure A.4 and Figure A.5.

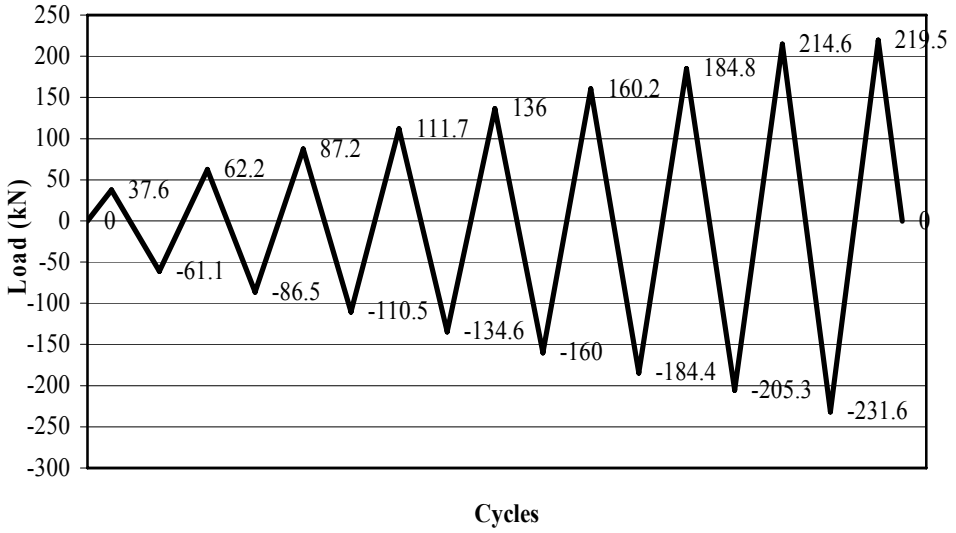

Figure A.1 - Loading History of Specimen 4XMesh

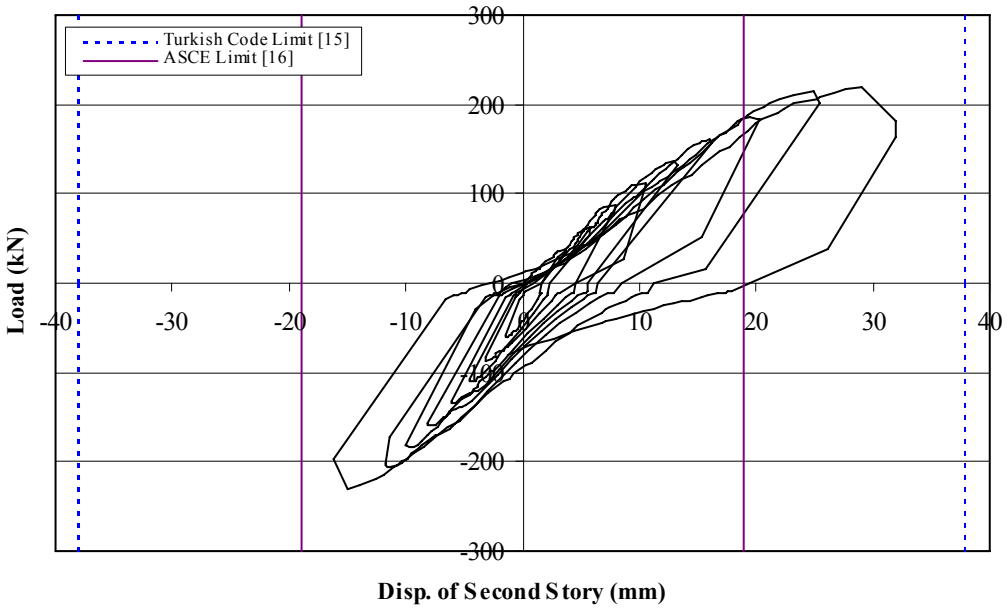

Figure A.2 - Load – Second Story Level Displacement Curve, Specimen 4XMesh

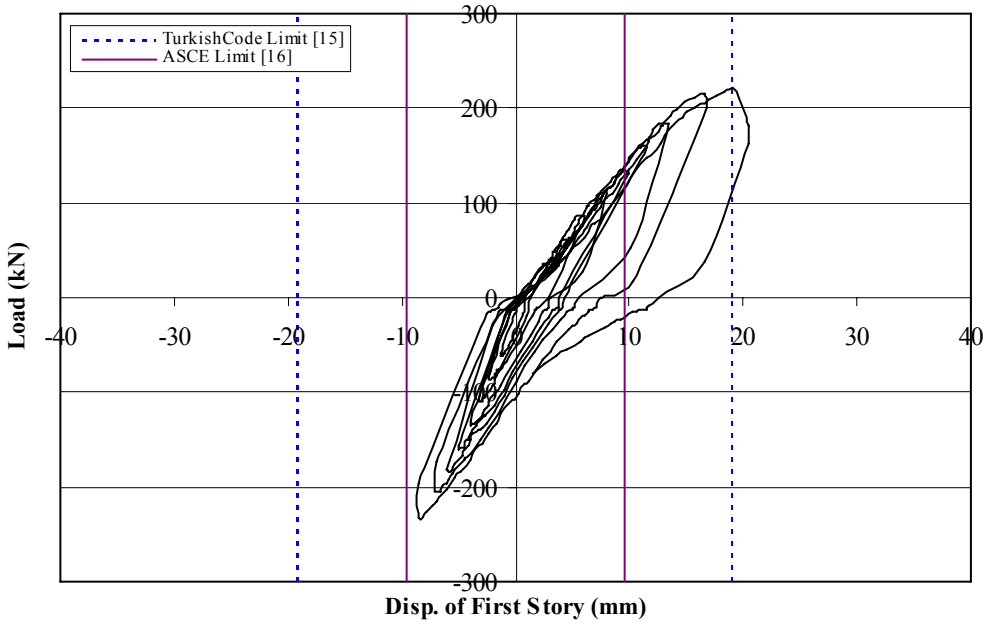

Figure A.3 - Load – First Story Level Displacement Curve, Specimen 4XMesh

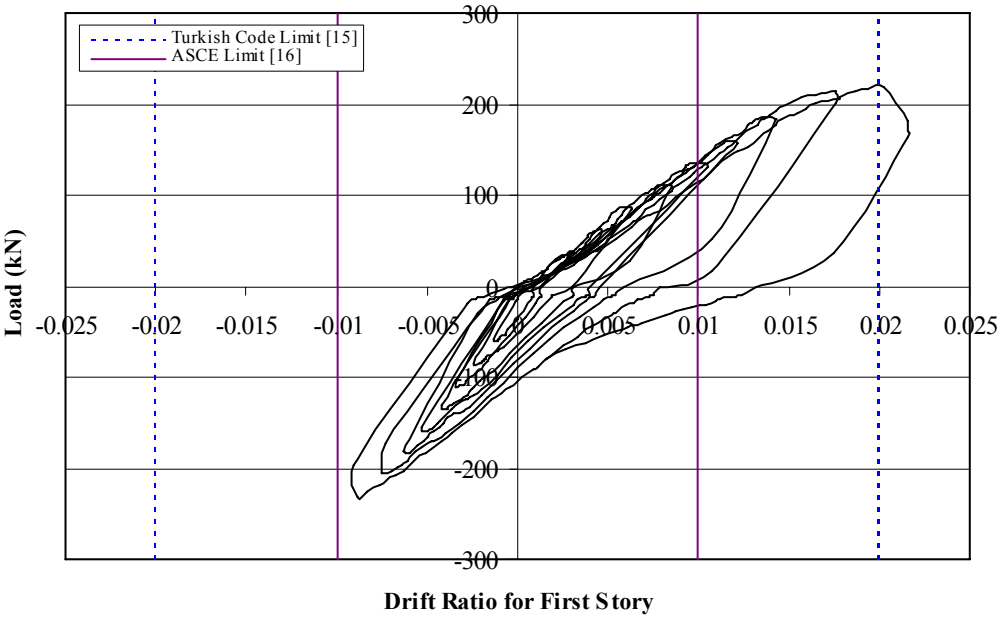

Figure A.4 - Load – First Story Drift Ratio Curve, Specimen 4XMesh

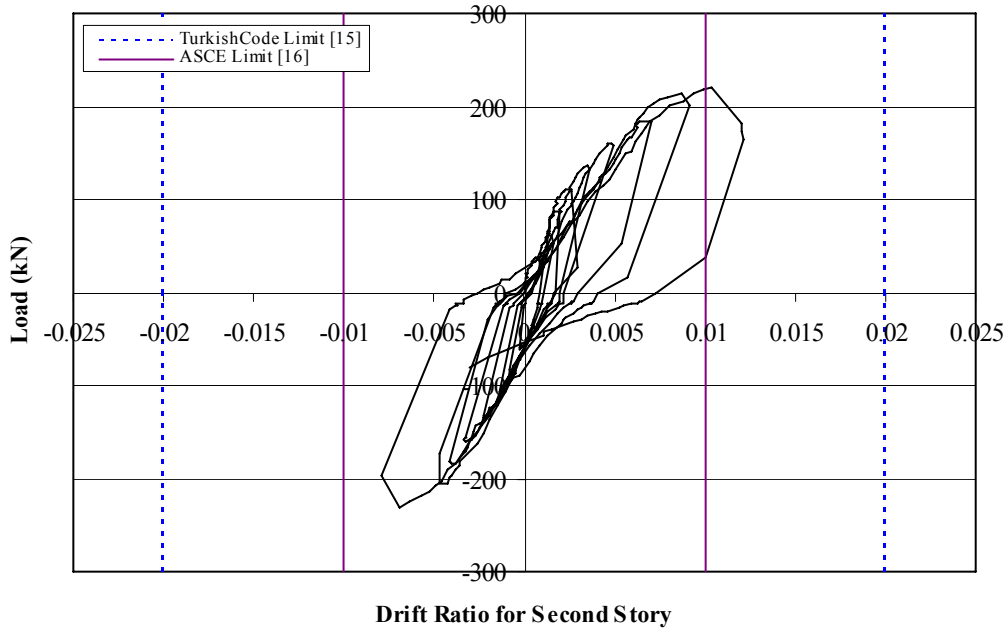

Figure A.5 - Load – Second Story Drift Ratio Curve, Specimen 4XMesh

Experimental observations for specimen 4-X-Mesh are given below:

- In the first two loading cycle, no cracking has occurred.
- In the third upward half cycle, hairline cracks were observed on the first story infills. These cracks remained from previous test. Due to loading cracks appeared again. In the next load stage symmetric cracks were observed.
- The previous diagonal cracks appeared during the continued four cycles but no separation between the frame and infills was observed.
- In the eighth upward half cycle, serious cracks formed at both column-foundation joints and previous cracks increased in number and length (Figure A.6). In the eighth downward half cycle, first story infills started to separate from the foundation with a thin crack. The cracking pattern is shown in Figure A.6. The maximum lateral load of 231.6 kN was recorded at this stage.

Figure A.6 - Column-Foundation Joint Crack (left) and Crack on the Infill (right)

- Since frame members especially first story columns and column-foundation joints were damaged seriously, the experiment was discontinued after the ninth upward cycle. Lateral load of 219.5 kN was reached at this cycle. The final view of the frame from front is given in Figure A.7.

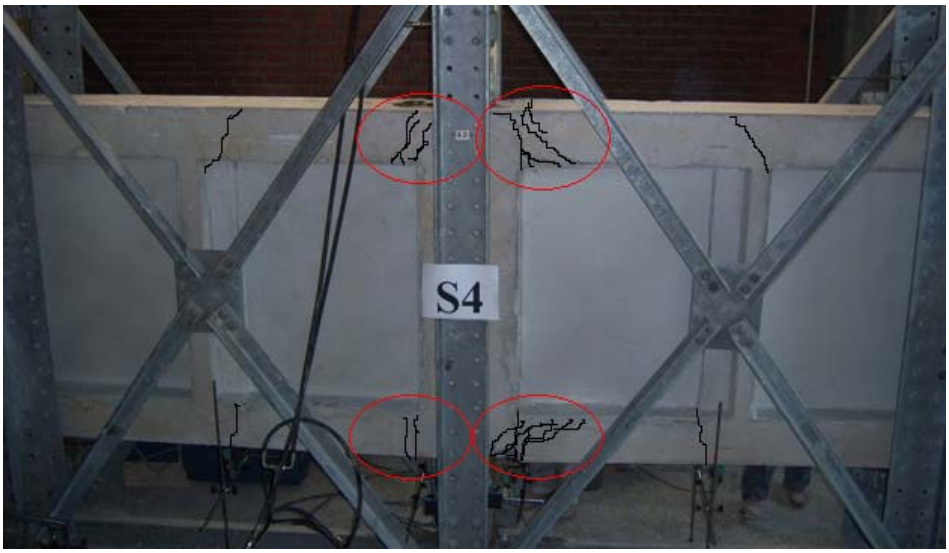

Figure A.7 - General View of Specimen after the Test

Test results are evaluated considering strength, stiffness and energy dissipation. Response envelope curve of the Specimen 4XMesh is given in Figure A.8. For comparison, curves of the other specimens are also given in the same graph. For each specimen, the maximum values of lateral loads are presented in Table A.1.

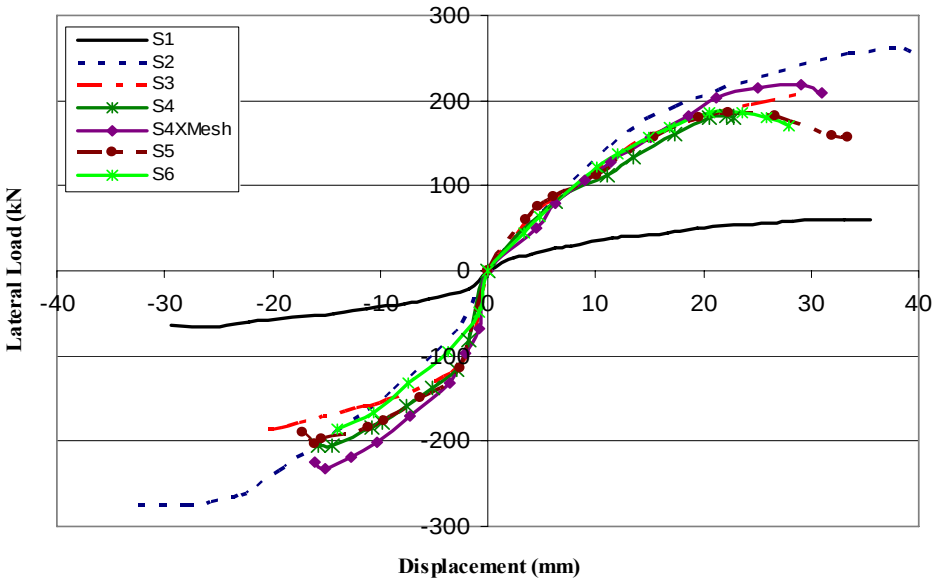

Figure A.8 – Response Envelope Curves of the Specimens

Table A.1 – Lateral Load Carrying Capacities of the Specimens

Specimen	Maximum upward load (kN)	Displacement at max. Load (mm)	Maximum downward load (kN)	Displacement at max. Load (mm)
S1	60.1	35.6	65.0	25.6
S2	262.0	39.2	276.4	28.0
S3	185.6	20.4	206.8	28.7
S4	182.0	22.2	205.3	15.0
S4XMesh	219.5	29.0	231.6	15.0
S5	184.7	22.4	203.5	16.1
S6	186.6	23.6	185.5	14.1

Test results showed that using FRCM to retrofit specimen increased the load carrying capacity significantly. Lateral load carrying capacity of specimen S4 increased 205.3 kN to 231.6 kN in spite of damaged specimen.

Initial stiffness value of the Specimen 4XMesh was calculated as 12.26 kN/mm which is lower than those of other strengthened specimens.

Using FRCM also increased the energy dissipated capacity of damaged specimen significantly. The results of the energy dissipation calculations for each specimen are given in Table A.2.

Table A.2 – Total Dissipated Energy for Test Specimens

Specimen	Dissipated Energy ($N_x m$)	Ratio of total energy to that of Reference Specimen
S1	2729	-
S2	25934	9.5
S3	10162	3.7
S4	9081	3.3
S4XMesh	13935	5.1
S5	12645	4.6
S6	7846	2.9